



Modelling of Acidic Solute Fluxes from Sediments to the Water Column in the Lower Lakes of South Australia.

Freeman J Cook and Luke Mosley

Report: FCA1_12

Prepared for: South Australian Department of Environment, Water and Natural Resources as part of the South Australian Government's \$610 million Murray Futures program funded by the Australian Government's Water for the Future Initiative.

July 2012 – Freeman Cook & Associates and South Australian EPA



**Government
of South Australia**



Australian Government

Prepared by:

Freeman Cook: Freeman Cook and Associates Pty Ltd.

Luke Mosley: South Australia Environmental Protection Agency

Permissive licence

© State of South Australia through the Department of Environment, Water and Natural Resources (DEWNR).

Apart from fair dealings and other uses permitted by the *Copyright Act 1968* (Cth), no part of this publication may be reproduced, published, communicated, transmitted, modified or commercialised without the prior written approval of the Department of Environment and Natural Resources.

Written requests for permission should be addressed to: Coorong, Lower Lakes and Murray Mouth Program Department of Environment, Water and Natural Resources
GPO Box 1047 Adelaide SA 5001

Copyright©. This publication ©2012, entitled “Modelling of Acidic Solute Fluxes from Sediments to the Water Column in the Lower Lakes of South Australia” is copyright. Apart from any fair dealing for the purpose of private study, research, criticism or review, as permitted under the **Copyright Act** (Cth), no part may be reproduced by any means by any persons without the prior written permission of the copyright owners Freeman Cook and Associates Pty Ltd.

Disclaimer.

Freeman Cook and Associates Pty Ltd makes no representations or warranties as to the accuracy or completeness of the Report and disclaims all liability for all claims, expenses, losses, damages and costs any third party may incur as a result of them relying on the accuracy or completeness of the Report.

This report has been prepared by consultants for the Department of Environment, Water and Natural Resources (DEWNR) and views expressed do not necessarily reflect those of the DEWNR. The DEWNR cannot guarantee the accuracy of the report, and does not accept liability for any loss or damage incurred as a result of relying on its accuracy.

I. Cover Photograph: Aerial photograph of Boggy lake (foreground and Lake Alexandrina (background) – Source (DEWNR)

Table of Contents

Modelling of Acidic Solute Fluxes from Sediments to the Water Column in the Lower Lakes of South Australia	1
Table of Contents	3
List of Figures	3
List of Tables	6
ACKNOWLEDGMENTS	7
EXECUTIVE SUMMARY	8
1. INTRODUCTION	10
1.1 Modelling of Solute Transport in Sediments	10
1.1.1. Initial inundation of sediments	11
1.1.2. Modelling the exchange of solutes between saturated sediments and the water column	12
1.1.3. Modelling acidic solutes	14
1.2 Local Studies of Relevance to Acidity Transport	15
1.2.2. Acidity distribution and concentration in the lower lakes sediment	15
1.2.3. Physical properties of lower lakes sediments	17
1.2.4. Acid flux from sediment to water	17
1.2.5. Sulfate reduction/neutralisation in submerged sediments	18
2. MODELLING OF ACID FLUXES	19
2.1 Diffusion	19
2.1.1. Comparison with data from specific lower lakes sites	25
2.2 Advection Plus Diffusion	33
2.2.1 Comparison with data from specific lower lakes sites	40
3. MODELLING OF ACID NEUTRALISATION IN THE SURFACE WATER	47
3.1 Results for an Isolated Water Body : Diffusion	50
3.2 Results for an Isolated Water Body: Advection Plus Diffusion	56
3.3 Comparison to EPA Monitoring Results	61
4. DISCUSSION	62
5. CONCLUSIONS	65
5.1 Recommendations	67
6. REFERENCES	68
APPENDIXES	72
II.	
III.	

List of Figures

Figure 1. Penetration depths for one-dimensional infiltration of water and solutes into a soil profile (from Clothier and Scotter (1985)	11
Figure 2. Example of acidity distribution in pore water from Finniss River Site FC1029 (from Fitzpatrick et al. 2011).	16

Figure 3. Example of acidity distribution within the sediments for the Boggy Creek mecosystems (from Hick et al. 2009).....	17
Figure 4. Relative concentration (C^*) versus depth at $t = 0$, and $t = 100$ day for a range of values of the dispersion coefficient, D . The value of $c_1 = 10 \times 10^{-3} \text{ kg m}^{-3}$, $c_2 = c_0 = 0$ and $z_1 = 0.5 \text{ m}$	20
Figure 5. Initial acidity flux as a function of the dispersion coefficient (D), with $c_1 = 10 \times 10^{-3} \text{ kg m}^{-3}$, $c_2 = c_0 = 0$ and $z_1 = 0.5 \text{ m}$	21
Figure 6. Flux of acidity to the water column versus time for various values of D (see legend) with $c_1 = 10 \times 10^{-3} \text{ kg m}^{-3}$, $c_2 = c_0 = 0$ and $z_1 = 0.5 \text{ m}$	21
Figure 7. Cumulative acidity flux with time for various values of D (see legend) with $c_1 = 10 \times 10^{-3} \text{ kg m}^{-3}$, $c_2 = c_0 = 0$ and $z_1 = 0.5 \text{ m}$. Trapezoidal integration of the data in figure 6 was used to provide the data for this figure.	22
Figure 8. Relative concentration (C^*) versus depth for a range of z_1 values from 0.1 to 1 m, with $c_1 = 10 \times 10^{-3} \text{ kg m}^{-3}$, $c_2 = c_0 = 0$ and $D = 5 \times 10^{-4} \text{ m}^2 \text{ day}^{-1}$	22
Figure 9. Flux of acidity to the water column versus time for various values of z_1 with $c_1 = 10 \times 10^{-3} \text{ kg m}^{-3}$, $c_2 = c_0 = 0$ and $D = 5 \times 10^{-4} \text{ m}^2 \text{ day}^{-1}$	23
Figure 10. a) Concentration versus depth for various values of c_1 , b) relative concentration versus depth. These profiles were calculated with $z_1 = 0.5 \text{ m}$, $c_2 = c_0 = 0$ and $D = 5 \times 10^{-4} \text{ m}^2 \text{ s}^{-1}$	24
Figure 11. Flux versus time for a) various values of c_1 and b) relative flux ($\text{flux}(t)/\text{flux}(t = 0)$) versus time. These fluxes were calculated with $z_1 = 0.5 \text{ m}$, $c_2 = c_0 = 0$ and $D = 5 \times 10^{-4} \text{ m}^2 \text{ day}^{-1}$	25
Figure 12. Acidity flux versus time from total acidity, Fe^{2+} , Al^{3+} , H^+ , and the sum of Fe^{2+} , Al^{3+} and H^+ fluxes for the Boggy Creek fresh water site.....	26
Figure 13. Initial dimensionless concentration (C^*) and concentration of the ions after 100 days for the Boggy Creek fresh water site.....	27
Figure 14. Acidity flux versus time from total acidity, Fe^{2+} , Al^{3+} , H^+ , and the sum of Fe^{2+} , Al^{3+} and H^+ fluxes for the Boggy Creek salt water site.....	28
Figure 15. Initial dimensionless concentration (C^*) and concentration of the ions after 100 days for the Boggy Creek salt water site.....	29
Figure 16. Acidity flux versus time from total acidity and H^+ for the Point Sturt fresh water site. The fluxes were calculated using two different values of z_1 of 0.4 and 1 m. and the sum of Fe^{2+} , Al^{3+} and H^+ fluxes.	29
Figure 17. Dimensionless concentration (C^*) versus depth for $t = 0$ and $t = 100$ day for $z_1 = 0.4$ and 1 m for the Point Sturt fresh water site.	30
Figure 18. Acidity fluxes from the sediment to the water column with time for; a) total acidity, b) Fe^{2+} , c) Al^{3+} and d) H^+ , for the scenarios in Table 6 for the Point Sturt salt water site.....	32
Figure 19. Concentration profiles for a) total acidity and b) Fe^{2+} and Al^{3+} for modelling scenarios where $c_2 > 0$ (Table 6) for the Point Sturt salt water site.	33
Figure 20. Relative concentration (C^*) versus depth at $t = 0$, and $t = 100$ day for a range of values of the dispersion coefficient, D . The value of $c_1 = 10 \times 10^{-3} \text{ kg m}^{-3}$, $c_2 = c_0 = 0$, $v = 1 \times 10^{-2} \text{ m day}^{-1}$ and $z_1 = 0.5 \text{ m}$	35
Figure 21. Flux of acidity to the water column versus time with $c_1 = 10 \times 10^{-3} \text{ kg m}^{-3}$, $c_2 = c_0 = 0$, $v = 1 \times 10^{-2} \text{ m day}^{-1}$ and $z_1 = 0.5 \text{ m}$	36
Figure 22. Relative concentration (C^*) versus depth for a range of z_1 values from 0.1 to 1 m, with $c_1 = 10 \times 10^{-3} \text{ kg m}^{-3}$, $c_2 = c_0 = 0$, $v = 1 \times 10^{-2} \text{ m day}^{-1}$ and $D = 5 \times 10^{-4} \text{ m}^2 \text{ day}^{-1}$	37
Figure 23. Flux of acidity to the water column versus time for various values of z_1 with $c_1 = 10 \times 10^{-3} \text{ kg m}^{-3}$, $c_2 = c_0 = 0$, $v = 1 \times 10^{-2} \text{ m day}^{-1}$ and $D = 5 \times 10^{-4} \text{ m}^2 \text{ day}^{-1}$	37
Figure 24. a) concentration versus depth for various values of c_1 , b) relative concentration versus depth. These profiles were calculated with $z_1 = 0.5 \text{ m}$, $c_2 = c_0 = 0$, $v = 1 \times 10^{-2} \text{ m day}^{-1}$ and $D = 5 \times 10^{-4} \text{ m}^2 \text{ day}^{-1}$	38
Figure 25. Flux versus time for various values of c_1 and with $z_1 = 0.5 \text{ m}$, $c_2 = c_0 = 0$, $v = 1 \times 10^{-2} \text{ m day}^{-1}$ and $D = 5 \times 10^{-4} \text{ m}^2 \text{ day}^{-1}$	39

Figure 26. . Flux versus time for various values of v and with $z_1 = 0.5$ m, $c_2 = c_0 = 0$, $c_1 = 1 \times 10^{-2}$ kg m ⁻³ and $D = 5 \times 10^{-4}$ m ² day ⁻¹	39
Figure 27. Concentration versus depth for various values of v , with $z_1 = 0.5$ m, $c_2 = c_0 = 0$, $c_1 = 1 \times 10^{-2}$ kg m ⁻³ and $D = 5 \times 10^{-4}$ m ² day ⁻¹	40
Figure 28. Acidity flux versus time from total acidity, Fe ²⁺ , Al ³⁺ , H ⁺ , and the sum of Fe ²⁺ , Al ³⁺ and H ⁺ fluxes for the Boggy Creek fresh water site.....	41
Figure 29. Initial dimensionless concentration (C^*) and concentration of the ions after 100 days for the Boggy Creek fresh water site.	42
Figure 30. Acidity flux versus time from total acidity, Fe ²⁺ , Al ³⁺ , H ⁺ , and the sum of Fe ²⁺ , Al ³⁺ and H ⁺ fluxes for the Boggy Creek salt water site.	43
Figure 31. Initial dimensionless concentration (C^*) and concentration of the ions after 100 days for the Boggy Creek salt water site.....	44
Figure 32. Acidity flux versus time from total acidity and H ⁺ for the Point Sturt fresh water site. The fluxes were calculated using two different values of z_1 of 0.4 and 1 m.	45
Figure 33. Dimensionless concentration (C^*) versus depth for $t = 0$ and $t = 100$ day for $z_1 = 0.4$ and 1 m, for the Point Sturt fresh water site.	45
Figure 34. Acidity fluxes from the sediment to the water column with time for; a) total acidity, b) Fe ²⁺ , c) AL ³⁺ and d) H ⁺ , for the scenarios in Table 6 for the Point Sturt salt water site.....	46
Figure 35. Concentration profiles for total acidity and when $c_2 > 0$ (Table 6) for Point Sturt salt water site.....	47
Figure 36. Modelled surface water pH and alkalinity for the Boggy Creek freshwater site with different starting alkalinities in a 1m (top) and 0.1m (bottom) water column (0.0001, 0.001, 0.002, and 0.004 eq L ⁻¹).....	52
Figure 37. Modelled surface water pH and alkalinity for the Boggy Creek saltwater site with different starting alkalinities in a 1m water column (0.0001, 0.001, 0.002, and 0.004 eq L ⁻¹).....	53
Figure 38. Modelled surface water pH and alkalinity for the Pt Sturt freshwater site with different starting alkalinities in a 0.5m water column (0.0001, 0.001, 0.002, and 0.004 eq L ⁻¹) for $z = 0.4$ and $z = 1$ m.....	54
Figure 39. . Modelled surface water pH and alkalinity for the Pt Sturt salt water site with different starting alkalinities in a 0.5m water column (0.0001, 0.001, 0.002, and 0.004 eq L ⁻¹) for $z = 0.4$ and 1m and $c_2 > 0$	55
Figure 40. Modelled surface water pH and alkalinity for the Boggy Creek freshwater site with different starting alkalinities in a 0.5m (TOP) and 0.1m (BOTTOM) water column (0.0001, 0.001, 0.002, and 0.004 eq L ⁻¹) including advection.....	58
Figure 41. Modelled surface water pH and alkalinity for the Boggy Creek salt water site with different starting alkalinities in a 1m (top) and 0.1m (bottom) water column (0.0001, 0.001, 0.002, and 0.004 eq L ⁻¹) including advection.	58
Figure 42. . Modelled surface water pH and alkalinity for the Point Sturt freshwater site for a 0.5m water column with different starting alkalinities (0.0001, 0.001, 0.002, and 0.004 eq L ⁻¹) for $z = 0.4$ and $z = 1$ m including advection.	59
Figure 43. Modelled surface water pH and alkalinity for the Point Sturt saltwater site for a 1m water column with different starting alkalinities (0.0001, 0.001, 0.002, and 0.004 eq L ⁻¹) for $z = 0.4$ and $z = 1$ m including advection.	61
Figure 44. Modelled surface water pH and alkalinity for the Point Sturt salt water site for a 0.5m water column with different starting alkalinities (0.0001, 0.001, 0.002, and 0.004 eq L ⁻¹) and $c_2 > 0$	61
Figure 45. Measured acidity and alkalinity in the Boggy and Hunter's Creek region of Lake Alexandrina (Source: EPA).	62
Figure 46. Long term modelling of worst case scenario at each of the four sites of Hicks et al. (2009) for a) flux of acidity and b) cumulative acidity.	64

IV.

List of Tables

Table 1. Laboratory data summary of pH testing and sulfate chemistry from Fitzpatrick et al. 2010	16
Table 2. The depth of constant concentration (D) and the concentration (C_d) used to parameterise the flux equation used by Hicks et al. (2009) to estimate the acidity flux rates.	18
Table 3. Calculated and measured flux rates ($\text{mol H}^+ \text{ m}^{-2} \text{ day}^{-1}$) from Hicks et al. (2009, Table 8). Negative values indicate flux from the soil to the water column and positive values from the water column to the soil. The range for the long term measured values is shown in brackets.	18
Table 4. Values of c_1 , D , and z_1 used in the sensitivity analysis. The base case is the value when this parameter is not varying.	19
Table 5. Molecular diffusion of ions in water (DiToro, 2000; Vanýsek, 1992).	26
Table 6. Settings for c_1 , c_2 and z_1 for the modelling runs for Point Sturt salt water site.....	31
Table 7. Values of c_1 , D , v and z_1 used in the sensitivity analysis. The base case is the value when this parameter is not varying.	34
Table 8. Pore water velocities for the four sites from Hicks et al. (2009).	40

ACKNOWLEDGMENTS

The author would like to acknowledge funding for this work from the South Australian Department of Environment, Water and Natural Resources (DEWNR). The authors would like to thank Dr Liz Barnett (DEWNR), Ann-Marie Jolley (DEWNR) for their assistance with obtaining the funding. Drs John Knight (CSIRO, Griffith University), and Liz Barnett, and Ms Ann-Marie Jolley and Emily Leyden (SA EPA) are thanked for their useful comments on the manuscript. Lesley Cook is thanked for her administrative assistance.

EXECUTIVE SUMMARY

During the recent drought in the Murray-Darling Basin in flow to the lower lakes was severely restricted which led to a reduction in the lake levels to as low as -1.0 m AHD. This resulted in exposure of sediments with pyritic minerals and the subsequent oxidation of these to produce acidic sediments. Upon refilling of the lower lakes these sediments were inundated providing a pathway for this acidity to be transport to the lake water. The rate of acidity transport to the lake water, the time course of acidity transport and the possible effects on the lake water alkalinity are not known. In order to provide some guidance on these issues models to; estimate the flux of this acidity to the lake water, and the reactions in the water column of this acidity with the alkalinity in the lake water. Short term measurements of fluxes using mesocosms had shown that acid fluxes decreased rapidly with time but these studies, by the nature of the flow regime had significant advection of water into the sediments which could have reduced the acid fluxes. Using the modelling here we are able to consider situations where there is no advection or the advection is out of the sediments. Under these situations we postulate that the acid fluxes to the lake water will occur for longer and the total flux will be greater.

A review of modelling of solute transport in benthic sediments is presented and shows that analytical solute transport models compiled by van Genuchten and Alves (1982) are applicable. Measurements and relevant information on the acidity and acid fluxes for the lower lakes is reviewed in relation to the modelling that was carried out.

A model based on van Genuchten and Alves (1982) A5 solution was developed for both diffusion-only and advection plus diffusion solute transport. The sensitivity of this model was tested using the likely range of dispersion coefficient (D), concentration (c_1), depth of the acidity (z_1) and pore water velocity (v).

For diffusion-only transport the initial flux is proportional to the value of D and the flux and cumulative flux also increase as D increases. Flux is sensitive to the value of z_1 but only up to a certain value of $z_1 = 0.75$ m for the parameters used here. When $z_1 > 0.75$ m there was little change in the flux. Again the flux increased with c_1 but now in a linear manner which meant that the scaled flux was the same for all values of c_1 .

When advection was introduced the decrease in flux with decrease in D was dramatically greater than with diffusion-only, when the advection was into the sediment. This is because the solutes get transported down the sediment profile and the distance that the solutes now need to diffuse to get to the sediment surface increases with time. Advection also decreased the effect of z_1 on the flux with the value of z_1 at which the flux becomes similar was 0.5 m with a value of v of 1×10^{-2} m day⁻¹.

Sites where measurements of the acidity flux were by Hicks et al. (2009) viz Boggy Creek fresh water, Boggy Creek salt water, Point Sturt fresh water and Point Sturt salt water were modelled using the measured values of c_1 , z_1 , and v . The dispersion coefficient was taken as the molecular diffusion coefficient for the H^+ , Fe^{2+} and Al^{3+} ions modelled. The model was able to give reasonable estimates of the fluxes when compared to the measured fluxes. The diffusion-only model tended to overestimate

the flux while the advection plus diffusion model occasionally underestimated the flux. The fact that advection of alkalinity into the sediments is not taken into account meant that the model overestimated the flux at the Point Sturt salt water site. However, the modelled results were generally within one order of magnitude of the measured values.

A model of the water chemistry for an isolated water column was developed and the fluxes from the modelling at the four measurement sites used. The results show that at the Boggy Creek salt water site the water is likely to go acidic in < 25 days when the diffusion-only flux is used. This is more rapid than the measurements showed. The diffusion plus advection increased this time to 100 days similar to the measurements. The Boggy Creek salt water site when fluxes from the diffusion plus advection model indicated rapid acidification of the water column.

However, for the Point Sturt site the model showed no acidification occurring for either diffusion-only or diffusion and advection, which was similar to that measured.

The model for acid flux was run for the worse case scenarios for a time period of 1000 days. The cumulative acidity was then compared with the alkalinity of the lakes. For Lake Alexandrina the alkalinity of the lake and the rate of replenishment suggests that as a whole acidification is highly unlikely, however, acidification could occur in localised areas. For Lake Albert by comparison where the amount of alkalinity is much smaller, the rate of replenishment is unknown and the area of acidic sediments is larger, the worst case cumulative acid flux after 1000 days is greater than the lake's alkalinity. This means that the main water-body of Lake Albert has a much greater risk of acidifying than Lake Alexandrina.

The modelling carried out here necessarily simplified the processes in the sediments and no account was made of the effects of alkalinity input to the sediments from the lake water, sulfate reduction or iron and manganese oxidation at the redox boundary or hydrolysis at the sediment:water interface are taken into account. Some if not all of these processes could be included by extending these models.

This report recommends:

Enhance the present models with the addition of zero-order and first-order source/sink terms, including modelling the sulfide production rate of the sediments.

Monitor the diffusion processes and water quality in shallow embayments to determine the nature and time course of the acidity fluxes and effect on water alkalinity.

Ongoing monitoring of the alkalinity in the lakes, especially Lake Albert should be continued until reliable measurements of the acid fluxes are known.

Model the oxidation and hydrolysis of metal acidity (Mn, Al, Fe) at the redox boundary and sediment:water interface.

Modelling of the depth of oxygen penetration into the sediments to determine the oxic/anoxic boundary.

Combine acid flux measurements with benthic ecotoxicological experiments.

Measure the respiration rate of the sediments.

1. INTRODUCTION

The drought in the Murray Darling Basin in the recent years led to a reduction in the water level in the lower lakes (Lake Alexandrian and Lake Albert), to as low as -1.0 m AHD. This resulted in the formation of acidic sediments due to oxidation of sulfides in the sediments (Fitzpatrick et al., 2008) and surface and groundwater turning acidic on the lake margins (EPA 2012). In 2009, the lakes started to refill, covering the sediments and beginning the process of recovery in terms of the water levels, water quality and ecosystems. However, it is difficult to know the length of this recovery, given acidity is still present in the sediments. In particular, the potential for toxic effects on the benthic community, a major component of the ecosystem is currently unknown. The rate of the acidity flux from the sediments to the water column as a function of time and the effect of this on the alkalinity of the lake water is likely to have an effect on the recovery of the ecosystem in the lower lakes.

The initial stages of the rewetting of the sediments in the lower lakes will have consisted of a process of water table rise due to the increase in the level of the lakes and inundation of the sediments once the Lake level was greater than the surface level of the sediments. The first process is likely to push solutes up the sediment profile and cause solutes to increase near the surface of the sediments. The rate of water table rise in the sediments, compared to the lake water level rise, will depend on the sediments physical characteristics. The water table rise will result in advection of the solutes towards the sediment surface. Once inundation occurs the advection will take place in the opposite direction with the solutes being pushed into the sediments and diffusing towards the sediment: water surface. These processes can be estimated using some simple concepts for penetration depth in Clothier and Scotter (1985).

Once inundation of the sediments has occurred, models used for transport in saturated porous media and benthic systems become appropriate. There are a number of modelling approaches that have been taken in modelling the benthos in freshwater, estuarine and marine sediments. This study will review these various models and choose an appropriate model that will assist in understand the rate of acidity release to the water column and the solute transport in the benthos of the lower lake sediments.

1.1 Modelling of Solute Transport in Sediments

The modelling of solute fluxes in sediments from the benthos in the lower lakes following drying and then rewetting will follow three phases;

1. an initial inundation,
2. non-steady flux due to diffusion and advection,
3. and finally steady-state as the fluxes return to processes governed by diagenesis.

We will consider in detail the first two of these processes and touch briefly on the third which is covered in depth by DiToro (2000).

1.1.1. Initial inundation of sediments

For infiltration into unsaturated soil Clothier and Scotter (1985) showed that the simple concept of using piston flow to estimate the penetration front position (figure 1) was often quite accurate at estimating the centre of mass of the solute front.

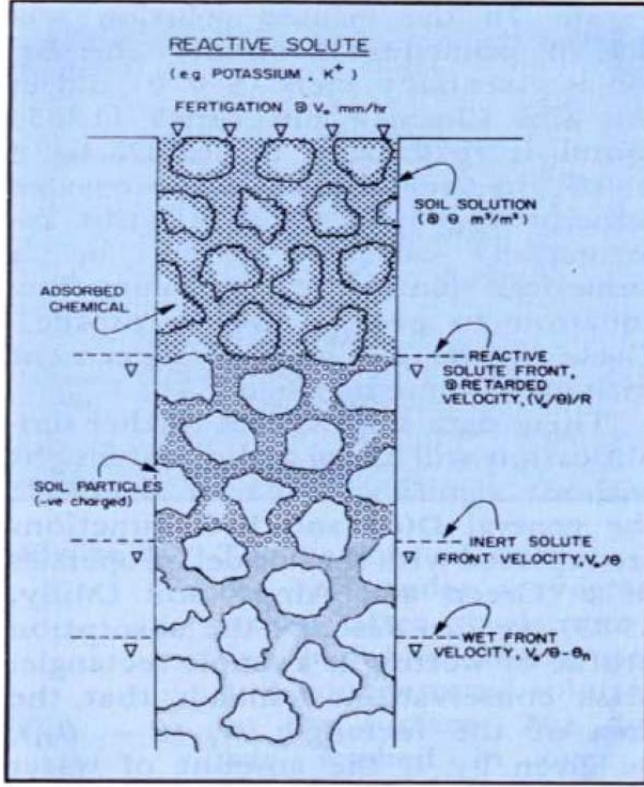


Figure 1. Penetration depths for one-dimensional infiltration of water and solutes into a soil profile (from Clothier and Scotter (1985)).

For an inert solute the penetration front ($\lambda_s(t)$) with time (t) can be given by:

$$\lambda_s(t) = \frac{V(t)}{\theta_n} \quad (1.1)$$

where $V(t)$ is the cumulative infiltration with time and θ_n is that water content at an infiltration rate of V . For a retarded solute the penetration depth is then given by:

$$\lambda_r = \frac{\lambda_s}{R} = \frac{V}{\theta_n R} \quad (1.2)$$

where R is the retardation with:

$$R = 1 + \rho_b \frac{f'(c)}{\theta} = 1 + \rho_b \frac{S_0}{\theta c_0} \quad (1.3)$$

where ρ_b is the bulk density and $f'(c)$ is the derivative of the relationship between the solute in solution and that adsorbed by the solids (isotherm), S_0 is the solute adsorbed at the influent concentration (c_0).

Where the inundation of the sediments occurs due to rapid overtopping (in comparison to gradually water table rise) this simple approach can be used to determine where the solute front is expected to be. The infiltration can be calculated using the infiltration equation of (Philip 1957; Philip 1987), based on the soil physical properties.

When the water table rises slowly towards the surface, the inundation of the surface can occur at the same time as the water table reaches the surface. With this scenario the sediment is saturated at inundation and no or little infiltration can occur. The slow water table rise is likely to move the solutes towards the sediment surface and lead to an initially high acidity flux upon inundation.

1.1.1. Modelling the exchange of solutes between saturated sediments and the water column

Numerous models have been developed to predict the transport of solutes to and from sediments. These vary from the simple box models (Marion et al. 2003) to full description of all processes (Meysman et al. 2007). This study started with the full Darcy-Brinkman-Forchheimer equation for flow (Meysman et al. 2007):

$$\rho \left[\frac{1}{\phi} \frac{\partial v_d}{\partial t} + \frac{1}{\phi} (v_d \cdot \nabla) v_d \right] = -\nabla p + \rho g \nabla z + \tilde{\mu} \nabla^2 v_d - \rho \frac{C_f}{\sqrt{k}} \|v_d\| v_d \quad (1.4)$$

where k is the permeability, μ is the dynamic viscosity, $\tilde{\mu}$ is the effective viscosity ρ is the pore water density, C_f a dimensional drag coefficient, g gravity and z the vertical coordinate. The Darcy velocity v_d is related to the actual velocity of the pore water (v) by $v_d = \phi v$ where ϕ is the porosity. The non-linear drag (Forchheimer) is negligibly small particularly in sands and can be ignored. The Brinkman term is only important in the interface between the benthos and the water where the velocity term shows strong curvature ($\nabla^2 v_d$ large). The region of importance is of the order of the grain diameter, so in sands is approximately 2 mm and again in most circumstances can be ignored. This then leaves the Darcy equation for flow:

$$v_d = -\frac{k}{\mu} (\nabla p - \rho g \nabla z) \quad (1.5)$$

When combined with the continuity equation this gives (Meysman et al. 2007):

$$\frac{\partial C}{\partial t} = \nabla \cdot (D \cdot \nabla C + vC) + R_r \quad (1.6)$$

where C is the solute concentration, D is the dispersion tensor and R_r is an overall production rate for the chemical species.

There are many variations on equation 1.4 with processes such as bioturbation and bio-irrigation (Glud and Fenchel 1999; Volkenborn et al. 2010; Braeckman et al. 2011), wave induced pressure effects (Webster, 2003) and ripples on the bottom (Marion, et al. 2003; Marion et al., 2002). All these processes can be considered to enhance the exchange of solutes and increase the apparent dispersion in the

sediments. This means that the apparent dispersion (D_m) can be written as (van Rees et al. 1996):

$$D_m = D_s + D_b + D_i + D_{wc} \quad (1.7)$$

where D_s is the molecular diffusion $D_s = \tau D_o$, (D_o is molecular diffusion in water and τ the tortuosity), D_b due to particle mixing, D_i is irrigation by benthic organisms and D_{wc} is due to wave action and current mixing. Van Rees et al. (1996) found for Lake Okeechobee that for $D_s = 0.9$ to $1.29 \text{ cm}^2/\text{day}$, the value of D_m increased from 1.98 - $4.14 \text{ cm}^2/\text{day}$, 1.35 - $4.74 \text{ cm}^2/\text{day}$ and 1.52 - $24.78 \text{ cm}^2/\text{day}$ for sand, mud and littoral sediments respectively. The large value for the littoral sediments was due to the macro benthos.

Wave action was found by Webster (2003) to be able to enhance apparent dispersion by orders of magnitude depending on the wave frequency, amplitude and sediment grain size.

Volkernborn et al. (2010) also concluded that the solute transport in the sediment pore water was dependent on the flow regime in the overlying water. Dade (1993) presents a review of the modelling approaches for turbulent transport in the water column above the sediments, based on transport equations for fluid mechanics. Here the study will only concentrate on the transport in the sediments but the boundary conditions with the overlying water are important. The boundary layer was found by (Arnon et al., 2007) to often be the rate determining step for solute mass transfer from the water column to the sediments. This can be a rate-limiting process for nutrient transport to the sediments and hence ecosystem-level metabolism (Duff and Triska, 2000; Larned et al., 2004). The presence of oxygen can also result in the oxidation of redox-sensitive, and acidity producing, soluble metals such as Fe and Mn (Di Toro 2000). The regime in the lower lakes may be similar to that in Lake Rotorua sediments, where they found for oxygen that the boundary layer was 0.8 mm .

Simpler box models have also been used to describe the exchange between the sediments and overlying water. Marion et al. (2003) described the transient storage model for a stream bed, where the concentration in the stream bed (C_b) is considered to be the average mixed value, and exchange is given by:

$$\frac{dC_b}{dt} = \alpha \frac{A}{A_s} (C_w - C_b) \quad (1.8)$$

A = cross-sectional area of the stream, A_s = cross sectional area of the storage zone, α = mass transfer coefficient and C_w = concentration of solute in stream. They compared this with a pumping model and showed that there was not a lot of difference. However, determining the value of α is critical for this model. Marion et al. (2002) also presented a model for exchange which considers the effect of the bed geometry on solute transport. They were able to show that the bed geometry could have an effect of the solute transfer especially in coarse sediments. These kind of models are used more in river systems and larger estuarine systems (Robson et al. 2008).

With regard to sulfidic sediments, Lichtschlag et al. (2010) have studied the fluxes of sulfides ($\text{H}_2\text{S} + \text{HS}^- + \text{S}^{2-}$) in the bottom waters of the Black sea. In their study sulfide reduction was driven by methane from volcanic vents which provided the carbon source. The methane sulfate and oxygen diffuse into sediments against an upward

welling pore water advection. This results in two sulfide peaks, one near the water interface and the other at 3-15 cm below the sediment surface. The peaks indicate zones of net sulfide reduction separated by a sulfide sink. Ankley et al. (1994) have reviewed the transport of metals in sediments and Di Toro (2000) has provided an extensive review of modelling such processes, as well as online EXCEL spreadsheet for computation of steady state fluxes.

Equation (1.6) above is similar to those used for transport of solutes into any porous media. Analytical solutions for equation (1.6) subject to various boundary and initial conditions were collated by van Genuchten and Alves (1982) with the general form of the equation given by:

$$\frac{\partial}{\partial x} \left(\theta D \frac{\partial c}{\partial x} - qc \right) - \frac{\partial}{\partial t} (\theta c + \rho S) = \mu_w \theta c + \mu_s \rho S - \gamma_w \theta - \gamma_s \rho \quad (1.9)$$

where c is the concentration in the solution [$M L^{-3}$], S is the adsorbed concentration [$M M^{-1}$], θ is the water content [$M^3 M^{-3}$], D is the dispersion coefficient [$L T^{-2}$], q is Darcy flux [$L T^{-1}$], ρ is bulk density [$M L^{-3}$], x is distance [L] and t is time [T]. The coefficients μ_w and μ_s are rate constants [T^{-1}] for first order transformations in the liquid and solid phases respectively. The coefficients γ_w [$M L^{-3} T^{-1}$] and γ_s [T^{-1}] are zero order transformation processes for liquid and solid phases respectively. We can use the solutions in van Genuchten and Alves (1982) with appropriate values of D , q , θ and ρ to compute the distribution within the sediment and flux at the sediment surface for different solutes. For example for a pulse input into a sediment ($c = c_1$, $t \geq 0$) with constant initial concentration (c_0) and a semi-infinite bottom boundary condition ($\partial c / \partial x \rightarrow 0$, $x \rightarrow \infty$) the solution is:

$$c(x, t) = c_0 + \frac{(c_1 - c_0)}{2} \left\{ \operatorname{erfc} \left[\frac{Rx - qt}{2\sqrt{DRt}} \right] + \exp \left(\frac{qx}{D} \right) \operatorname{erfc} \left[\frac{Rx + qt}{2\sqrt{DRt}} \right] \right\} \quad (1.10)$$

where R is the retardation given in equation (1.3) and erfc is the complimentary error function. The solutions become more complicated as the boundary and initial conditions, and processes become more complicated. The main difference from the use of solutions such as equation (1.10) in submerged sediments is that the dispersion coefficient is now the apparent dispersion given by equation (1.7).

Steady-state (time invariant) solutions for the flux of solutes from sediments in relation to the input of sediment from the water column have been developed by Di Toro and co-workers and published by Di Toro (2000). These are more relevant to future development of the sediments in relation to continued formation of sulfides in the sediments. They are dependent on the rate of sedimentation which has been estimated by Bourman and Barnett (1995) and the composition (Aldridge et al., 2009). The study will not attempt to model the steady-state processes here but suggest it would be a useful exercise in the future to assist with understanding the rate of sulfide formation.

1.1.2. Modelling acidic solutes

The pore water acidity in submerged acid sulfate soils can be comprised of different solutes, typically H^+ , $Fe^{+2/+3}$, Mn^{+2} and Al^{+3} ions. The H and Fe in the first instance result from the pyrite oxidation reactions while the Mn and Al commonly are released by subsequent acid dissolution of silicate, carbonate, and oxide minerals. Dissolved

metals release acidity to solution (or consume base) by hydrolysis reactions (e.g. $\text{Fe}^{+3} + 3 \text{H}_2\text{O} = \text{Fe}(\text{OH})_{3(\text{aq})} + 3 \text{H}^+$).

The complete hydrolysis of Fe^{+3} , Fe^{+2} , Mn^{+2} and Al^{+3} will generate 3, 2, 2, and 3 protons (H^+) respectively. The establishment of hydrolysis equilibria is generally very fast and there is a general tendency for metals to precipitate as pH increases and hydrolysis begins (Stumm and Morgan 1996). For the purposes of this study we have considered the flux of individual ions contributing to acidity (Fe^{+3} , Mn^{+2} , Al^{+3} , H^+) and the sum of these ions (total acidity expressed as H^+ equivalents). In the surface water, the effect of total acidity only is considered with the implicit assumption that hydrolysis of metal ions has proceeded to completion with equivalent H^+ ions generated. Water that initially has near-neutral pH (6–7) and contains dissolved metals can have both alkalinity and acidity and ultimately could have acidic pH (<4.5) after oxidation, hydrolysis, and precipitation of Fe, Mn, and other metals (Kirby and Cravotta 2005).

1.2 Local Studies of Relevance to Acidity Transport

The initial and boundary conditions are needed for modelling for purposes, as are the parameter estimates or ranges for the sediments. A number of studies of the sediments in the lower lakes have been undertaken and these provide some, if not all, of the parameters required for the modelling.

These studies have also provided profiles and estimates of the fluxes of solutes from the sediments. These will be useful in providing comparisons with the model output. These studies are summarised below.

1.2.1. Acidity distribution and concentration in the lower lakes sediment

Fitzpatrick et al. (2008, 2009, 2010) found that the acidic horizon in the exposed sediments of the lower lakes was generally concentrated in the top 30 cm of the exposed sediment profile, although it sometimes extended deeper in sandy sediments. This indicates the depth zone for the establishment of the acidity diffusion gradient.

The studies of Fitzpatrick et al. also give guidance as to the concentration and distribution of acidity in the lower lakes sediment. The results from both exposed and submerged sediments samples are shown below in Table 1. The parameters of titratable available acidity (TAA) and retained acidity (RA, minerals such as jarosite) indicate the acidity fraction available in theory for diffusion to surface water. The sum of the RA and titratable acidity (TA) mean and maximum values in Table 1 is 5.8 and 395 mole H^+ /tonne respectively. Higher maximum TAA values (>2400 mol H^+ /tonne) have been measured in some samples in the Currency-Finniss tributary region (Fitzpatrick et al. 2009).

Sediment peeper measurements have also provided more detailed information on the acidic with depth until reaching a maximum at 15 cm to 20 cm below the sediment water interface, where they begin to decrease, reaching concentrations similar to those of the surface water in the top 2 cm. Similar results are shown for the clay sediment mecosystem experiments of Hicks et al. (2009, see Figure 2). These submerged profile acidity distributions are generally consistent with the acidity distribution in the exposed sediments.

Table 1. Laboratory data summary of pH testing and sulfate chemistry from Fitzpatrick et al. (2010).

Parameter	Description	Units	Minimum	Median	Mean	Maximum	Count
SEC	Electrical conductivity	mS/cm	0.09	2.3	2.90	17.92	707
pHw	pH in water	pH unit	2.18	7.47	7.01	11.79	707
pHFOX	pH after peroxide treatment	pH unit	1.22	2.66	3.68	8.70	707
pHincubation	pH after ageing 8 weeks	pH unit	1.6	4.21	4.74	8.28	707
pHKCl	pH in KCl	pH unit	3.15	7.34	7.42	9.81	707
SCR	Cr-reducible sulfur	%SCr	0	0.06	0.43	3.05	707
TAA	Titratable actual acidity	mole H+/tonne	0	0	4.47	270.45	707
RA	Retained acidity	mole H+/tonne	0	0	1.33	124.62	707
ANC	Acid neutralising capacity as %CaCO ₃	%CaCO ₃	0	0.41	1.36	45.07	707
NA	Net acidity	mole H+/tonne	-5859.72	10.34	123.79	1772.41	707

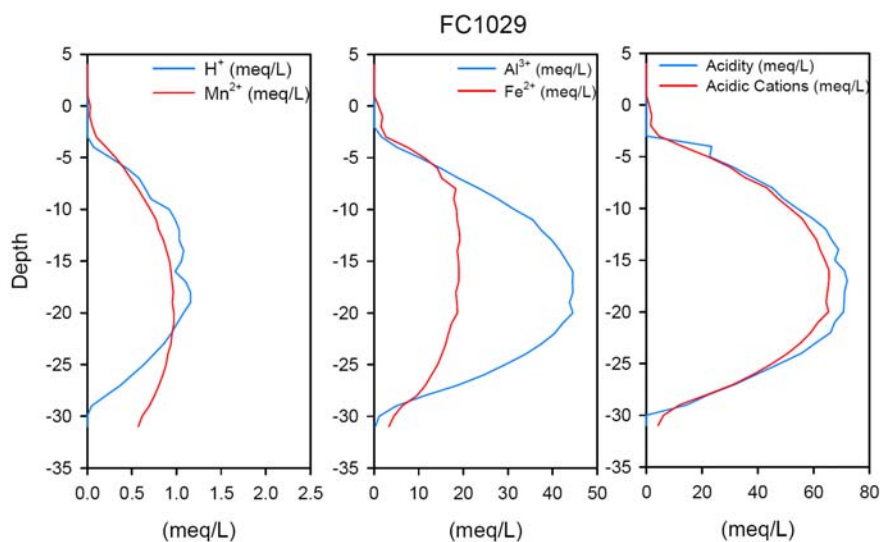


Figure 2. Example of acidity distribution in pore water from Finniss River Site FC1029 (from Fitzpatrick et al. 2011).

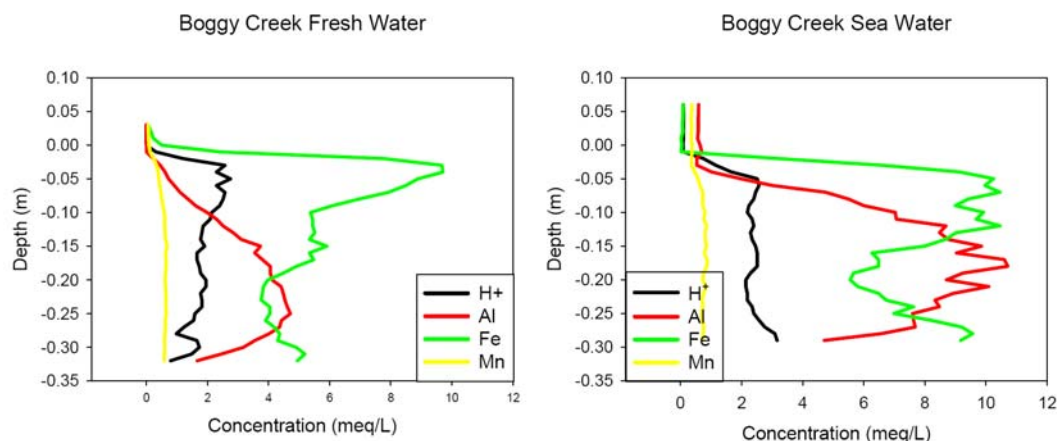


Figure 3. Example of acidity distribution within the sediments for the Boggy Creek mecosms (from Hick et al. 2009).

1.2.2. Physical properties of lower lakes sediments

The physical properties of the sediments at some sites (e.g. porosity) of the lower lakes sediment relevant to diffusion processes are found in Cook et al. (2011). Other properties such as the seepage rates can be estimated from the studies of Hipsey et al. (2010) and Hicks et al. (2009).

1.2.3. Acid flux from sediment to water

Hicks et al. (2009) used mecosm experiments and diffusion calculations to estimate sediment:water diffusion parameters and flux rates (see Table 2). The calculations predicted the measured flux for the clay soils reasonably well. The long term measured and calculated flux rates for the clay soil at Boggy Creek on Hindmarsh Island are around four times the calculated value for both treatments. At Point Sturt, Lake Alexandrina, the predicted values from applying the flux equation estimate that there will be a net flux from the overlying water into the soil. The measured values are in agreement with the direction, but are an order-of-magnitude less. A possible explanation is that sparingly soluble acid oxidation products such as natrojarosite in the near surface provide an ongoing flux of acidity. The initial flux rate is two orders of magnitude higher than the long term flux rate (Table 3).

The simulations of Cook et al. (2011), in agreement with the previous study of Hicks et al (2009), indicated that a rapid release of acidity would occur upon rewetting of the lower lakes sediments with almost no further release from the flat sandy sediments and a slow continued release from the clay peds. Cook et al. (2011) also modelled (using HYDRUS2D/3D) diffusion from the cracked and non-cracked sediments and showed that the cracking of the sediments would result in enhanced transport of acidity to the surrounding water by up to 30%.

Laboratory column experiments undertaken by Sullivan et al. (2010) found that inundation of the lower lakes sediments had the potential to have an impact on inundating water quality for up to 136 days (duration of their experiments) if diffusion is the dominant contaminant transport process operating within the sediment.

Table 2. The depth of constant concentration (D) and the concentration (C_d) used to parameterise the flux equation used by Hicks et al. (2009) to estimate the acidity flux rates.

		H ⁺		Al ³⁺		Fe ²⁺		Mn ²⁺	
		D (m)	C _d (mol m ⁻³)	D (m)	C _d (mol m ⁻³)	D (m)	C _d (mol m ⁻³)	D (m)	C _d (mol m ⁻³)
Boggy Creek clay	Fresh water	0.04	1.0	0.04	1.5	0.04	5.0	0.04	0.4
	Sea water	0.06	1.0	0.14	3.0	0.05	5.0	0.07	0.3
Point Sturt sand	Fresh water	0.19	1.0	0.50	0.03	0.11	0.50	0.17	0.004
	Sea water	0.10	0.15	0.10	0.30	0.10	0.08	0.10	0.22

Table 3. Calculated and measured flux rates (mol H⁺ m⁻² day⁻¹) from Hicks et al. (2009, Table 8). Negative values indicate flux from the soil to the water column and positive values from the water column to the soil. The range for the long term measured values is shown in brackets.

Location	Calculated			Measured	
	Acid	Alkalinity	Net		
	(Acid+ Alkalinity)				
Boggy Creek				Day 1	Day 7 -102
Fresh water	-1.5x10 ⁻²	2.2x10 ⁻³	-1.3x10 ⁻²	-1.61±0.02x10 ⁻¹	-6.0(-13 to 2)x10 ⁻³
Sea water	-1.1x10 ⁻²	2.1x10 ⁻³	-8.5x10 ⁻³	-5.3±0.05x10 ⁻¹	-22(-73 to 0)x10 ⁻³
Point Sturt				Day 1	Day 12 -100
Fresh water	-5.4x10 ⁻⁴	3.6x10 ⁻²	3.5x10 ⁻²	-1.38±0.09x10 ⁻¹	5(-3 to 19)x10 ⁻³
Sea water	-6.1x10 ⁻⁴	2.1x10 ⁻²	2.0x10 ⁻³	-2.8±0.05x10 ⁻¹	7(0 to 17)x10 ⁻³

1.2.4. Sulfate reduction/neutralisation in submerged sediments

Baker et al. (2011) analysed temporal changes in the acid distribution in the lower lakes sediment (pre- and post-reinundation). They found that neutralisation is proceeding in a slow and limited manner at many previously acidic lower lakes sites. Their results indicated that this neutralisation was driven by sulfate reduction at some sites (measured increase in CrS) and flushing of acidity from surface sediments had likely occurred.

Sullivan et al. (2011) undertook detailed sulfate reduction research and found prolonged (>6 months) inundation allowed appreciable reduction to occur in the 0 -

2.5 cm sediment layer, with rates ranging from 25 to 170 nmol g⁻¹ day⁻¹ depending on previous vegetation type (phragmites highest rates). There was limited sulfate reduction (i.e. < 10 nmol g⁻¹ day⁻¹) occurring down to the 20 cm layer in some treatments. Sulfate reduction has not been included in the modelling presented in this report but could be added to these models as a zero-order flux reaction.

2. MODELLING OF ACID FLUXES

2.1 Diffusion

First, this study considered the diffusion-only transport of acidity out of the sediments and into the overlying water column. The initial condition is considered to be described by acidity at a constant concentration of c_1 from the surface to a depth z_1 , and from z_1 to infinity the concentration is $c_2 = 0$. Obviously a value other than zero could also be chosen for c_2 . For the purposes of the modelling a very low value (other than zero) can also be chosen for c_2 and some scenarios tested below use values of $c_2 \neq 0$. The surface concentration will be taken as $c_0 = 0$. The appropriate solution in van Genuchten and Alves (1982) is their A5 solution, which is modified below for $\nu = 0$:

$$\begin{aligned} c(z,t) &= c_2 + (c_1 - c_2) A(z,t) + (c_0 - c_1) \\ A(z,t) &= \frac{1}{2} \operatorname{erfc} \left[\frac{R(z - z_1)}{2\sqrt{RDt}} \right] + \frac{1}{2} \operatorname{erfc} \left[\frac{R(z + z_1)}{2\sqrt{RDt}} \right] \\ B(z,t) &= \operatorname{erfc} \left[\frac{Rz}{2\sqrt{RDt}} \right] \end{aligned} \quad (2.1)$$

For acidity the study considered there to be no retardation, so $R = 1$. The flux from the sediments to the water column was calculated by $-Ddc/dz \approx -D(c_0 - c(z = 0.001))/(0 - 0.001)$. The modelling carried out was firstly a sensitivity analysis of how the concentration and flux varied in relation to changes in c_1 , D , and z_1 . The range of values for these parameters chosen for the sensitivity analysis is given in Table 4.

Table 4. Values of c_1 , D , and z_1 used in the sensitivity analysis. The base case is the value when this parameter is not varying.

Parameter and units	Base Case	Range
c_1 (kg m ⁻³)	10×10^{-3}	$(1-100) \times 10^{-3}$
D (m ² day ⁻¹)	5×10^{-4}	$(0.5-25) \times 10^{-4}$
z_1 (m)	0.5	0.1-1

The range of values of D chosen represent the range for molecular diffusion of Al^{3+} of $0.47 \times 10^{-4} \text{ (m}^2 \text{ day}^{-1}\text{)}$ to the maximum value for dispersion measured by Hargrave (1972) of $25 \times 10^{-4} \text{ (m}^2 \text{ day}^{-1}\text{)}$. As D increases, the relative concentration $c^* = (c - c_0)/(c_1 - c_0)$ spreads out through the sediment profile and the maximum concentration after 100 days is reduced and occurs at a greater depth in the sediment (figure 4).

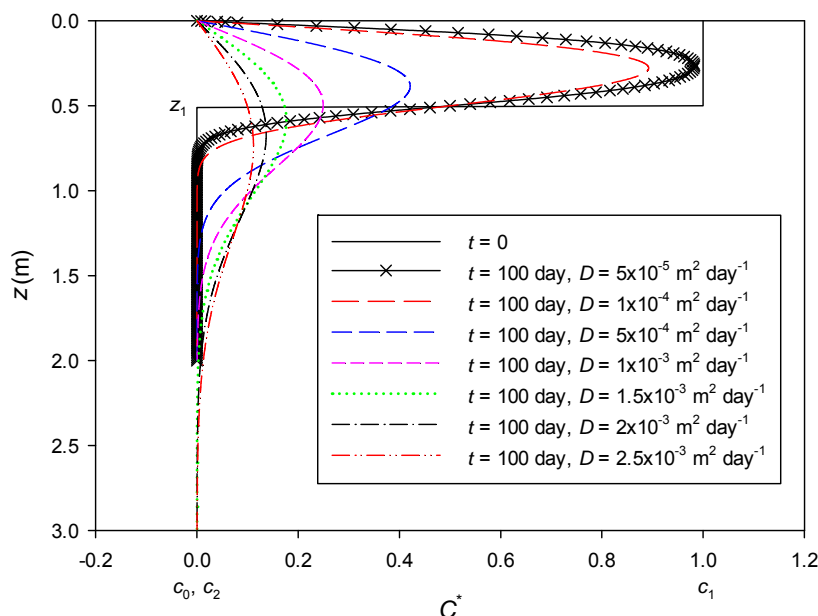


Figure 4. Relative concentration (C^*) versus depth at $t = 0$, and $t = 100$ day for a range of values of the dispersion coefficient, D . The value of $c_1 = 10 \times 10^{-3} \text{ kg m}^{-3}$, $c_2 = c_0 = 0$ and $z_1 = 0.5 \text{ m}$.

The larger dispersion coefficient results in a higher initial flux in acidity transport to the sediment (figure 5). This initial flux ranges from 5×10^{-4} to $2.5 \times 10^{-2} \text{ kg m}^{-2} \text{ day}^{-1}$ a 50 fold range.

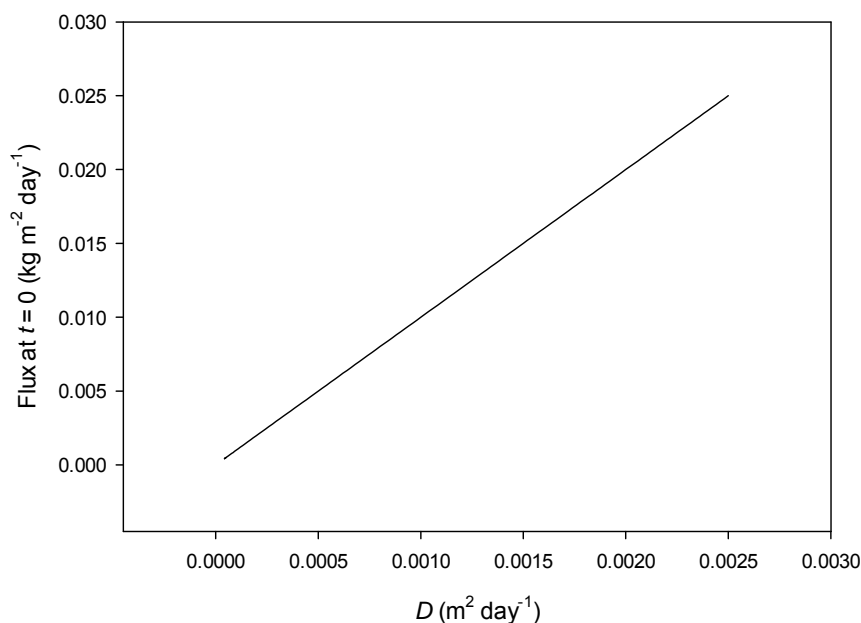


Figure 5. Initial acidity flux as a function of the dispersion coefficient (D), with $c_1 = 10 \times 10^{-3} \text{ kg m}^{-3}$, $c_2 = c_0 = 0$ and $z_1 = 0.5 \text{ m}$.

However, due to dispersion of the acidity down the sediment results in the flux decreases more rapidly with time (figure 6). Introduction of benthic organisms into the sediments, which could increase D , could result in increased initial acidity release but longer term the rate would decrease. However, although a lower dispersion coefficient results in a lower initial rate of acidity release the release of acidity to the water column will for a much longer time period.

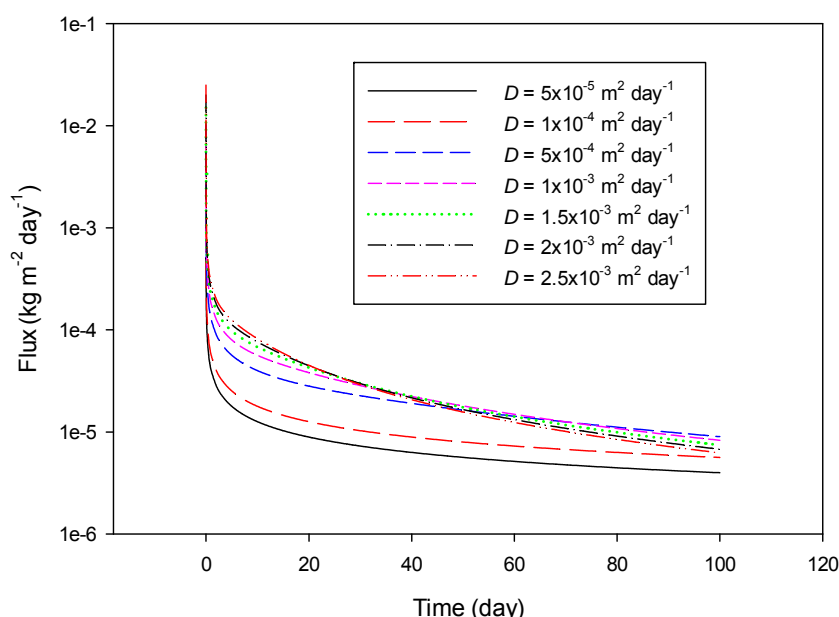


Figure 6. Flux of acidity to the water column versus time for various values of D (see legend) with $c_1 = 10 \times 10^{-3} \text{ kg m}^{-3}$, $c_2 = c_0 = 0$ and $z_1 = 0.5 \text{ m}$.

When the cumulative flux of acidity from the sediment is calculated from the integral of the flux with time we can see that even with a continual slow rate of increase the amount of acidity release after 100 days is still more for $D = 2.5 \times 10^{-3} \text{ m}^2 \text{ day}^{-1}$ than with $D = 5 \times 10^{-5} \text{ m}^2 \text{ day}^{-1}$ by a factor of 4.6 (figure 7). This has decrease significantly from the ratio of the difference at day 20 of 6.8, but will only decrease slowly from day 100 onward with time.

The depth that the acidity extends to down the profile prior to inundation indicates that the maximum concentration in the profile increases as z_1 increases, but the depth where this maximum occurs also increases (figure 8).

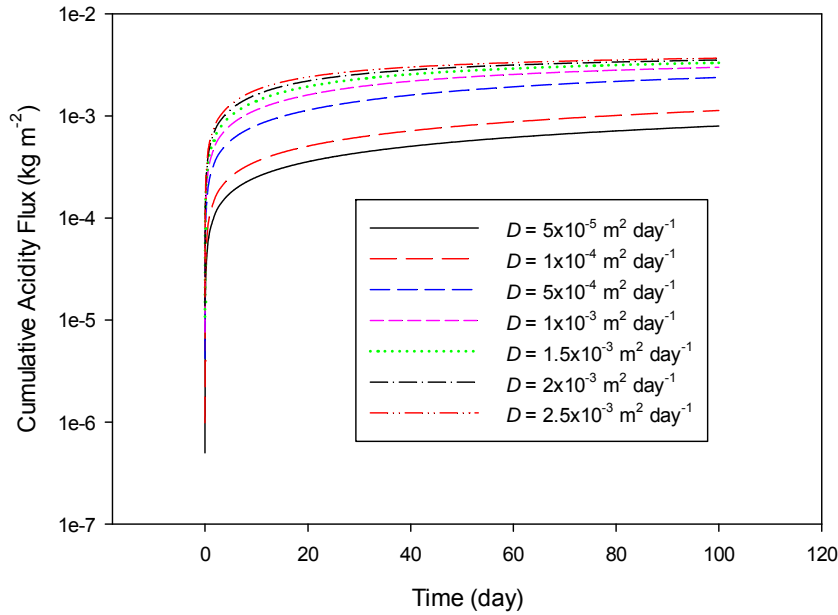


Figure 7. Cumulative acidity flux with time for various values of D (see legend) with $c_1 = 10 \times 10^{-3} \text{ kg m}^{-3}$, $c_2 = c_0 = 0$ and $z_1 = 0.5 \text{ m}$. Trapezoidal integration of the data in figure 6 was used to provide the data for this figure.

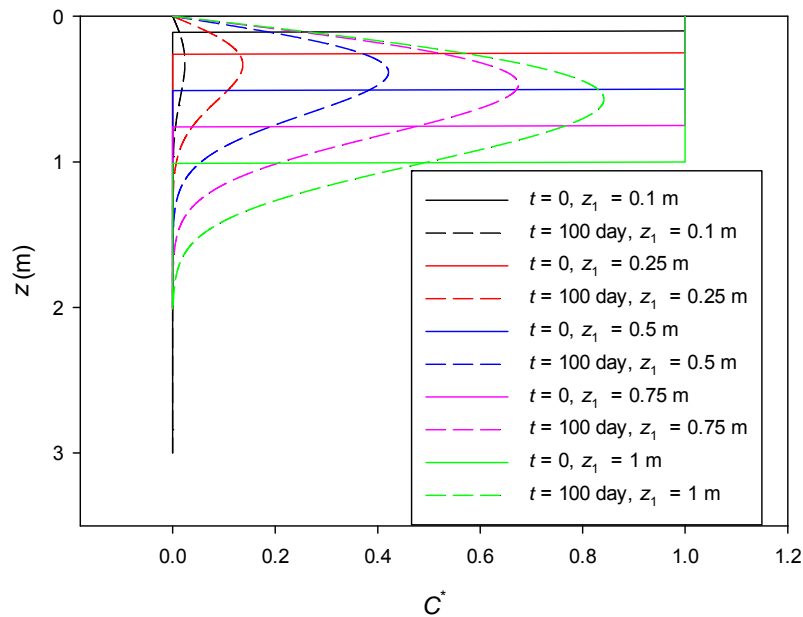


Figure 8. Relative concentration (C^*) versus depth for a range of z_1 values from 0.1 to 1 m, with $c_1 = 10 \times 10^{-3} \text{ kg m}^{-3}$, $c_2 = c_0 = 0$ and $D = 5 \times 10^{-4} \text{ m}^2 \text{ day}^{-1}$.

The increased amount of acidity still stored in the profile does not result in large increases in the flux of acidity to the water column as z_1 increases beyond approximately 0.75 m (figure 9). The rate of decrease in the flux is also decreased as z_1 increases.

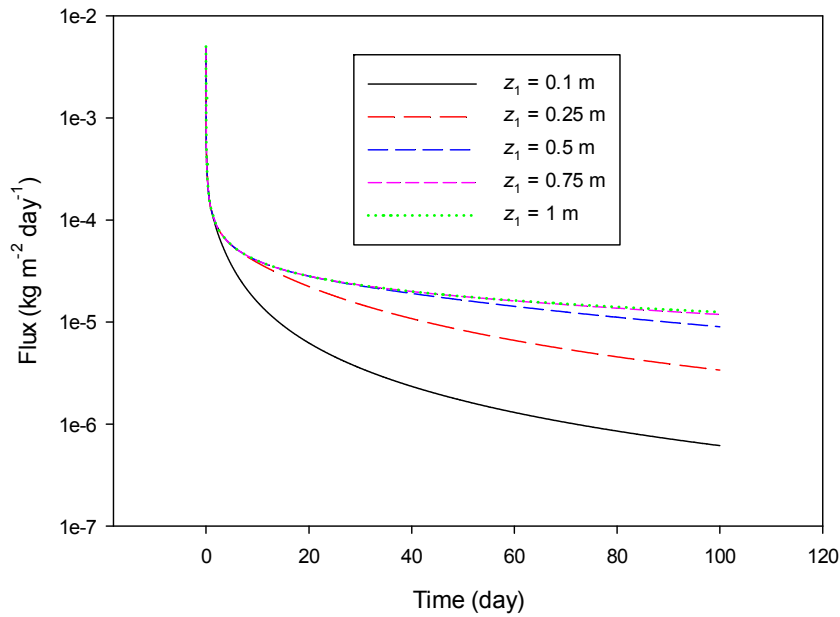


Figure 9. Flux of acidity to the water column versus time for various values of z_1 with $c_1 = 10 \times 10^{-3} \text{ kg m}^{-3}$, $c_2 = c_0 = 0$ and $D = 5 \times 10^{-4} \text{ m}^2 \text{ day}^{-1}$.

Varying the initial concentration (c_1) of the acidity results in the amount of solute left in the sediment after 100 days being greater (figure 10a). The position of the peak concentration is the same for all values of c_1 . When the relative concentration is plotted as a function of depth all these concentration profiles collapse to one profile (figure 10b).

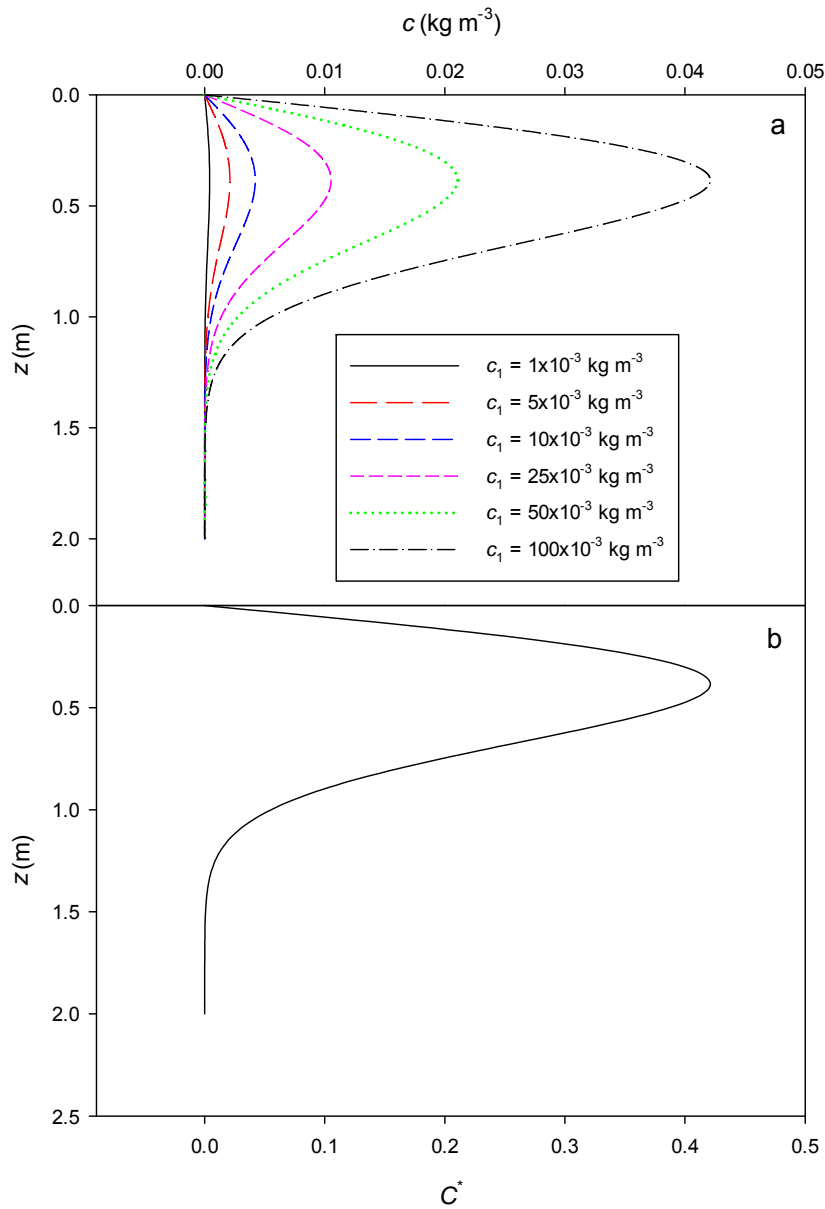


Figure 10. a) Concentration versus depth for various values of c_1 , b) relative concentration versus depth. These profiles were calculated with $z_1 = 0.5 \text{ m}$, $c_2 = c_0 = 0$ and $D = 5 \times 10^{-4} \text{ m}^2 \text{ s}^{-1}$.

The flux also increases with c_1 (figure 11a) but again when scaled with the flux at $t = 0$ the relative flux is the same for all values of c_1 (figure 11b).

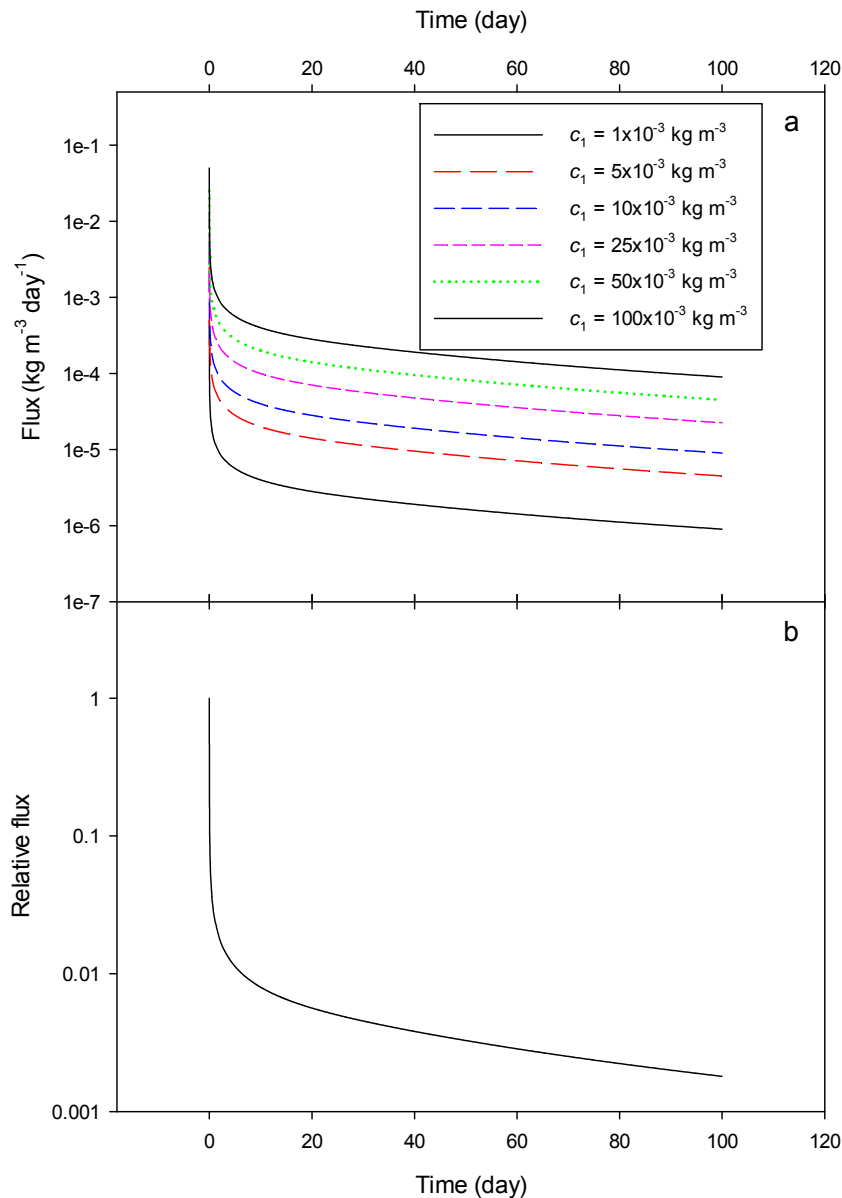


Figure 11. Flux versus time for a) various values of c_1 and b) relative flux ($\text{flux}(t)/\text{flux}(t=0)$) versus time. These fluxes were calculated with $z_1 = 0.5 \text{ m}$, $c_2 = c_0 = 0$ and $D = 5 \times 10^{-4} \text{ m}^2 \text{ day}^{-1}$.

The collapse of both the profile and fluxes when plotted in dimensionless form mean that only one computation is needed, and any others can be derived from the dimensionless form of the solution. This could be particularly useful for assessing the range of acidity profiles found in the lower lakes in terms of their relative (to each other) acidity fluxes to the water column.

2.1.1. Comparison with data from specific lower lakes sites

Hicks et al. (2009) measured the acidity profiles at four sites and this study used the profiles of H^+ , Fe^{2+} , Al^{3+} and total acidity (sum of molar equivalents for H^+ , Fe^{2+} , and Al^{3+}) to estimate the fluxes and profiles with time at these sites. The profiles were shown above for the Boggy creek site (Figure 1). The dispersion coefficient was

taken as the molecular diffusion for the species of H^+ , Fe^{2+} , Al^{3+} and the dispersion coefficient for H^+ used for the total acidity (Table 5).

Table 5. Molecular diffusion of ions in water (DiToro, 2000; Vanýsek, 1992).

Ion	$D \text{ (m}^2 \text{ day}^{-1}\text{)}$
H^+	8.06×10^{-4}
Fe^{2+}	0.61×10^{-4}
Al^{3+}	0.47×10^{-4}

Boggy Creek fresh water site

The value of z_1 at this site based on the data of Hicks et al. (2009) was assumed to be 0.4 m. The values for c_1 for total acidity, Fe^{2+} , Al^{3+} and H^+ were 12×10^{-3} , 0.22×10^{-3} , 0.24×10^{-3} and $2 \times 10^{-3} \text{ kg m}^{-3}$ respectively based on Hicks et al. (2009). The flux of acidity is seen to drop off rapidly with time during the first 100 days (figure 12). The sum of acidity flux is similar to, but not the same as, the total acidity due the lower diffusion coefficients for Fe^{2+} and Al^{3+} (Table 5) and a small contribution rounding when estimating c_1 .

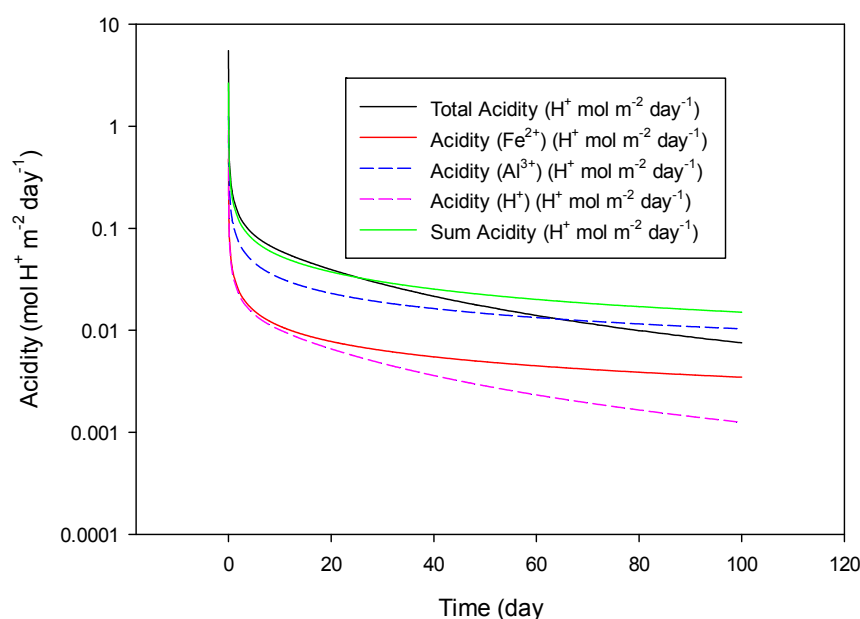


Figure 12. Acidity flux versus time from total acidity, Fe^{2+} , Al^{3+} , H^+ , and the sum of Fe^{2+} , Al^{3+} and H^+ fluxes for the Boggy Creek fresh water site.

The value for average acid flux during the first day from the total acidity is $0.39 \text{ mol H}^+ \text{ m}^2 \text{ day}^{-1}$ and from the sum of the acidities is $0.33 \text{ mol H}^+ \text{ m}^2 \text{ day}^{-1}$. These estimates of the flux are greater than, but similar to, the value of $0.161 \text{ mol H}^+ \text{ m}^2 \text{ day}^{-1}$ that Hicks et al. (2009) measured. Hicks et al. (2009) also suggested that the flux was between 13 and $2 \times 10^{-3} \text{ mol H}^+ \text{ m}^2 \text{ day}^{-1}$ for days 7 to 102 with an average flux of $6 \times 10^{-3} \text{ mol H}^+ \text{ m}^2 \text{ day}^{-1}$. The modelling suggested fluxes of 7.5 to $73 \times 10^{-3} \text{ mol H}^+ \text{ m}^2 \text{ day}^{-1}$ from the total acidity and 15 to $64 \times 10^{-3} \text{ mol H}^+ \text{ m}^2 \text{ day}^{-1}$ for the sum of the acidities with the average flux of 22 and $25 \times 10^{-3} \text{ mol H}^+ \text{ m}^2 \text{ day}^{-1}$ for the total acidity and sum of the acidities respectively. Again the modelled fluxes are greater

than the measured flux but we have not considered the effect of advection on the flux or tortuosity on the dispersion coefficient.

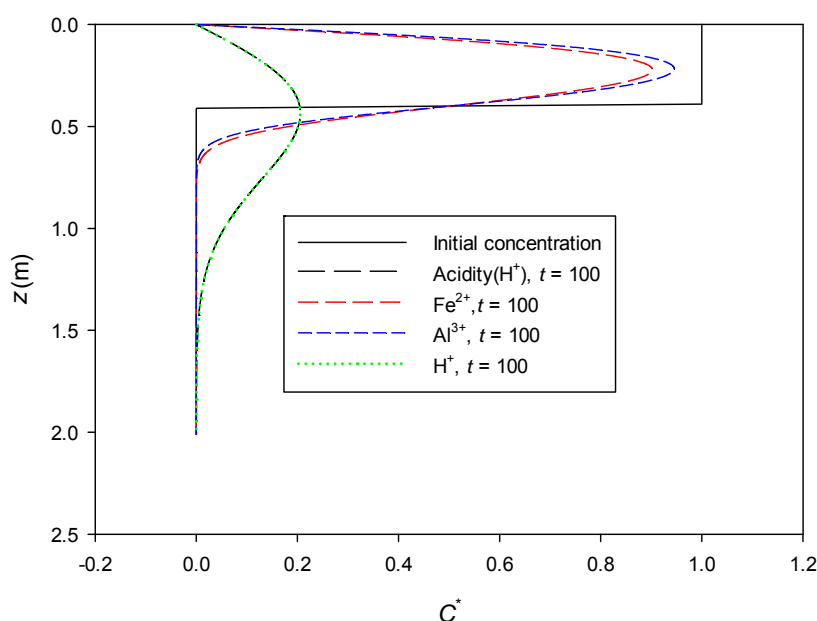


Figure 13. Initial dimensionless concentration (C^*) and concentration of the ions after 100 days for the Boggy Creek fresh water site.

The flux based on either total acidity or sum of the acidity are initially similar but start to diverge as time increases. This is due to the lower diffusion coefficient for Fe^{2+} and Al^{3+} which mean that these ions are not as readily diffused down into the sediments (figure 13) and their flux to the water column does not decrease as quickly (figure 12).

Boggy Creek salt water site

The value of z_1 at this site based on the data of Hicks et al. (2009) was assumed to be 0.4 m except for Al^{3+} where $z_1 = 0.32$ m was used. The values for c_1 for total acidity, Fe^{2+} , Al^{3+} and H^+ were 19×10^{-3} , 1.0, 0.065 and $2 \times 10^{-3} \text{ kg m}^{-3}$ respectively, based on Hicks et al. (2009). At this site the contribution of H^+ to the acidity was negligible and was not modelled. The flux of acidity is seen to drop off rapidly with time during the first 100 days (figure 14). The flux based on the sum of acidities is similar to, but not the same as, the total acidity, due to rounding when estimating c_1 and due to the different diffusion coefficients for the H^+ , Fe^{2+} and Al^{3+} (Table 5).

The modelled average flux during the first day was 0.62 and $0.91 \text{ mol m}^{-2} \text{ day}^{-1}$ from total acidity and sum of the acidities respectively; this is greater than but close to that measured by Hicks et al. (2009) of $0.53 \text{ mol m}^{-2} \text{ day}^{-1}$. The flux from day 7 to 102 measured by Hicks et al. (2009) of 0.073 to $0 \text{ mol m}^{-2} \text{ day}^{-1}$ (mean of $0.022 \text{ mol m}^{-2} \text{ day}^{-1}$) is less than modelled flux range of 0.11 to $0.012 \text{ mol m}^{-2} \text{ day}^{-1}$ from total acidity from total acidity and 0.18 and $0.045 \text{ mol m}^{-2} \text{ day}^{-1}$ from sum of the acidities. The modelled mean flux was 0.034 and $0.073 \text{ mol m}^{-2} \text{ day}^{-1}$, again greater than that measured by Hicks et al. (2009). The ratio of the over estimation by the modelling for both the fresh water and salt water of the average fluxes is in a similar range of 2 to 4 for the fresh water site and 1 to 3 for the salt water site. This would suggest that there

is not an increase in the flux due to the use of salt (sea) water beyond that due to the different initial concentrations of the acidity at these sites.

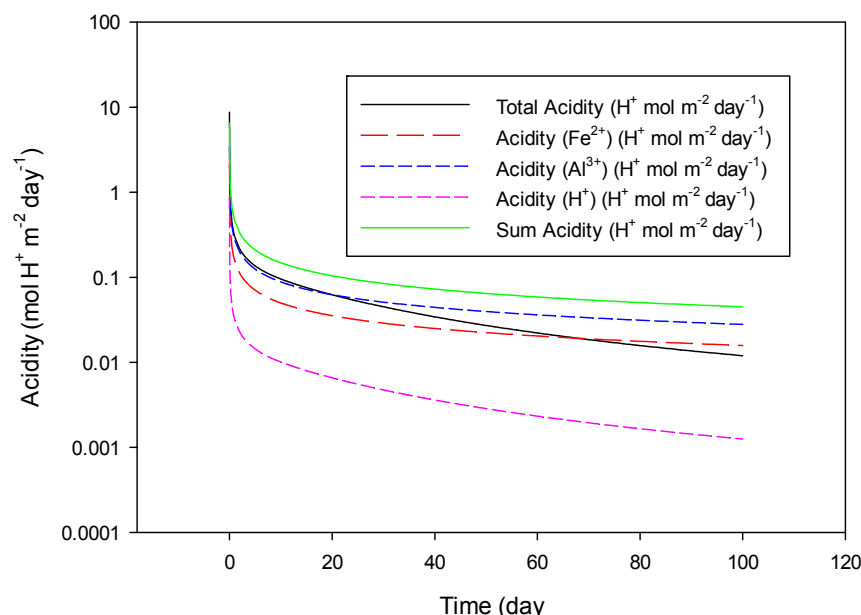


Figure 14. Acidity flux versus time from total acidity, Fe²⁺, Al³⁺, H⁺, and the sum of Fe²⁺, Al³⁺ and H⁺ fluxes for the Boggy Creek salt water site.

The flux from the sum of the acidity is now greater than the flux calculated from the total acidity, apart from initially when the fluxes are similar. This is because the total acidity is now dominated by Fe²⁺ and Al³⁺ and the diffusion coefficient for H⁺ which is greater than that for Fe²⁺ and Al³⁺ was used in calculating the acidity flux for the total acidity. This use of the H⁺ diffusion coefficient results in the acidity diffusing further down the soil profile than the Fe²⁺ and Al³⁺ (figure 15) resulting in the difference in the acidity flux when the total acidity is used rather than the sum of the acidities.

The salt water site results in both a higher initial and continuing acidity flux to the water column than was estimated for the fresh water site. This is most likely due to the acidity being dominated by Fe²⁺ and Al³⁺. The modelled increase was also found by Hicks et al. (2009) in the measured flux (Table 3).

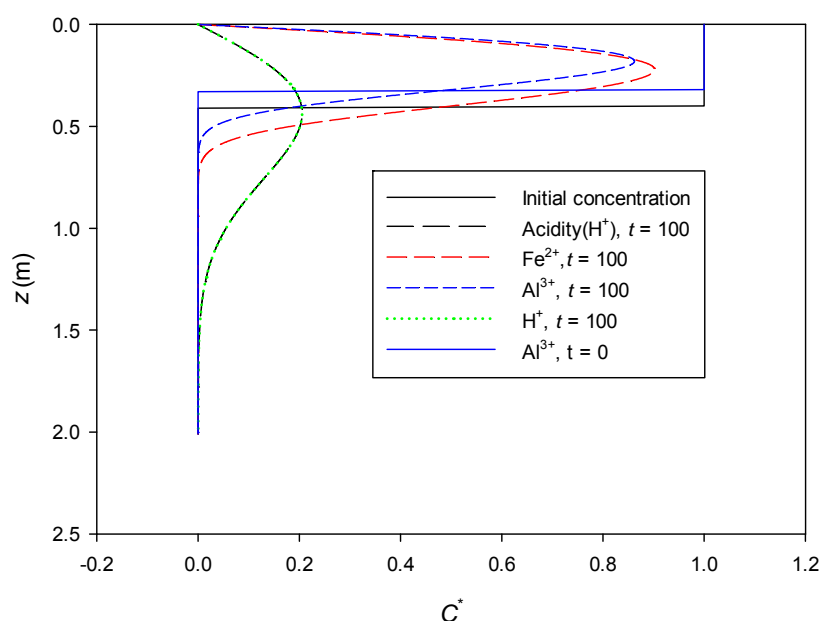


Figure 15. Initial dimensionless concentration (C^*) and concentration of the ions after 100 days for the Boggy Creek salt water site.

Point Sturt fresh water site

The value of z_1 at this site based on the data of Hicks et al. (2009) was difficult to estimate, as the acidity had not diminished by maximum depth (0.35 m) in figure 30 of Hicks et al. (2009), so two values 0.4 and 1 m were used in the calculations. This site had very little acidity associated with Fe^{2+} and Al^{3+} so modelling was not carried out for these ions.

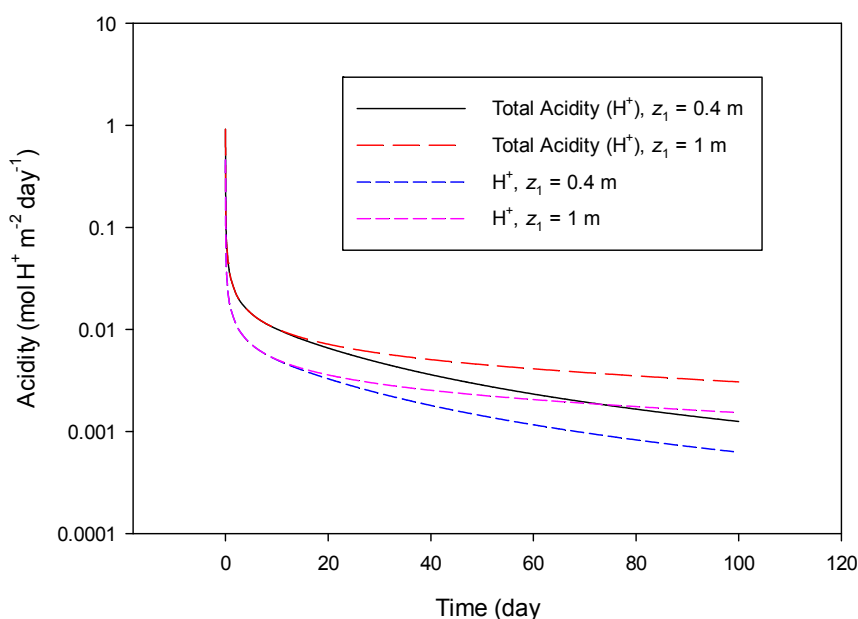


Figure 16. Acidity flux versus time from total acidity and H^+ for the Point Sturt fresh water site. The fluxes were calculated using two different values of z_1 of 0.4 and 1 m. and the sum of Fe^{2+} , Al^{3+} and H^+ fluxes.

Based on Hicks et al. (2009), the value for c_1 for acidity (H^+), was 2×10^{-3} and for H^+ was $1 \times 10^{-3} \text{ kg m}^{-3}$. The flux of acidity is seen to drop off rapidly with time during the first 100 days (figure 16). The effect of the z_1 is only seen after about 15 days when the larger value of z_1 results in larger fluxes being calculated.

Hicks et al. (2009) measured the average acidity flux from this site as $0.138 \text{ mol m}^{-2} \text{ day}^{-1}$ for the first day. Our modelling suggested the flux of acidity to be $0.065 \text{ mol m}^{-2} \text{ day}^{-1}$ for the first day which is an underestimate. It is unlikely that this is due to the effect of the value of z_1 as the same average flux over the first day was calculated for both values of z_1 . However, increasing the dispersion coefficient to being greater than the diffusion coefficient for H^+ , or increasing the initial concentration, could increase the acidity flux during this first day (see figures 7 and 11).

For the period from 12 to 100 days Hicks et al. (2009) measured the flux of acidity to range from 3 to $-19 \times 10^{-3} \text{ mol m}^{-2} \text{ day}^{-1}$ (here negative indicates a flux into the sediment), while we model the flux over the same period to be from 3 to $9 \times 10^{-3} \text{ mol m}^{-2} \text{ day}^{-1}$ when $z_1 = 1 \text{ m}$ and from 1×10^{-3} to $9 \times 10^{-3} \text{ mol m}^{-2} \text{ day}^{-1}$ when $z_1 = 0.4 \text{ m}$. The measured average flux in this period to be $-5 \times 10^{-3} \text{ mol m}^{-2} \text{ day}^{-1}$ while the modelled average flux was 3 and $5 \times 10^{-3} \text{ mol m}^{-2} \text{ day}^{-1}$ for $z_1 = 0.4 \text{ m}$ and $z_1 = 1 \text{ m}$ respectively. We cannot model directly the flux of alkalinity into the sediment with the modelling approach used here, so although we are able to show that the flux decreases rapidly we cannot show a net alkalinity as Hicks et al. (2009) measured.

The larger value of z_1 results in a higher concentration of H^+ closer to the sediment surface which results in the increased flux (figure 17).

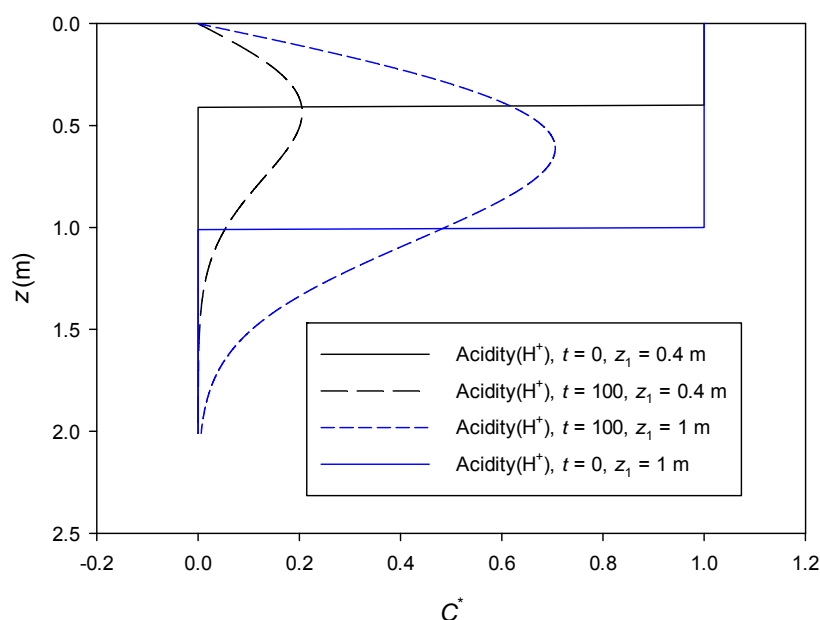


Figure 17. Dimensionless concentration (C^*) versus depth for $t = 0$ and $t = 100$ day for $z_1 = 0.4$ and 1 m for the Point Sturt fresh water site.

Point Sturt salt water site

The profile at this site is more complicated than at the previous sites, so a number of modelling runs were done for each ion (Table 6).

Table 6. Settings for c_1 , c_2 and z_1 for the modelling runs for Point Sturt salt water site.

Ion	c_1 (kg m ⁻³)	c_2 (kg m ⁻³)	z_1 (m)
Acidity	6×10^{-3}	0	0.4
	10×10^{-3}	0	1
	5×10^{-3}	15×10^{-3}	0.27
Fe ²⁺	0.17	0	0.4
	0.34	0	1
	0	1	0.15
Al ³⁺	0.16	0	0.4
	0.38	0	1
	0.081	0.405	0.27
H ⁺	2×10^{-3}	0	0.4
	2×10^{-3}	0	1

The results show that the effect of the total acidity, Fe²⁺ and Al³⁺ being deeper in the profile has an effect on the flux of acidity to the water column (figure 18). For the total acidity this results in the flux remaining almost constant with time after the initial decrease in the first 10 days (figure 18a). For Fe²⁺ the inclusion of a large source of acidity at depth and none in the top 0.15 m of sediment results in a rise in the acid flux from this source during the first 60 days and a flux at 100 days similar to that if the source was considered closer to the surface but extending to 1 m in depth (figure 18b). The inclusion of a deeper source of acidity by contrast has little effect on the modelled acidity flux to the water column from this source (figure 18c). Modelling the acidity due to the H⁺ ion, with the source occurring to a greater depth, results in a lower rate of decrease in acidity flux to the water column after about 20 days (figure 18d).

The modelled flux from the sediment using the total acidity scenarios gives an average flux during the first day of between 486 and 196×10^{-3} mol m⁻² day⁻¹ depending on which scenario (Table 6) was used. The modelled average flux is greater than the measured flux of 2.8×10^{-3} mol m⁻² day⁻¹ by Hicks et al. (2009) by more than an order of magnitude. The modelled flux from days 12 to 100 were in the range of 72 to 4×10^{-3} mol m⁻² day⁻¹ compared to the measured flux range of 0 to -17×10^{-3} mol m⁻² day⁻¹. Again the measured flux was a net flux of alkalinity into the sediment, while the modelled fluxes are of a flux of acidity to the water column. The high infiltration rate and advection at this site will have contributed to the disparity between the modelled and measured fluxes. This will be examined a bit more below when advection is included in the modelling as fluxes are likely to be reduced due to solutes being advected away from the sediment:water interface.

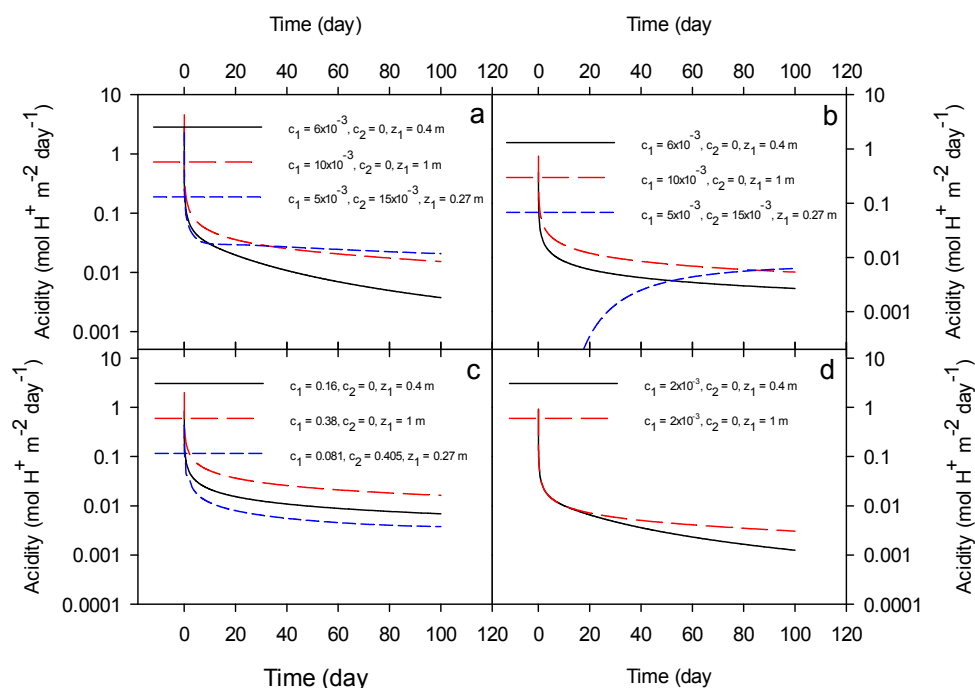


Figure 18. Acidity fluxes from the sediment to the water column with time for; a) total acidity, b) Fe^{2+} , c) Al^{3+} and d) H^+ , for the scenarios in Table 6 for the Point Sturt salt water site.

When the ions are concentrated near the surface, the concentration profiles are similar to those above (figures 13, 15, 17) for total acidity, Fe^{2+} , Al^{3+} and H^+ . The concentration profiles when the ions are concentrated deeper in the profile show the depletion of ions due to diffusion to the water column near the surface but there is still a large concentration at depth in the profile (figure 19). This is especially the case for both Fe^{2+} and Al^{3+} which have lower diffusion coefficients than H^+ , with the depth of depletion after 100 days for the former being approximately 0.5 m (figure 19b) while for the latter this was about 1.5 m (figure 19a).

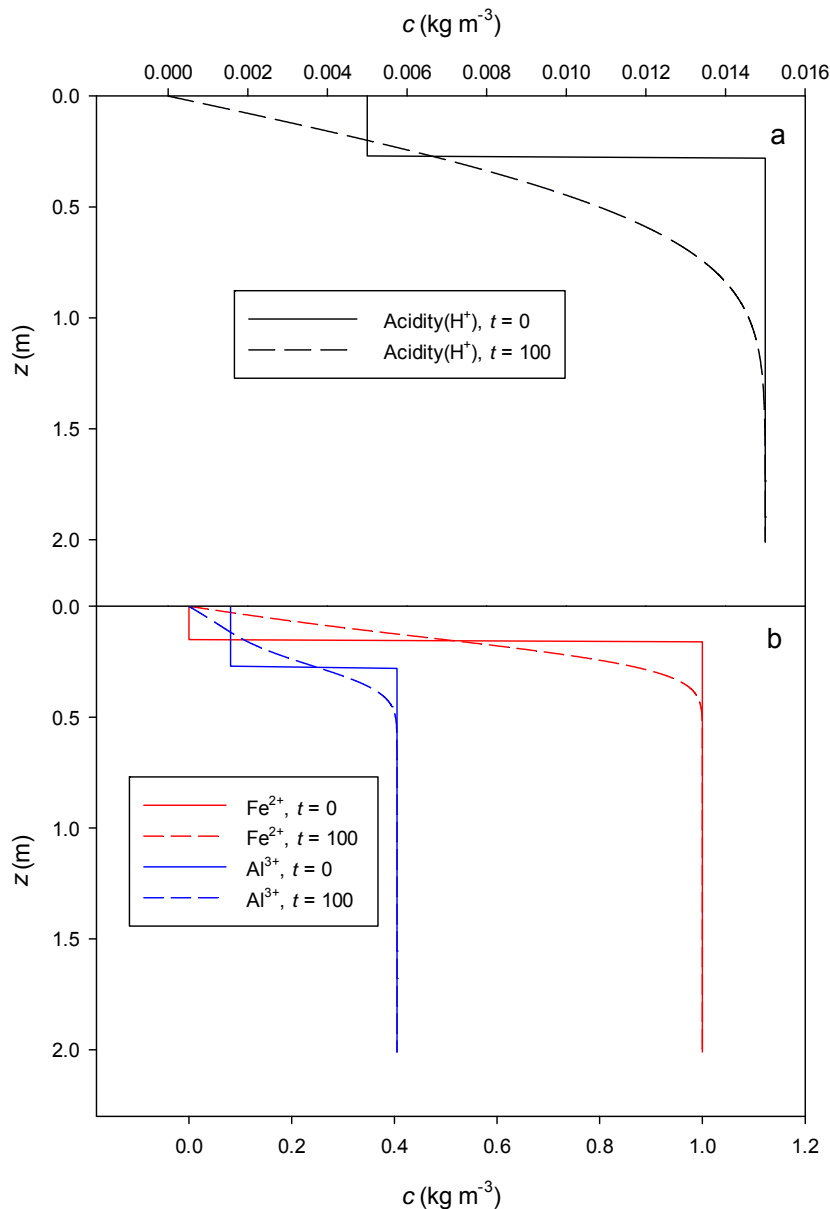


Figure 19. Concentration profiles for a) total acidity and b) Fe²⁺ and Al³⁺ for modelling scenarios where $c_2 > 0$ (Table 6) for the Point Sturt salt water site.

Sediment profiles where the acidic ions are concentrated in the lower part of the sediment profile could constitute a greater risk of acidic fluxes continuing, albeit at a low rate for a considerable period of time. Also the introduction of benthic organisms into such sediments with a concomitant increase in the dispersion coefficient, could result in an increase in the flux of acidity to the water column, until a new equilibrium is reached.

2.2 Advection Plus Diffusion

Now we will consider both advection and diffusion as the processes causing the transport of acidity in the sediments. When the pore water velocity (v) is positive the

water flow is into the sediment from the water column. This will tend to decrease the flux of acidity out of the sediments as only diffusion will be driving this flux and advection will move the acidic ions further down into the sediments. The data of Hicks et al. (2009) provides four sites where measurements of v and the acidity flux were made and these will be used to compare with the modelled fluxes. Hipsey et al. (2010) estimated the seepage rate to the lakes and using this we calculated the pore water velocities to be -2.8×10^{-5} and -2.1×10^{-5} m day $^{-1}$ for sandy and clayey sediments respectively.

Again solution A5 in van Genuchten and Alves (1982) is used but now with velocity included:

$$\begin{aligned}
 c(z, t) &= c_2 + (c_1 - c_2) A(z, t) + B(c_0 - c_1) \\
 A(z, t) &= \frac{1}{2} \operatorname{erfc} \left[\frac{R(z - z_1)}{2\sqrt{RDt}} \right] + \frac{1}{2} \exp \left(\frac{vz}{D} \right) \operatorname{erfc} \left[\frac{R(z + z_1)}{2\sqrt{RDt}} \right] \\
 B(z, t) &= \frac{1}{2} \operatorname{erfc} \left[\frac{Rz - vt}{2\sqrt{RDt}} \right] + \frac{1}{2} \exp \left(\frac{vz}{D} \right) \operatorname{erfc} \left[\frac{Rz + vt}{2\sqrt{RDt}} \right]
 \end{aligned} \tag{2.2}$$

For acidity we consider the retardation, R , to not occur, so $R = 1$. The flux from the sediments to the water column was calculated by $-Ddc/dz \approx -D(c_0 - c(z = 0.001)) / (0 - 0.001)$. The modelling carried out was firstly a sensitivity analysis of the effect of concentration and flux to c_1 , D , v and z_1 . The range of values for these parameters chosen for the sensitivity analysis is given in Table 7.

Table 7. Values of c_1 , D , v and z_1 used in the sensitivity analysis. The base case is the value when this parameter is not varying.

Parameter and units	Base Case	Range
c_1 (kg m $^{-3}$)	10×10^{-3}	$(1-100) \times 10^{-3}$
D (m 2 day $^{-1}$)	5×10^{-4}	$(0.5-25) \times 10^{-4}$
z_1 (m)	0.5	0.1-1
V (m day $^{-1}$)	1×10^{-2}	-1×10^{-5} to 4×10^{-2}

The justification for the range of values of D , c_1 and z_1 was given above and velocities by the range of seepage values from Hipsey et al. (2011) and the infiltration data from Hicks et al. (2009) discussed above.

Hipsey (2010) estimated the seepage rate to the lakes as $0.4 \text{ m}^3 \text{ day}^{-1}$. Assuming a 1 m wide strip at the lake edge and radii of the Lakes of 14.3 km for Lake Alexandrina and 7.4 km for Lake Albert the discharge rate was estimated to be 7.0×10^{-6} and $1.1 \times 10^{-5} \text{ m day}^{-1}$ respectively. The latter figure was then used along with the porosity values from Cook et al (2011) of $0.4 \text{ m}^3 \text{ m}^{-3}$ for the sandy sediments and $0.6 \text{ m}^3 \text{ m}^{-3}$ to calculate the pore water velocities. For case where the advection

was into the sediments the pore water velocity was taken from data by both Hicks et al. (2009) and Cook et al. (2011) to give the range of v in Table 7.

Increasing D results in the spreading out of the concentration but now due the advection of the solute the peak of the concentration occurs deeper in the soil (figure 20) and is not centred on the position of the initial peak as in the diffusion only case (figure 4). The peak has now been advected more than 1 m down the profile.

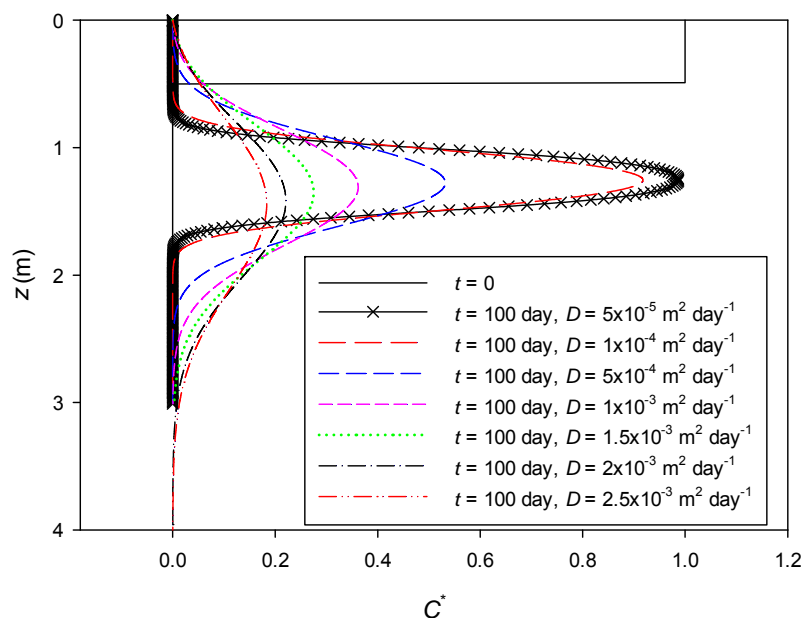


Figure 20. Relative concentration (C^*) versus depth at $t = 0$, and $t = 100$ day for a range of values of the dispersion coefficient, D . The value of $c_1 = 10 \times 10^{-3} \text{ kg m}^{-3}$, $c_2 = c_0 = 0$, $v = 1 \times 10^{-2} \text{ m day}^{-1}$ and $z_1 = 0.5 \text{ m}$.

Now both the effect of dispersion and advection means that the acidity flux decreases more rapidly with time (figure 21) compared with just diffusion alone (figure 13). This means if advection is considered as being into the sediments as in this modelling then the risk posed by the introduction of benthic organisms of causing an initial acidity spike in acidity is reduced. Now when high dispersion is combined with advection there is a very rapid decrease in acidity flux from the sediments (figure 21).

As with the case of diffusion-only and no advection the depth that the acidity extends down the profile prior to inundation indicates that this will result in the maximum concentration in the profile increasing as z_1 increases but the depth where this maximum occurs also increases (figure 22). The peak position is now shifted down the profile due to both the centre of where the mass was initially and additionally due to advection (figure 22).

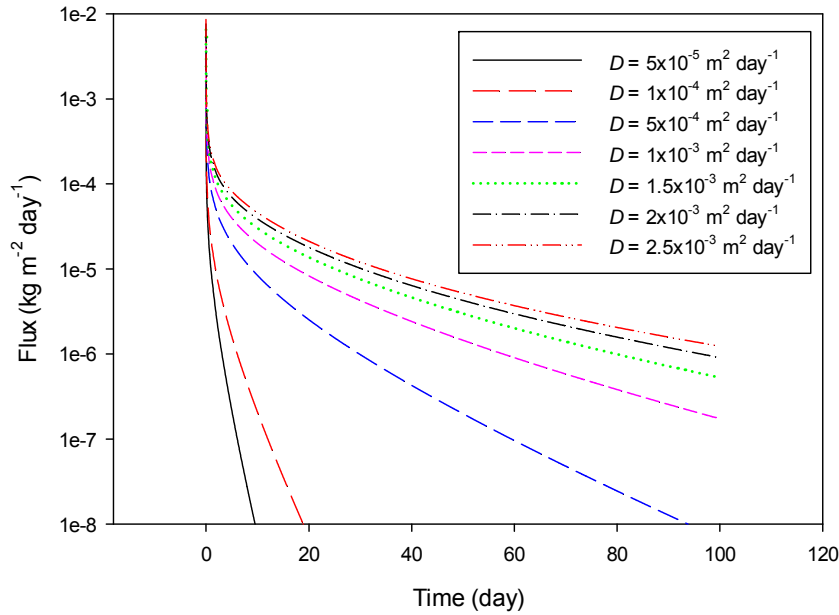


Figure 21. Flux of acidity to the water column versus time with $c_1 = 10 \times 10^{-3} \text{ kg m}^{-3}$, $c_2 = c_0 = 0$, $v = 1 \times 10^{-2} \text{ m day}^{-1}$ and $z_1 = 0.5 \text{ m}$.

Again the increased amount of acidity still stored in the profile due to the greater value of z_1 does not result in large increases in the flux of acidity to the water column as z_1 increases beyond approximately 0.5 m (figure 23). This depth at which the effect of z_1 on the flux is small is less than the 0.75 m for the diffusion only case due to advection of the solute peak down the sediment profile. The advection of the solute mass down the sediment profile means that the initial extent of acidity in does not have a large effect on the acid flux. We will examine the effect of the direction of the advection on the modelled acidity flux below.

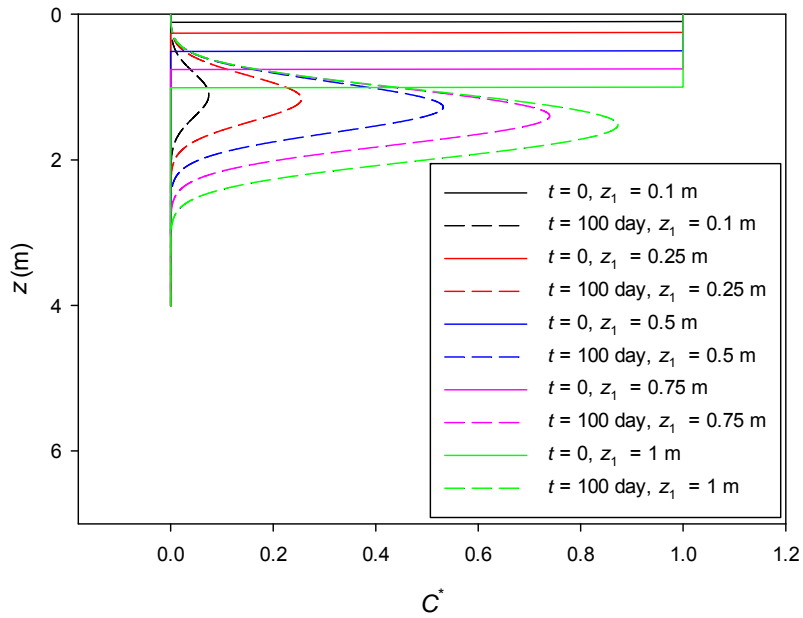


Figure 22. Relative concentration (C^*) versus depth for a range of z_1 values from 0.1 to 1 m, with $c_1 = 10 \times 10^{-3} \text{ kg m}^{-3}$, $c_2 = c_0 = 0$, $v = 1 \times 10^{-2} \text{ m day}^{-1}$ and $D = 5 \times 10^{-4} \text{ m}^2 \text{ day}^{-1}$.

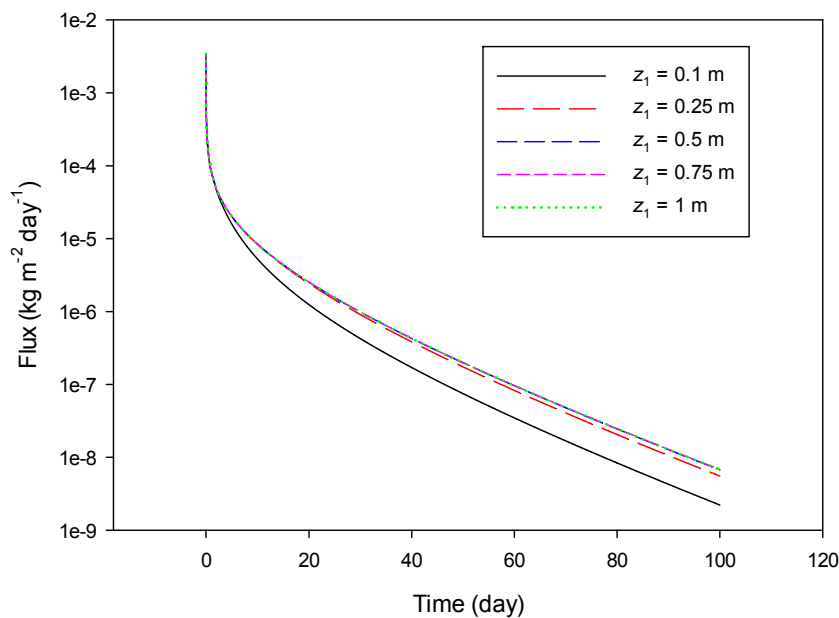


Figure 23. Flux of acidity to the water column versus time for various values of z_1 with $c_1 = 10 \times 10^{-3} \text{ kg m}^{-3}$, $c_2 = c_0 = 0$, $v = 1 \times 10^{-2} \text{ m day}^{-1}$ and $D = 5 \times 10^{-4} \text{ m}^2 \text{ day}^{-1}$.

Varying the initial concentration (c_1) of the acidity results in the amount of solute left in the sediment after 100 days being greater (figure 24a). The peak concentration is

greater than that found when only diffusion was used as the transport mechanism (figure 10a), as the peak is now shifted down the sediment profile and the flux is now less (figure 25 cf figure 11). The position of the peak concentration is again the same for all values of c_1 , so when the relative concentration is plotted as a function of depth all these concentration profiles collapse to one profile (figure 24b).

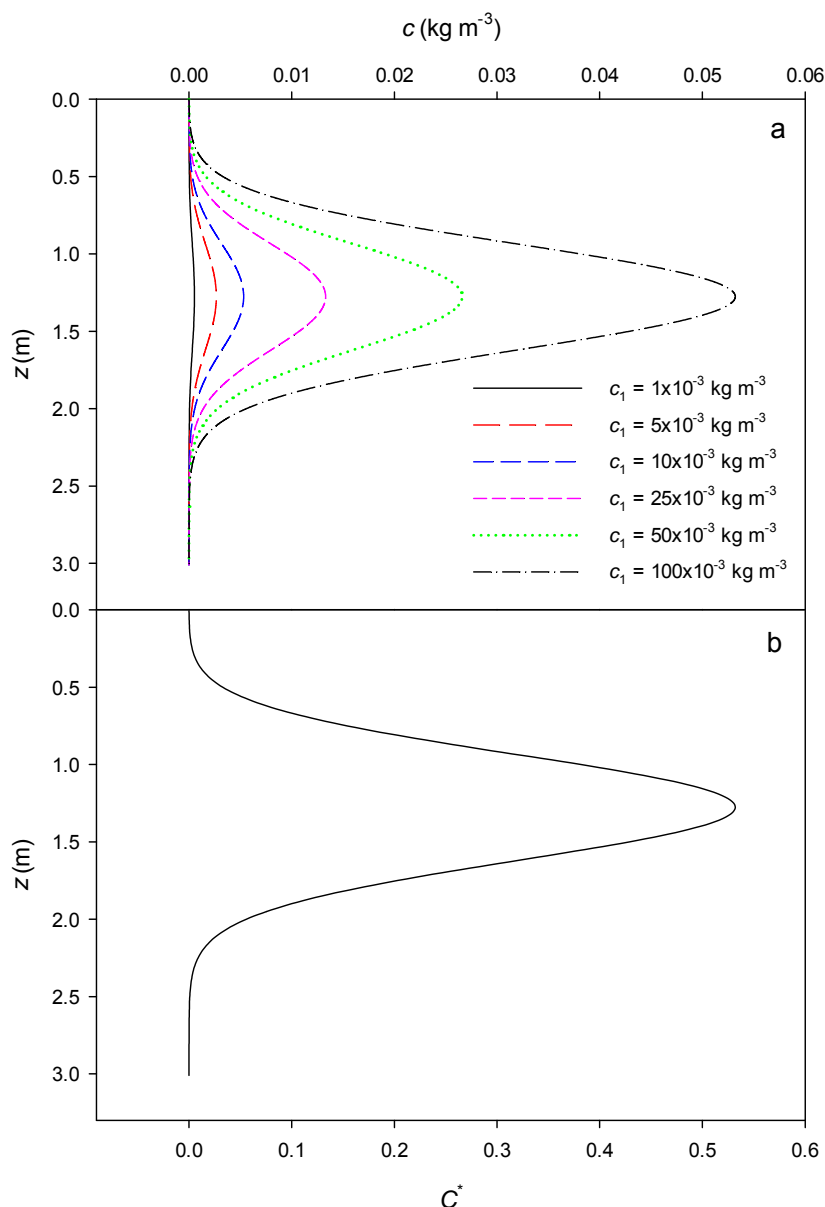


Figure 24. a) concentration versus depth for various values of c_1 , b) relative concentration versus depth. These profiles were calculated with $z_1 = 0.5 \text{ m}$, $c_2 = c_0 = 0$, $v = 1 \times 10^{-2} \text{ m day}^{-1}$ and $D = 5 \times 10^{-4} \text{ m}^2 \text{ day}^{-1}$.

The flux also increase with c_1 (figure 25) but now shows a continuing decrease with time, compared to the diffusion only case where the flux flattens out with time (figure 11a). This is due to advection moving the solute front down the sediment profile.

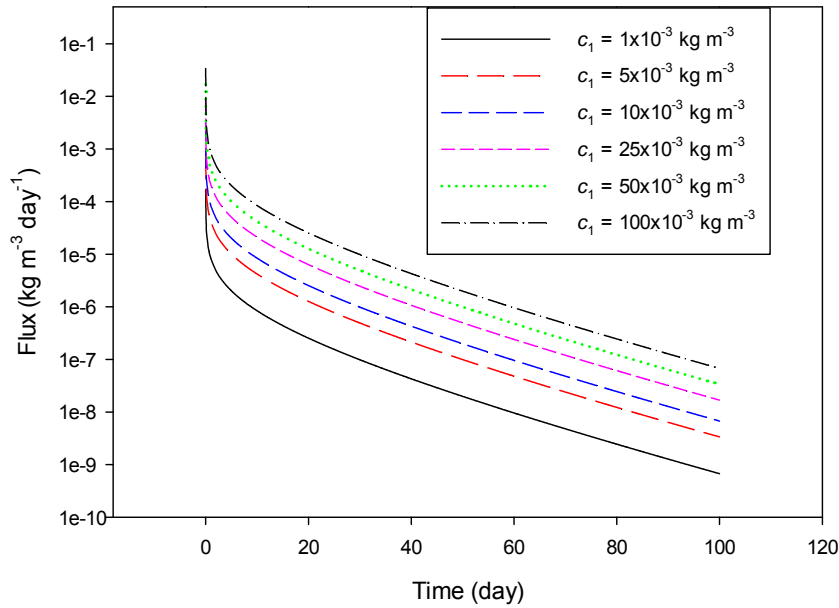


Figure 25. Flux versus time for various values of c_1 and with $z_1 = 0.5$ m, $c_2 = c_0 = 0$, $v = 1 \times 10^{-2}$ m day $^{-1}$ and $D = 5 \times 10^{-4}$ m 2 day $^{-1}$.

The sensitivity of the modelled acidity fluxes to the velocity is not great with the small seepage velocities ($v = -1$ to -10×10^{-5} m day $^{-1}$) and even the smallest infiltration flux ($v = 1 \times 10^{-3}$ m day $^{-1}$) (figure 26). However, with the negative values of v the solutes (figure 27) are now pushed up toward the surface and so the flux remains between 1 and 10×10^{-5} kg m 2 day $^{-1}$ for most of the 100 days, while the fluxes were shown to fall rapidly with time when the $v > 1 \times 10^{-3}$ m day $^{-1}$.

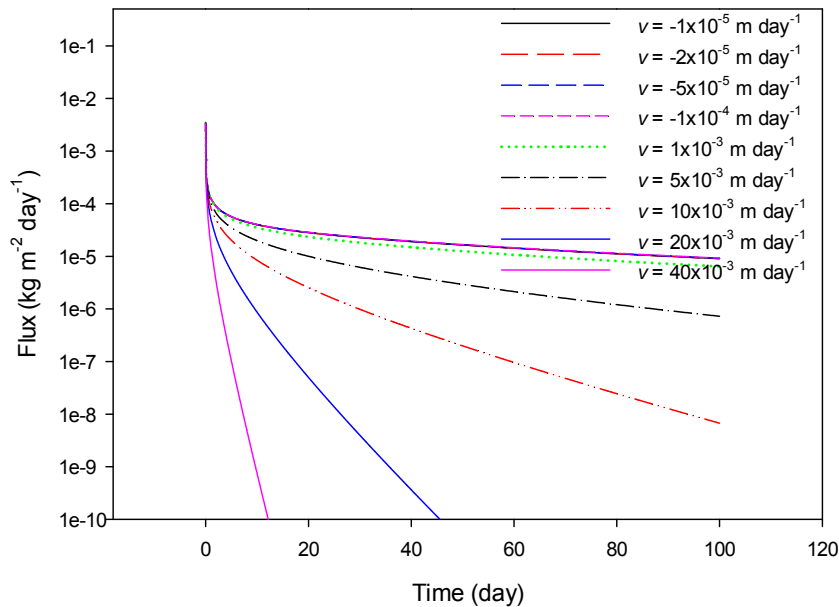


Figure 26. . Flux versus time for various values of v and with $z_1 = 0.5$ m, $c_2 = c_0 = 0$, $c_1 = 1 \times 10^{-2}$ kg m $^{-3}$ and $D = 5 \times 10^{-4}$ m 2 day $^{-1}$.

This difference in the solute profiles is dramatic, with the peak in concentration at approximately 0.5 m when $v < 0$ and below 4 m when $v > 40 \times 10^{-3} \text{ m day}^{-1}$. This illustrates that the process by which the sediments wet up will be critical to the acid fluxes that will occur. When infiltration occurs from the top of the sediment profile, the solutes will be pushed down the sediment profile and acidity flux will be restricted. However, if the sediments are wetted by a slow rise in the groundwater level, the opposite will occur and upon inundation high initial fluxes of acidity could occur.

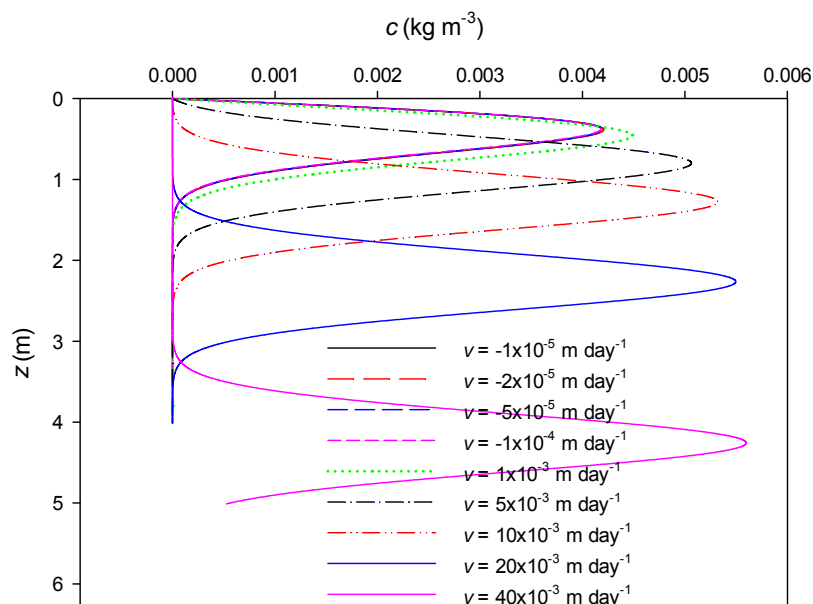


Figure 27. Concentration versus depth for various values of v , with $z_1 = 0.5 \text{ m}$, $c_2 = c_0 = 0$, $c_1 = 1 \times 10^{-2} \text{ kg m}^{-3}$ and $D = 5 \times 10^{-4} \text{ m}^2 \text{ day}^{-1}$.

2.2.1 Comparison with data from specific lower lakes sites

Hicks et al. (2009) measured the acidity profiles at four sites and we will use the profiles of H^+ , Fe^{2+} , Al^{3+} and acidity to estimate the fluxes and profiles with time at these sites. The profiles were shown above for the Boggy creek site (figure 3). The dispersion was taken as the molecular diffusion for the species of H^+ , Fe^{2+} , Al^{3+} and total acidity was assumed to be H^+ (Table 5). The advection velocity was taken as the infiltration from Hicks et al. (2009) or the seepage rate from Hipsey et al. (2010) and the values for the four sites given in Table 8.

Table 8. Pore water velocities for the four sites from Hicks et al. (2009).

Site	$v \text{ (m day}^{-1}\text{)}$
Boggy Creek fresh water	1.6×10^{-3}
Boggy Creek salt water	1.6×10^{-3}
Point Sturt fresh water	1.6×10^{-2}
Point Sturt salt water	2.8×10^{-2}

Boggy Creek fresh water site

The value of z_1 at this site based on the data of Hicks et al. (2009) was assumed to be 0.4 m. The values for c_1 for acidity (H^+), Fe^{2+} , Al^{3+} and H^+ were 12×10^{-3} , 0.22×10^{-3} , 0.24×10^{-3} and $2 \times 10^{-3} \text{ kg m}^{-3}$ respectively based on Hicks et al. (2009). The flux of acidity is seen to drop off rapidly with time during the first 100 days (figure 28). The sum of acidity flux is similar but not the same as the total acidity this is now due to a combined effect of advection pushing solute peaks down the profile (figure 29) and the lower diffusion coefficient for Fe^{2+} and Al^{3+} compared with H^+ resulting in a greater acidity flux from the sediments when the components of the acidity are summed. When diffusion alone was consider the opposite effect occurred (figure 12).

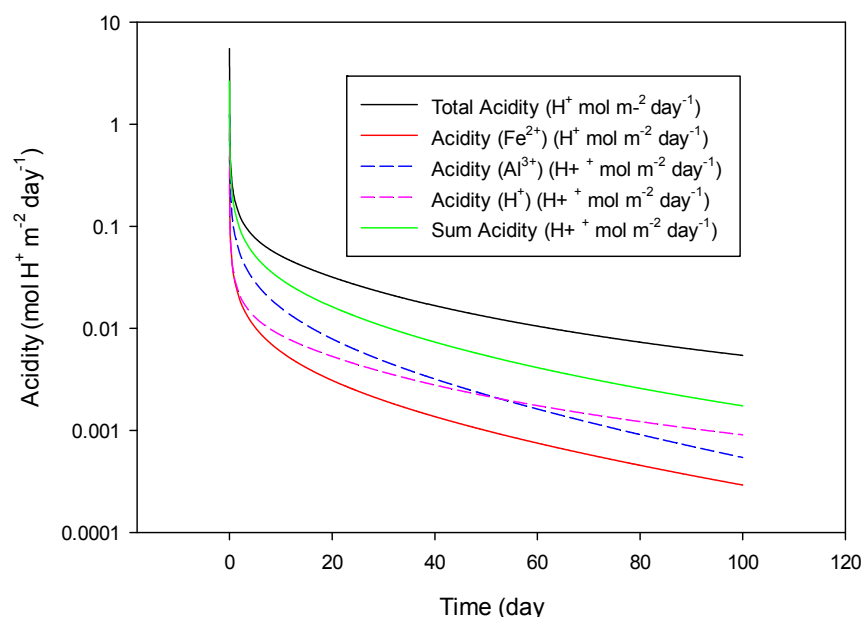


Figure 28. Acidity flux versus time from total acidity, Fe^{2+} , Al^{3+} , H^+ , and the sum of Fe^{2+} , Al^{3+} and H^+ fluxes for the Boggy Creek fresh water site.

The value of the average acid flux during the first day from the total acidity is $0.27 \text{ mol H}^+ \text{ m}^2 \text{ day}^{-1}$ and from the sum of the acidities is $0.34 \text{ mol H}^+ \text{ m}^2 \text{ day}^{-1}$. This is about double the value of 0.161 that Hicks et al. (2009) measured for the first day and similar to the average flux when diffusion only was used in the modelling. We have only used the long term infiltration rate in calculating the pore water velocity. The initial inundation is likely to have caused a greater initial pore water velocity and may have resulted in the lower flux measured. We have not included tortuosity in the dispersion coefficient which would also result in reducing the flux.

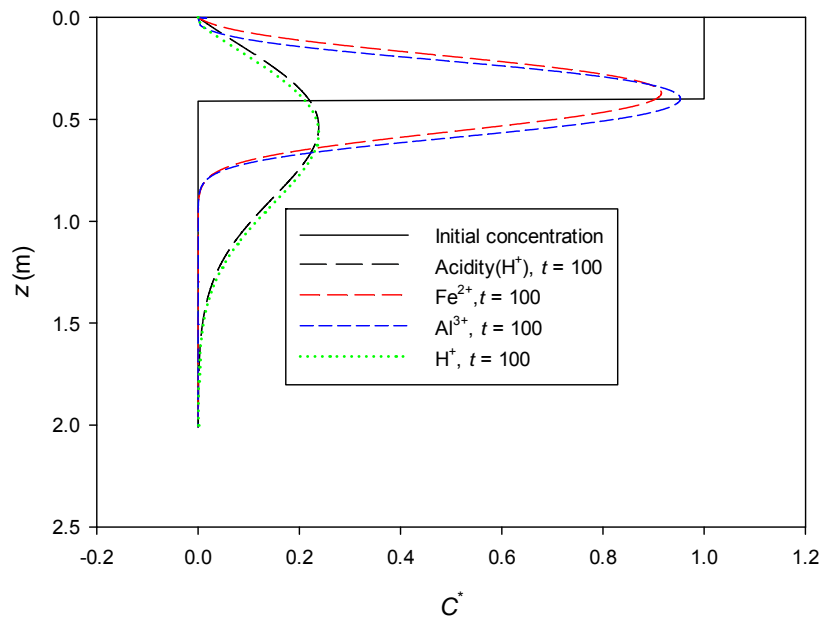


Figure 29. Initial dimensionless concentration (C^*) and concentration of the ions after 100 days for the Boggy Creek fresh water site.

Hicks et al. (2009) also suggested that the flux was between 13 and $2 \times 10^{-3} \text{ mol H}^+ \text{ m}^2 \text{ day}^{-1}$ for days 7 to 102, while the modelling suggested fluxes from 58 to $11 \times 10^{-3} \text{ mol H}^+ \text{ m}^2 \text{ day}^{-1}$, for the period of 7 to 100 days when the total acidity is used and 40 to $2 \times 10^{-3} \text{ mol H}^+ \text{ m}^2 \text{ day}^{-1}$ when the sum of the acidities is used. The average modelled flux during this time period is $17 \times 10^{-3} \text{ mol H}^+ \text{ m}^2 \text{ day}^{-1}$ for the total acidity and $9 \times 10^{-3} \text{ mol H}^+ \text{ m}^2 \text{ day}^{-1}$ for the sum of the acidities which is similar to the $6 \times 10^{-3} \text{ mol H}^+ \text{ m}^2 \text{ day}^{-1}$ measured by Hicks et al. (2009). of the same order of magnitude.

Boggy Creek salt water site

The value of z_1 at this site based on the data of Hicks et al. (2009) was assumed to be 0.4 m except for Al^{3+} where $z_1 = 0.32 \text{ m}$ was used. The values for c_1 for acidity (H^+), Fe^{2+} , Al^{3+} and H^+ were 19×10^{-3} , 1.0 , 0.065 and $2 \times 10^{-3} \text{ kg m}^{-3}$ respectively based on Hicks et al. (2009). At this site the contribution of H^+ to the acidity was negligible and not modelled. The flux of acidity is seen to drop off rapidly with time during the first 100 days (figure 30). The sum of acidity flux decreases more quickly than Total Acidity due advection of the solutes into the sediments and the different dispersion coefficients for the H^+ , Fe^{2+} and Al^{3+} . We can see the effect of the diffusion coefficient combined with advection in the rate of decrease in the flux for Fe^{2+} and Al^{3+} compared with that of H^+ .

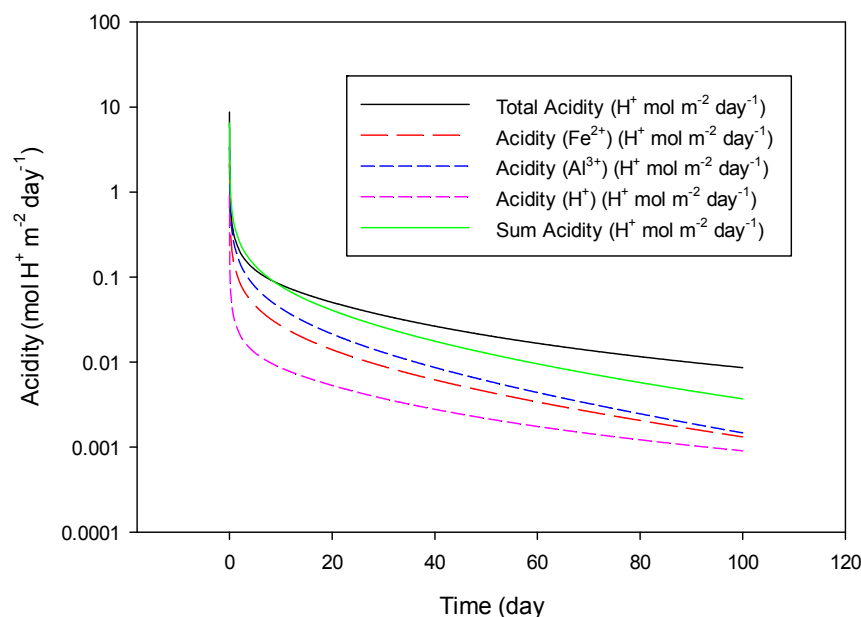


Figure 30. Acidity flux versus time from total acidity, Fe²⁺, Al³⁺, H⁺, and the sum of Fe²⁺, Al³⁺ and H⁺ fluxes for the Boggy Creek salt water site.

Again the average flux for the first day of 0.61 and 0.84 mol m⁻² day⁻¹ from total acidity and sum of acidity respectively is greater than but similar to that measured by Hicks et al. (2009) of 0.53 mol m⁻² day⁻¹. However, the flux from day 7 to 102 measured by Hicks et al. (2009) of 0.073 to 0 mol m⁻² day⁻¹ (mean of 22x10⁻³ mol m⁻² day⁻¹) is less than modelled flux range of 0.101 to 0.086 mol m⁻² day⁻¹ from total acidity and 0.105 and 0.004 mol m⁻² day⁻¹ from sum of the acidities. These values are however within the same order of magnitude as the measured fluxes. The average modelled fluxes are 27 and 20x10⁻³ mol m⁻² day⁻¹ for the total acidity and sum of the acidities respectively and the same as the measured flux. These results again suggest that the use of salt (sea) water as the water source has not contributed greatly to the acid flux seen at this site.

The flux from the sum of the acidity is now less than the flux calculated from the total acidity. This is because the total acidity is now dominated by Fe²⁺ and Al³⁺ and the diffusion coefficient for H⁺ which is greater than that for Fe²⁺ and Al³⁺ was used in calculating the acidity flux for the total acidity. This means that when the Fe²⁺ and Al³⁺ is advected down the sediment profile (figure 31) the lower diffusion coefficient means that less can now make it out of the sediment.

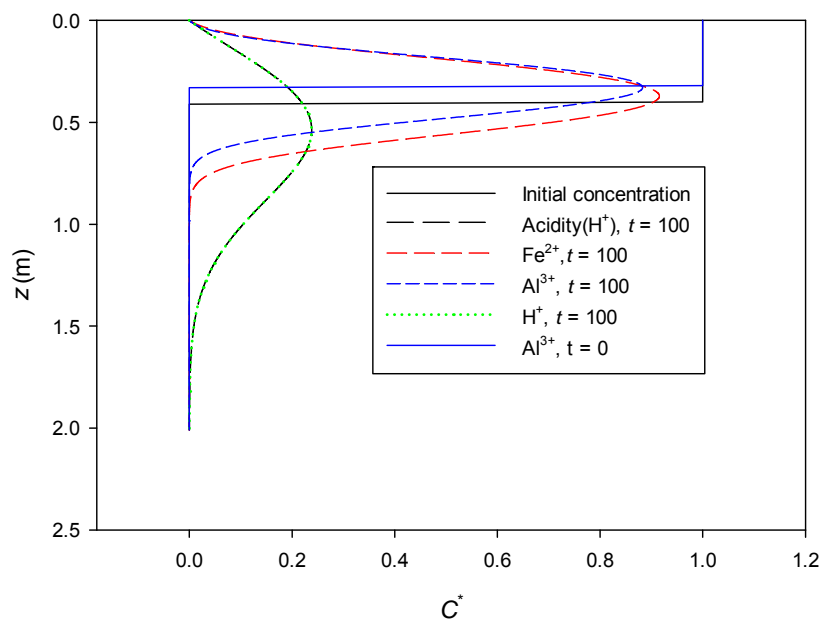


Figure 31. Initial dimensionless concentration (C^*) and concentration of the ions after 100 days for the Boggy Creek salt water site.

The salt water site due to the acidity being dominated by Fe^{2+} and Al^{3+} results in both higher initial and continuing acidity flux to the water column than the fresh water site (figure 14).

Point Sturt fresh water site

The two values of z_1 used in calculations at this site were 0.4 and 1 m, based on the data of Hicks et al. (2009). These two values were used as the profile data showed that the acidity had not diminished by maximum depth of the information in figure 30 of Hicks et al. (2009). This site had very little acidity associated with Fe^{2+} and Al^{3+} so modelling was not carried out for these ions. The values for c_1 for acidity (H^+), H^+ were 2×10^{-3} and $1 \times 10^{-3} \text{ kg m}^{-3}$ respectively based on Hicks et al. (2009). The flux of acidity is seen to drop off rapidly and continue to decrease with time during the first 100 days (figure 33). By comparison with the diffusion only modelling the effect of the z_1 (figure 16) is now very small as the effect of advection of the solutes into the sediments (figure 34) dominates compared to the value of z_1 .

Hicks et al. (2009) measured the average acidity flux for the first day from this site as $0.138 \text{ mol m}^{-2} \text{ day}^{-1}$ and we modelled the average flux for the same time period as $0.052 \text{ mol m}^{-2} \text{ day}^{-1}$. The modelled flux is now less than the measured flux. This difference may be due to the presence of dissolved acidic salts at the surface of this site which are not accounted for in the model.

For the period from 12 to 100 days, Hicks et al. (2009) measured a flux of acidity ranging from 3 to $-19 \times 10^{-3} \text{ mol m}^{-2} \text{ day}^{-1}$, while we model the flux over the same period to be from 9×10^{-4} to $5.9 \times 10^{-8} \text{ mol m}^{-2} \text{ day}^{-1}$ when $z_1 = 1 \text{ m}$ and from 9×10^{-4} to $6.2 \times 10^{-8} \text{ mol m}^{-2} \text{ day}^{-1}$ when $z_1 = 0.4 \text{ m}$. The modelling, like the measurements shows very little acidity flux in the period from 12 days onward. However, it cannot show the alkalinity flux into the sediment measured at this site as the simple model used does not incorporate this process. The average modelled flux for the period 12 to 100 days after inundation is virtually zero at $1.5 \times 10^{-4} \text{ mol m}^{-2} \text{ day}^{-1}$ for both values

of z_1 and compares well with the average value of Hicks et al. (2009) of $-5 \times 10^{-3} \text{ mol m}^{-2} \text{ day}^{-1}$ indicating a net alkalinity flux.

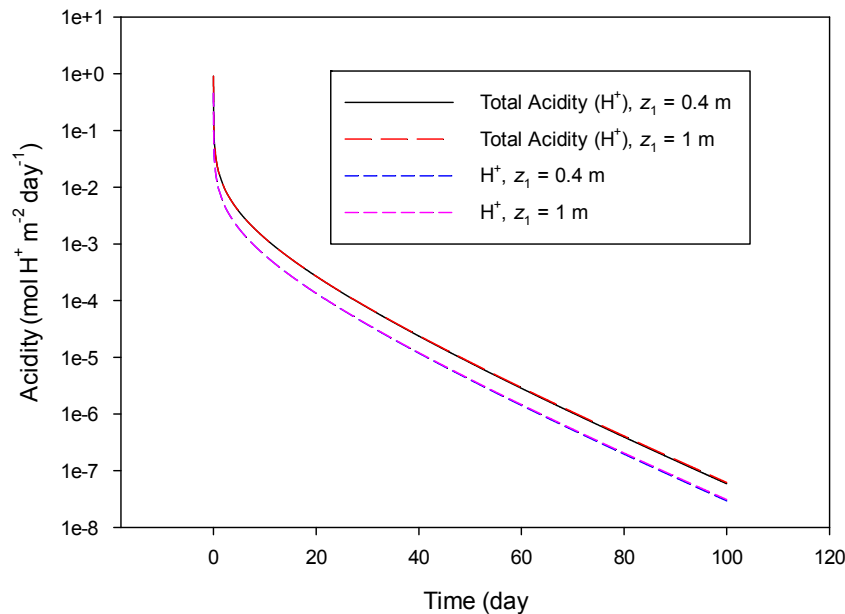


Figure 32. Acidity flux versus time from total acidity and H^+ for the Point Sturt fresh water site. The fluxes were calculated using two different values of z_1 of 0.4 and 1 m.

The advection of the solute mass into the sediment means that the peak of where the solute concentration occurs, is now nearer the surface for the smaller value of z_1 (figure 34) compared with diffusion only where the situation was reversed (figure 17).

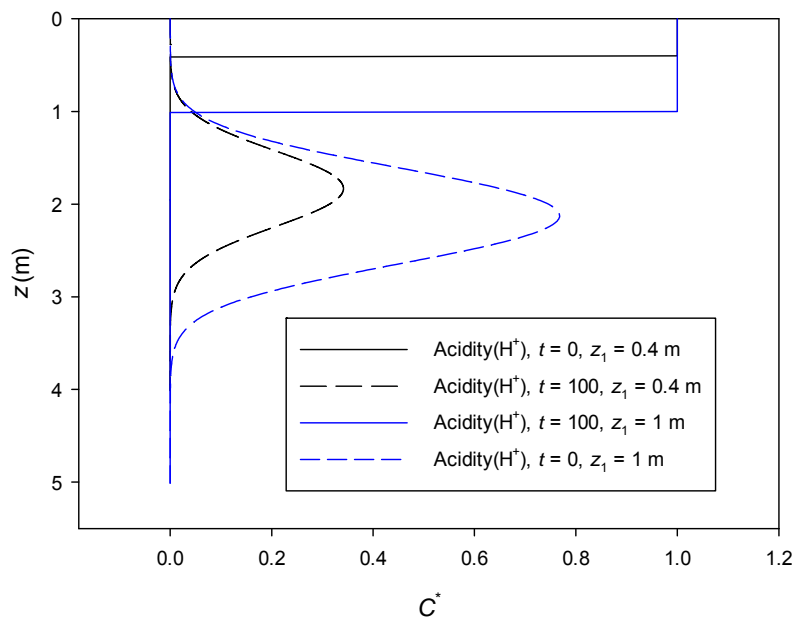


Figure 33. Dimensionless concentration (C^*) versus depth for $t = 0$ and $t = 100$ day for $z_1 = 0.4$ and 1 m, for the Point Sturt fresh water site.

Point Sturt salt water site

The profile at this site is considerably more complicated than at the previous sites, so a number of modelling runs were done for each ion and these were described previously in Table 6. For this site the pore water velocity is the largest for any of the sites at 2.8×10^{-2} m/day. This large velocity results in some numerical problems for calculating the complimentary error function so not all model results are complete for this site.

The results show that the effect of the total acidity, Fe^{2+} and Al^{3+} being deeper in the profile when advection occurs has little effect on the flux of acidity to the water column (figure 34). For the total acidity with diffusion only the flux remains almost constant with time after the initial decrease in the first 10 days (figure 18a), but now the acidity flux continues a decrease with time (figure 34a). For Fe^{2+} the inclusion of a large source of acidity at depth and none in the top 0.15 m of sediment now results in only a small difference in the flux (figure 34b). The inclusion of a deeper source of acidity from Al^{3+} has little effect on the modelled acidity flux to the water column from this source (figure 34c). Modelling the acidity due to the H^+ ion with the source occurring to a greater depth has no effect on the acidity flux to the water column (figure 34d).

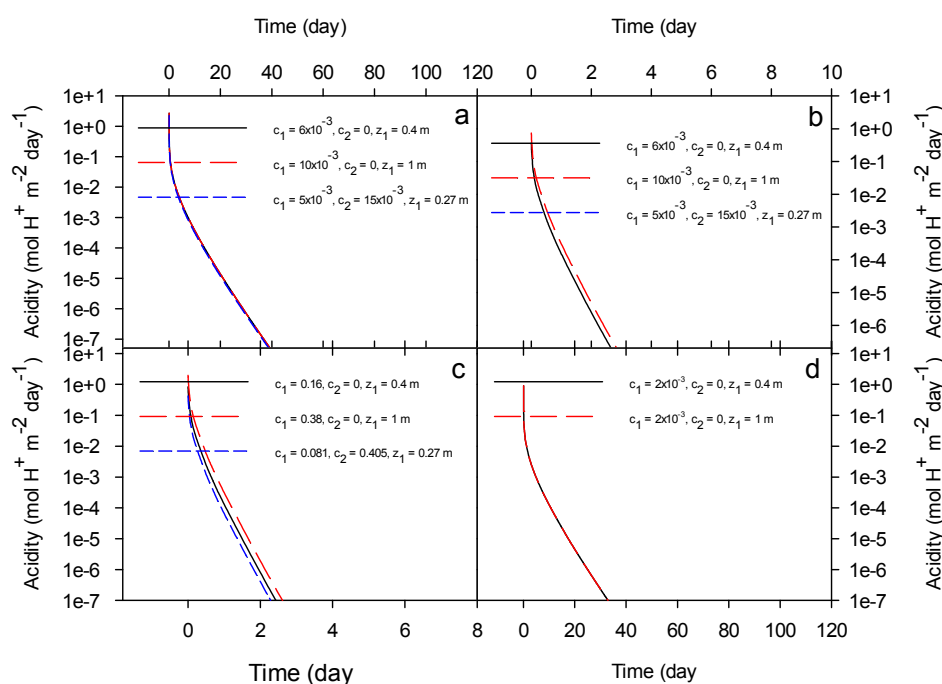


Figure 34. Acidity fluxes from the sediment to the water column with time for; a) total acidity, b) Fe^{2+} , c) Al^{3+} and d) H^+ , for the scenarios in Table 6 for the Point Sturt salt water site.

The modelled average flux from the sediment using the total acidity scenarios, give fluxes during the first day of between 153 and 60×10^{-3} $\text{mol m}^{-2} \text{ day}^{-1}$ which is much greater than the measured flux of 2.8×10^{-3} $\text{mol m}^{-2} \text{ day}^{-1}$ by Hicks et al. (2009) but now much closer than when diffusion alone is used to model the acidity flux. The modelled flux from days 12 to 100 were in the range of 2×10^{-4} to 0 $\text{mol m}^{-2} \text{ day}^{-1}$ compared to the measured flux range of 0 to -17×10^{-3} $\text{mol m}^{-2} \text{ day}^{-1}$. The measured fluxes indicate that no acidic flux occurs and only a flux of alkalinity into the

sediments. The modelling shows very little acid flux but is unable to indicate a flux of alkalinity.

When the ions are initially concentrated near the surface the concentration profiles are similar to above those above (figures 29, 32 and 33) for total acidity, Fe^{2+} , Al^{3+} and H^+ . The concentration profiles when the ions are concentrated deeper in the profile could only be modelled for the H^+ ion as the numerical problems occurred when computing the profiles for However, the effect will be similar for Fe^{2+} and Al^{3+} to that of H^+ with the solute getting advected down the sediment profile (figure 35).

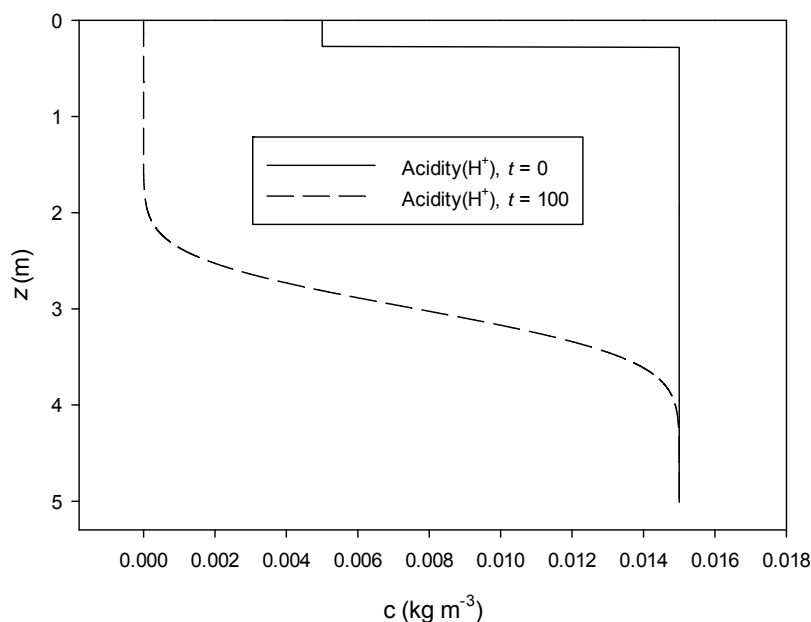


Figure 35. Concentration profiles for total acidity and when $c_2 > 0$ (Table 6) for Point Sturt salt water site.

When advection occurs, sediment profiles where the acidic ions are concentrated in the lower part of the sediment profile are no more of a risk of acidic fluxes than when they are nearer the surface. These results suggest that in rewetting of the sediments it would be advisable to do this quickly, so the advective flux into the sediments transported the acidic solutes deeper into the sediment profile. This may be a useful management tool for rewetting of billabongs where acidic sediments exist. Areas could be banded off and then sudden rewetted. This may assist in reducing the acidic solutes being transported to the water column.

3. MODELLING OF ACID NEUTRALISATION IN THE SURFACE WATER

It was also considered important to determine if an ongoing acid flux from the lower lakes sediments could impact on the surface water body. The alkalinity of water is its acid neutralising capacity and the higher the alkalinity the more acid input it requires to cause acidification. In most natural waters the bicarbonate (HCO_3^-), and to a less extent (CO_3^{2-}) carbonate, ions provide the ability to neutralise acid inputs by buffering increases in H^+ ion concentrations (Stumm and Morgan 1996). Disregarding the usually minor contribution of other weak H^+ ion acceptors such as organic acids, alkalinity can be defined as:

$$\text{Alkalinity} = [\text{HCO}_3^-] + 2[\text{CO}_3^{2-}] + [\text{OH}^-] - [\text{H}^+] = c_B - c_A \quad (3.1)$$

The right hand side of the equation ($c_B - c_A$) represents the alkalinity as a conservative and experimentally accessible parameter (via standard acid-base titration and/or measurement of base cations and acid anions), representing the excess of an arbitrary amount of strong base (c_B) over the amount of strong acid (c_A). Alkalinity is a conservative and easily measurable parameter which along with pH makes it the most useful CO_2 system parameter for considering mixing of water bodies of different composition (Mosley et al. 2010).

In the present context, acid diffusing out of the sediment ($c_{a(\text{sed})}$, $\text{mol H}^+ \text{ T}^{-1}$) consumes some the water alkalinity ($c_B - c_{A(t)}$) in exact proportion to the acid input. Additional inputs ($c_B - c_{A(\text{in})}$) of alkalinity could also occur (e.g. via horizontal turbulent diffusion or tributary inflows) in an acid-affected water body connected to a more alkaline one. Hence, after accounting for these potential fluxes, the change in alkalinity in the acid-affected water body over time (t) can be represented by:

$$\text{Alkalinity} = c_B - c_{A(t+1)} = (c_B - c_{A(t)}) - c_{A(\text{sed})(t)} + (c_B - c_{A(\text{in})(t)}) \quad (3.2)$$

This equation can be used to determine if a water body will turn acidic (alkalinity < zero), representing the point at which acid additions are sufficient to overcome the excess amount of base. A similar approach was successfully applied by Schofield et al. (1995) for predicting lake alkalinity changes resulting from acid rain deposition to their catchments.

The titration endpoint for the carbonate system to reach zero alkalinity is at $\text{pH} \approx 5$. As biological damages to ecosystems start above this ($\text{pH} \approx 6.5$) and increase with further lowering of pH (ANZECC 2000; Vinebrook et al. 2003), it is also useful to determine pH changes in addition to alkalinity consumption following acid additions. To calculate pH changes, the total mass-balance condition for the carbonate system (C_T , total inorganic carbon) must first be defined:

$$C_T = [\text{H}_2\text{CO}_3^*] + [\text{HCO}_3^-] + [\text{CO}_3^{2-}] \quad (3.3)$$

In most natural surface water bodies open to the atmosphere, the carbonic acid (H_2CO_3^*) level is fixed by the partial pressure of carbon dioxide in the water (pCO_2),

and the three components comprising C_T may be expressed in terms of a fraction ($\alpha_0 + \alpha_1 + \alpha_2 = 1$, see Stumm and Morgan 1996):

$$[H_2CO_3^*] = C_T \alpha_0 = K_H pCO_2 \quad (3.4)$$

$$[H_2CO_3^-] = C_T \alpha_1 \quad (3.5)$$

$$[CO_3^{2-}] = C_T \alpha_2 \quad (3.6)$$

where

$$\alpha_0 = \frac{1}{1 + K_1' / \{H^+\} + K_1' K_2' / \{H^+\}^2} \quad (3.7)$$

$$\alpha_1 = \frac{1}{K_1' / \{H^+\} + K_2' / \{H^+\}} \quad (3.8)$$

$$\alpha_2 = \frac{1}{1 + \{H^+\} / K_2' + \{H^+\}^2 / K_1' K_2'} \quad (3.9)$$

and $\{H^+\}$ is the hydrogen ion activity (NBS pH scale), K_H is the Henry's Law constant for gas-liquid phase equilibrium, and K_1' and K_2' are the first and second mixed acidity constants for dissociation of H_2CO_3 . By rearranging equation (3.3) for C_T , combining with equations (3.4), (3.5) and (3.6), and substituting into equation (3.1) leads to an equation that can be used to calculate changes in pH following additions of known amounts of acid and/or base to a system of a particular alkalinity and pH (Stumm and Morgan 1996):

$$\text{Alkalinity} = (c_B - c_A) = \frac{K_H pCO_2}{\alpha_0} (\alpha_1 + 2\alpha_2) + \frac{K_w'}{\{H^+\}} + \frac{\{H^+\}}{\gamma H} \quad (3.10)$$

where the additional terms, are the water self-dissociation constant, K_w' , and the activity coefficient for the hydrogen ion, γH . Thermodynamic equilibrium constant values for K_H , K_w' , K_1' , and K_2' in equations (3.7)-(3.10), were obtained from Stumm and Morgan (1996, Table 4.3) for zero ionic strength (also available for various temperatures from 5-40 °C). Values of the mixed acidity constants (K_w' , K_1' and K_2') with increasing ionic strength (I) were calculated using the Güntelberg approximation of the Debye-Huckel equation (Stumm and Morgan 1996, valid to $I \approx 0.1$):

$$pK' = pK + \frac{0.5(Z_{HB}^2 - Z_B^2)}{1 + \sqrt{I}} \quad (3.11)$$

where Z_{HB}^2 and Z_B^2 are the charges of the acid and base species in the respective dissociation reactions ($Z_{H_2CO_3} = 0$, $Z_{HCO_3^-} = -1$, $Z_{CO_3^{2-}} = -2$, $Z_{H_2O} = 0$, $Z_{OH^-} = -1$). γ_H was also calculated using the Güntelberg approximation for the single ion activity.

Changes in the alkalinity (left hand side of equation 3.10) following acid inputs from the sediment were calculated using equation (3.2). The acid inputs are given in $\text{mol m}^{-2} \text{ day}^{-1}$ and these were converted to mol L^{-1} in the water body by accounting for the overlying water depth in the model (in m, where $1\text{m}^3 = 1000\text{L}$). Calculation of pH ($-\log \{H^+\}$) at each time step was undertaken using the bisection method implemented in MATLABTM, with Equation (3.10) solved numerically by varying the $\{H^+\}$ systematically until the left hand side equalled the right hand side. pH predictions using equation (3.10) below the carbonate system endpoint are unlikely to be accurate as dissolved metals such as Al can begin to form a large component of the solution acidity and additional acid-base equilibria are required to be considered.

To represent the range of potential conditions in the lower lakes, (a) various starting water body alkalinities ($C_B - C_{A(t=0)}$) were used in the model scenarios; 0, 1, 1, 2, and 4 meq L^{-1} (corresponding to 5, 50, 100 and 200 mg L^{-1} alkalinity respectively). (b) two water depths were considered; 0.1 and 1m, and (c) two additional daily alkalinity inputs ($C_B - C_{A(in)(t)}$); 0 (no additional input, isolated water body). Only one typical temperature (25°C) and salinity ($0.6 \text{ g/L} \approx 1000 \mu\text{S cm}^{-1}$) were considered in the scenarios due to the relatively minor (compared to acid additions) effect of these parameters on the modelled pH and alkalinity.

3.1 Results for an Isolated Water Body : Diffusion

These simulations consider the acid fluxes to isolated water bodies (no additional alkalinity inputs, $C_B - C_{A(in)(t)} = 0$). Hence they can be considered worst case type outcomes although it is noted that isolated acidic water bodies occurred in the lower lakes during the 2007-2009 drought period (e.g. Currency Creek, Loveday Bay).

The pH and alkalinity following acid diffusion from the sediment at the Boggy Creek freshwater site is shown in figure 36. The acid flux from the sediment is predicted to turn a 1m overlying water body acidic for alkalinities $< 0.004 \text{ eq L}^{-1}$ or less within a 25 day period. However, the results for a 0.1 m water column show a much faster acidification due to the lower amount of acid neutralising capacity in the smaller volume of water. The results for the Boggy Creek saltwater site (figure 37) show that, due to the higher acid flux, acidification is. These simulations consider the acid fluxes to isolated water bodies (no additional alkalinity inputs, $C_B - C_{A(in)(t)} = 0$). Hence they can be considered worst case type outcomes although it is noted that isolated acidic water bodies occurred in the lower lakes during the 2007-2009 drought period (e.g. Currency Creek, Loveday Bay).

The model results for the Pt Sturt freshwater (figure 38) are also consistent with those of Hicks et al. (2009) as no acidification is observed at 0.002 eq/L used in their experiments. Acidification was only at the very low starting alkalinity modelled (0.0001 eq/L), which only occur in the situation of rainwater ponding on the sediment. The seawater treatments show a reasonably rapid acidification which differs from the Hicks et al. (2009) results (figure 39). This is likely due to the modelled sediment flux

being higher than that measured as noted above. Also additional alkalinity inputted via advection (water in Hicks et al. mecoscosms were topped up as required to maintain a stable level), and advection of solutes downward (see below), are not considered in these simulations.

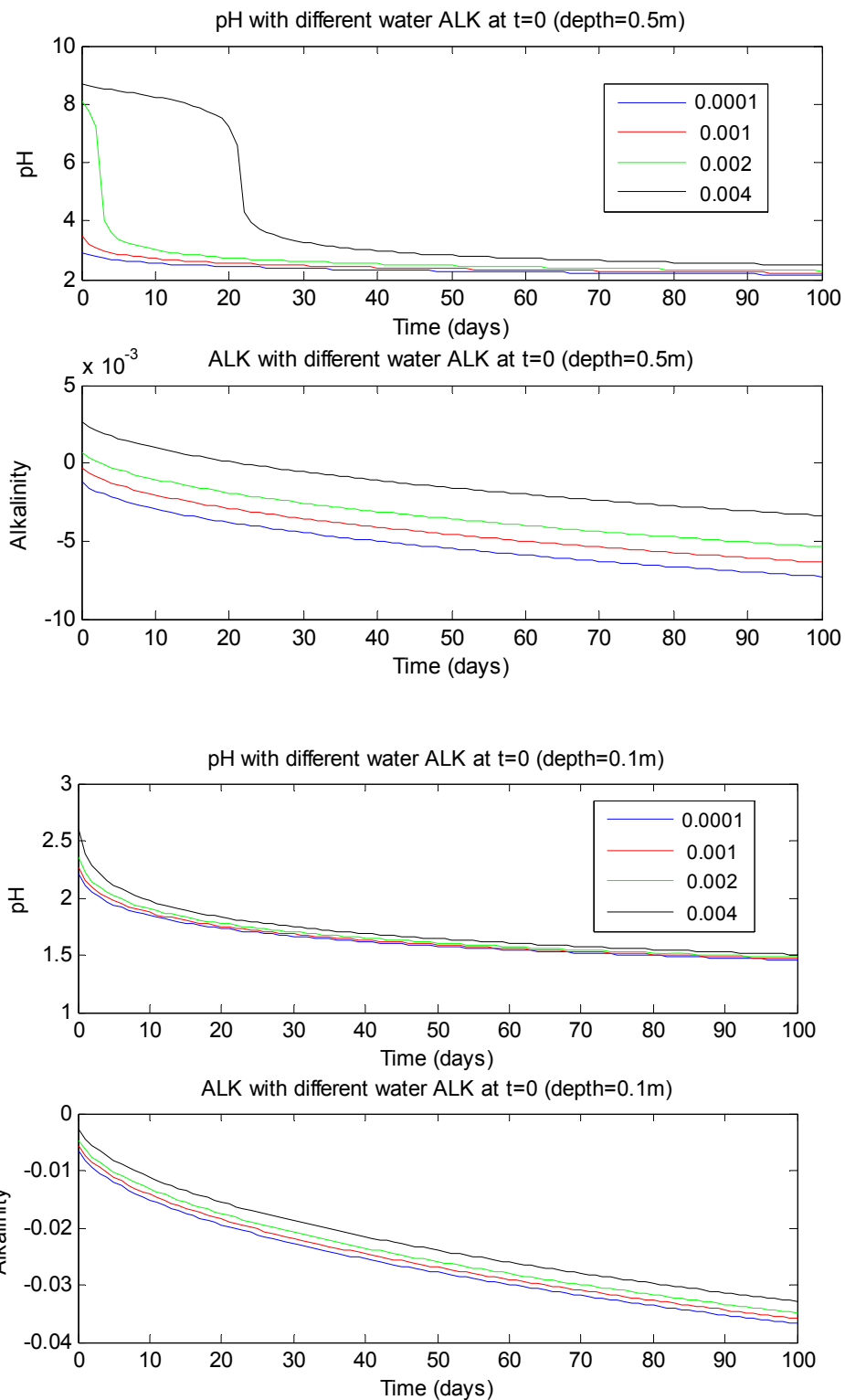


Figure 36. Modelled surface water pH and alkalinity for the Boggy Creek freshwater site with different starting alkalinities in a 1m (top) and 0.1m (bottom) water column (0.0001, 0.001, 0.002, and 0.004 eq L⁻¹)

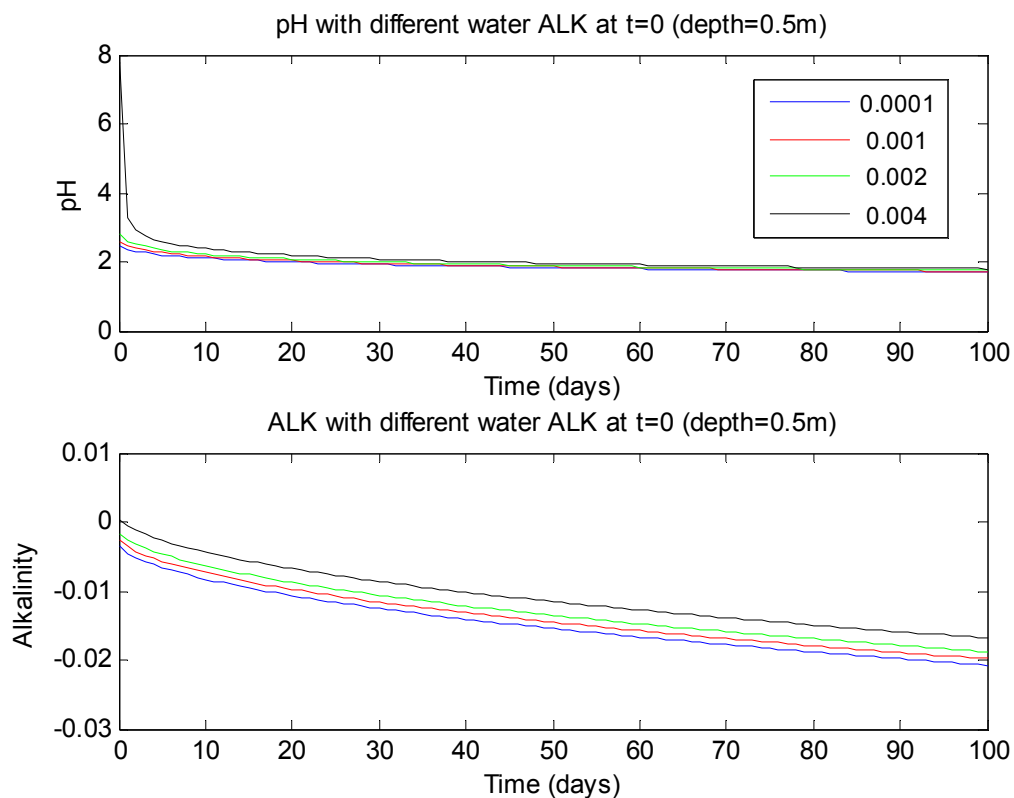


Figure 37. Modelled surface water pH and alkalinity for the Boggy Creek saltwater site with different starting alkalinities in a 1m water column (0.0001, 0.001, 0.002, and 0.004 eq L⁻¹).

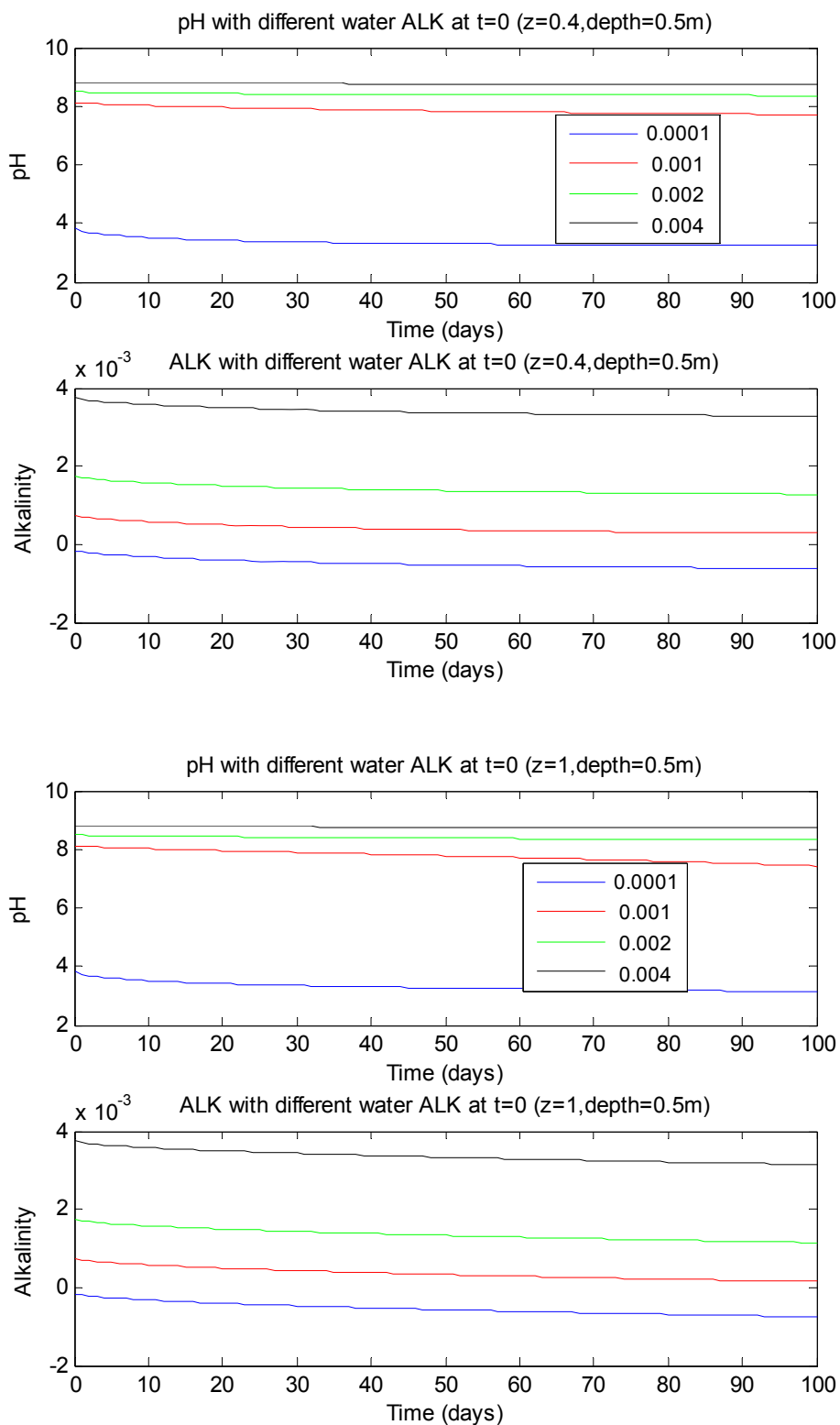


Figure 38. Modelled surface water pH and alkalinity for the Pt Sturt freshwater site with different starting alkalinities in a 0.5m water column (0.0001, 0.001, 0.002, and 0.004 eq L⁻¹) for z=0.4 and z=1m.

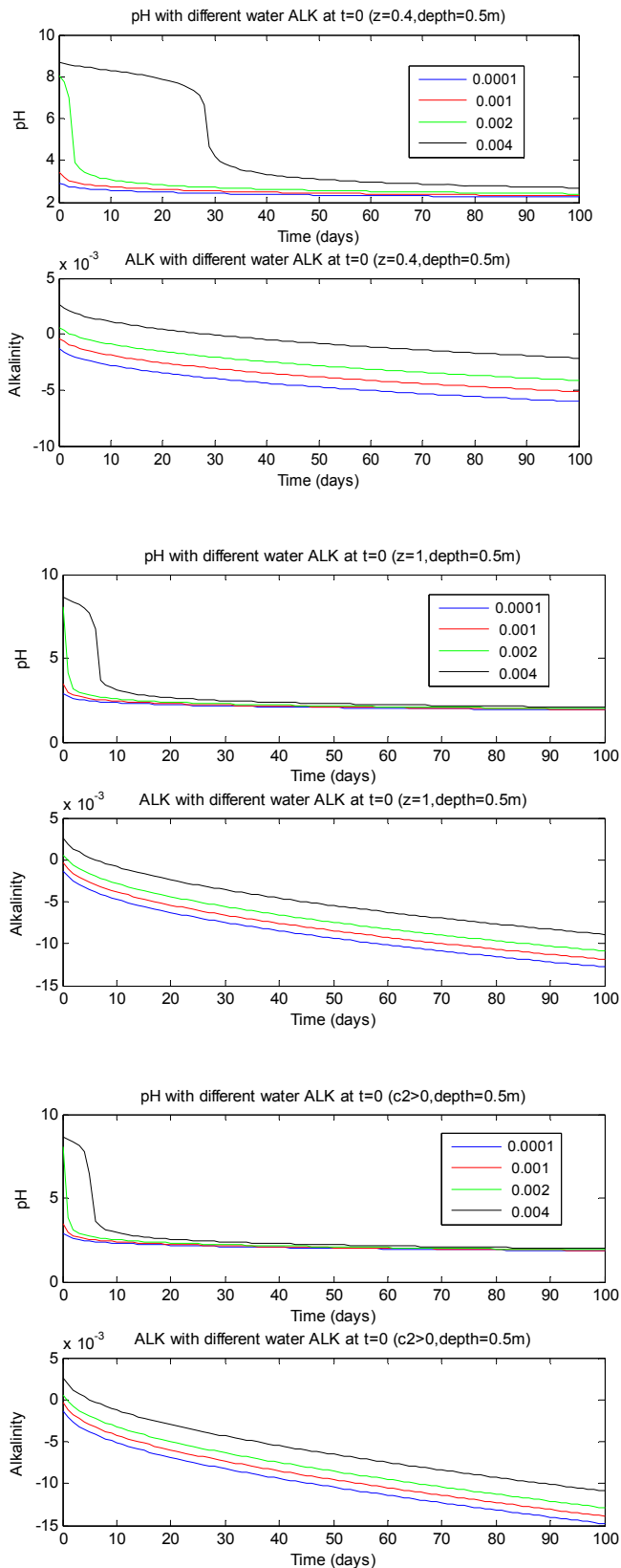


Figure 39. . Modelled surface water pH and alkalinity for the Pt Sturt salt water site with different starting alkalinities in a 0.5m water column (0.0001, 0.001, 0.002, and 0.004 eq L⁻¹) for z=0.4 and 1m and c₂>0.

3.2 Results for an Isolated Water Body: Advection Plus Diffusion

The pH and alkalinity following acid diffusion from the sediment at the Boggy Creek freshwater site is shown in figure 40. The acid flux from the sediment is predicted to turn a 0.5 m overlying water body acidic for alkalinities $\leq 0.002 \text{ eq L}^{-1}$ within the 100 day time period although the alkalinity for the 0.004 eq L^{-1} starting alkalinity is still declining so this would turn acidic at a later date. The acidification process is slower compared to the same simulations with diffusion only (figure 36). The results for the Boggy Creek saltwater site (figure 41) show that, due to the higher acid flux, acidification is much more rapid than for freshwater and results are similar to the diffusion-only simulation (figure 37).

The advection-diffusion model results for the Pt Sturt freshwater (figure 42) show that acidification occurred only at the very low starting alkalinity modelled (0.0001 eq L^{-1}), which would only occur in the situation of rainwater ponding on the sediment. The seawater treatments also only showed acidification at the low starting alkalinity value (figures 43-44) which differs from the rapid acidification indicated by the diffusion-only simulations (figure 39), but is similar to the results of Hicks et al. (2009). These results suggest advection has the potential to greatly reduce acid flux from submerged sandy sediments but has less impact in clay sediments. As noted above the additional input of alkalinity, as occurred in the mecoscosms to maintain water levels, is not considered in these simulations.

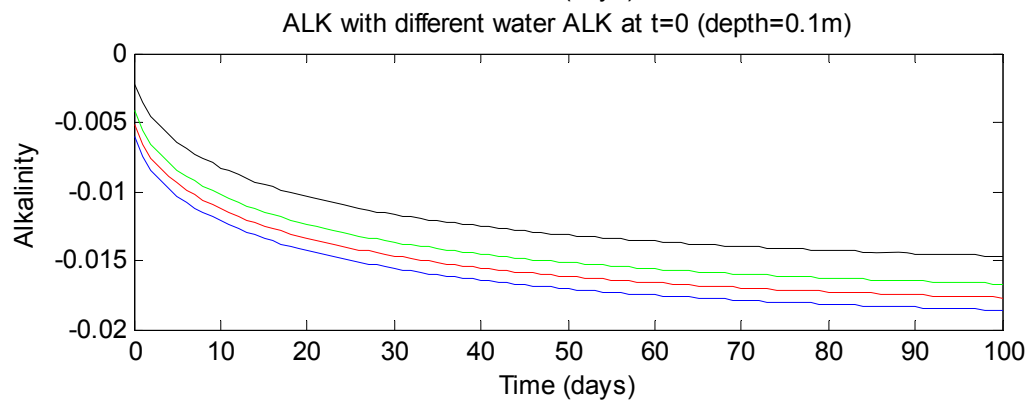
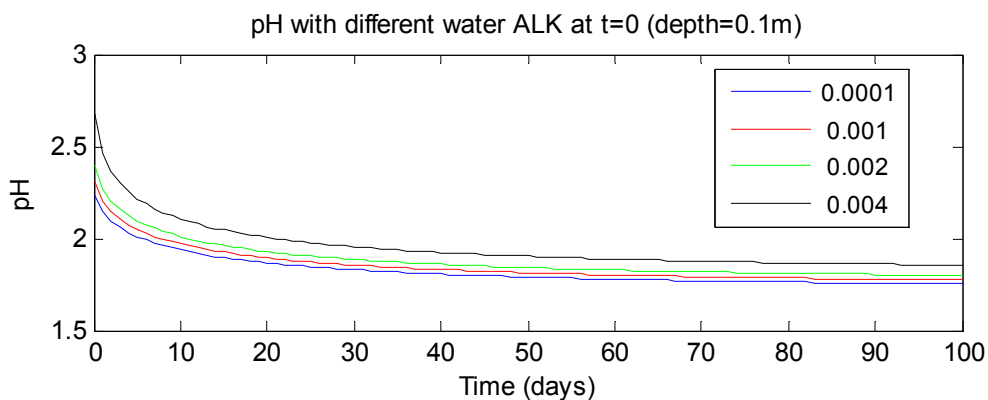
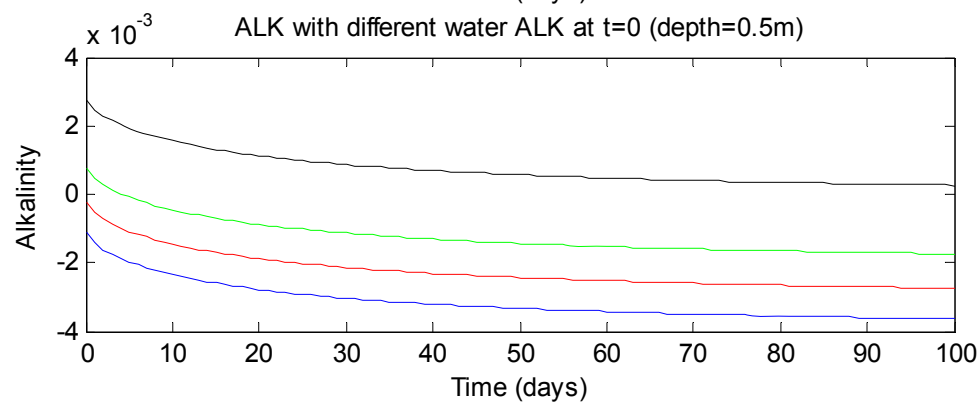
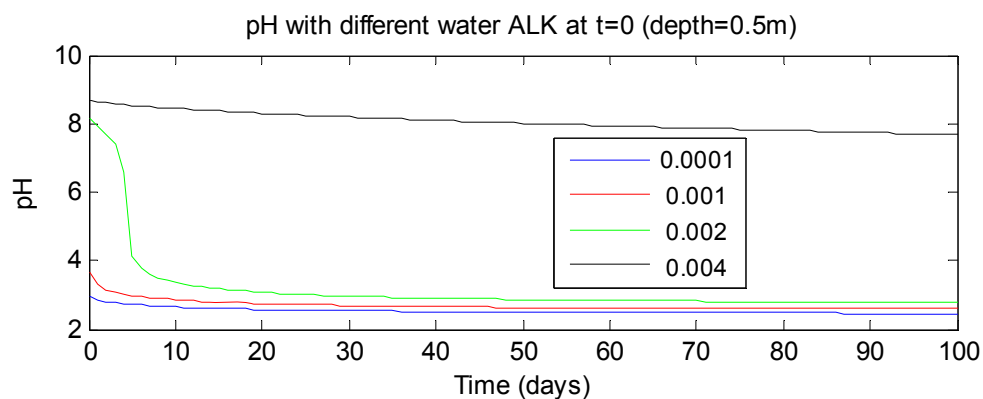


Figure 40. Modelled surface water pH and alkalinity for the Boggy Creek freshwater site with different starting alkalinities in a 0.5m (TOP) and 0.1m (BOTTOM) water column (0.0001, 0.001, 0.002, and 0.004 eq L⁻¹) including advection.

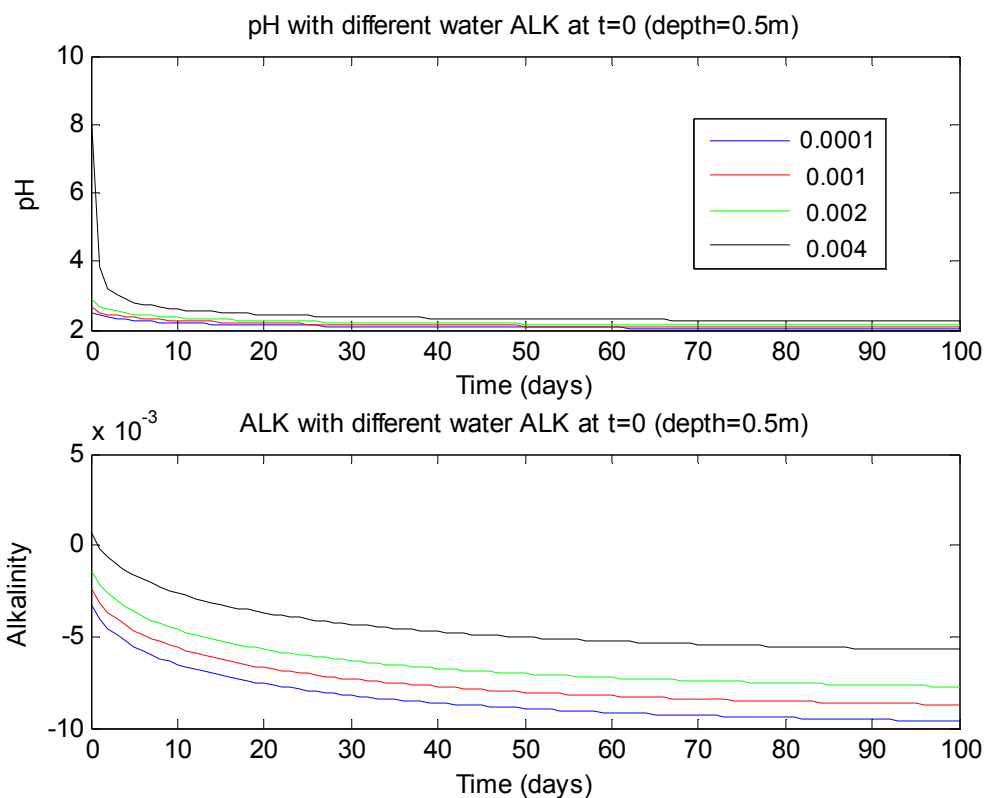


Figure 41. Modelled surface water pH and alkalinity for the Boggy Creek salt water site with different starting alkalinities in a 1m (top) and 0.1m (bottom) water column (0.0001, 0.001, 0.002, and 0.004 eq L⁻¹) including advection.

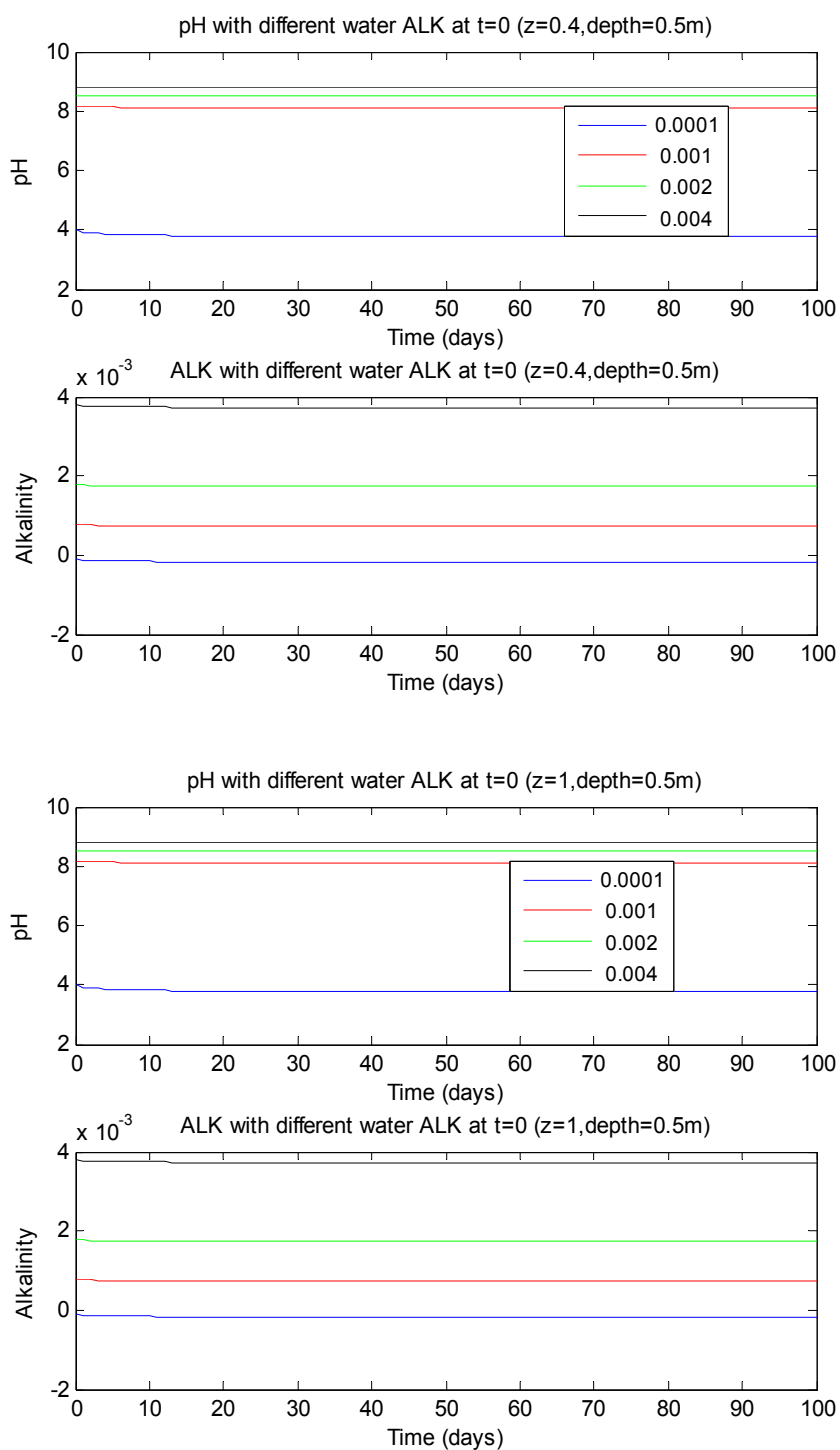


Figure 42. . Modelled surface water pH and alkalinity for the Point Sturt freshwater site for a 0.5m water column with different starting alkalinities (0.0001, 0.001, 0.002, and 0.004 eq L⁻¹) for $z=0.4$ and $z=1$ m including advection.

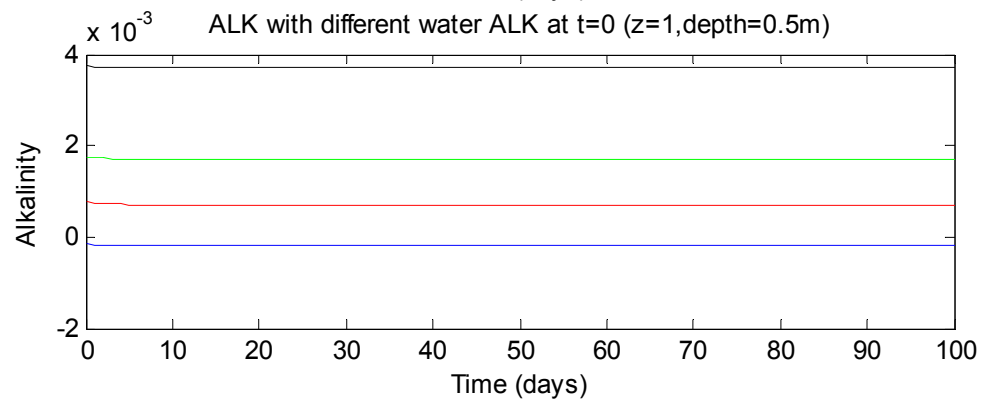
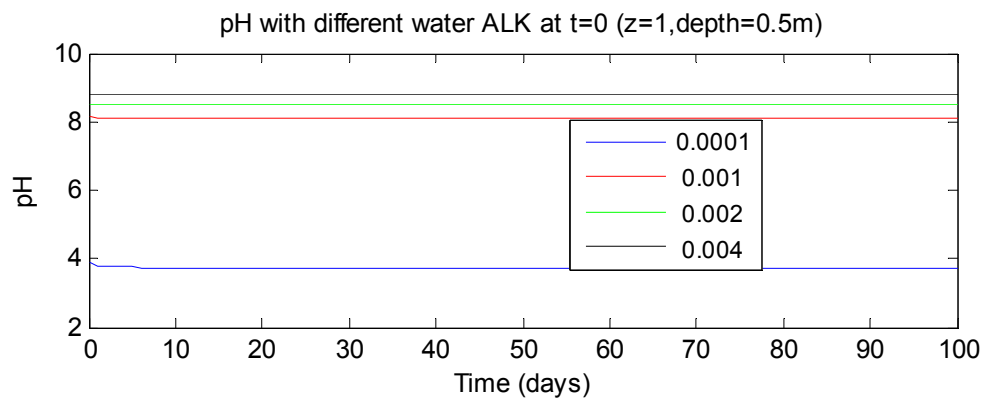
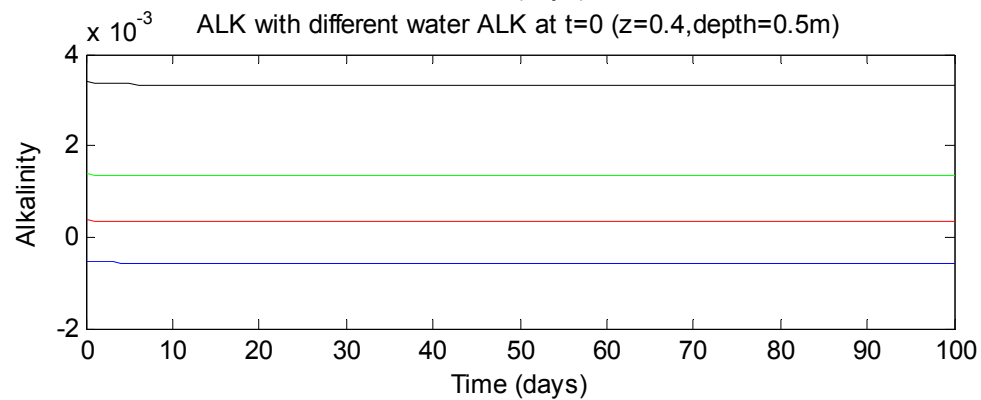
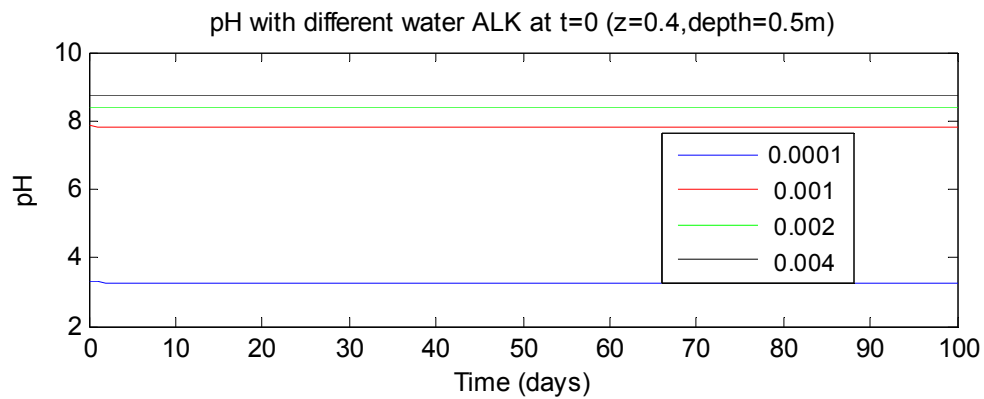


Figure 43. Modelled surface water pH and alkalinity for the Point Sturt saltwater site for a 1m water column with different starting alkalinities (0.0001, 0.001, 0.002, and 0.004 eq L⁻¹) for z=0.4 and z=1m including advection.

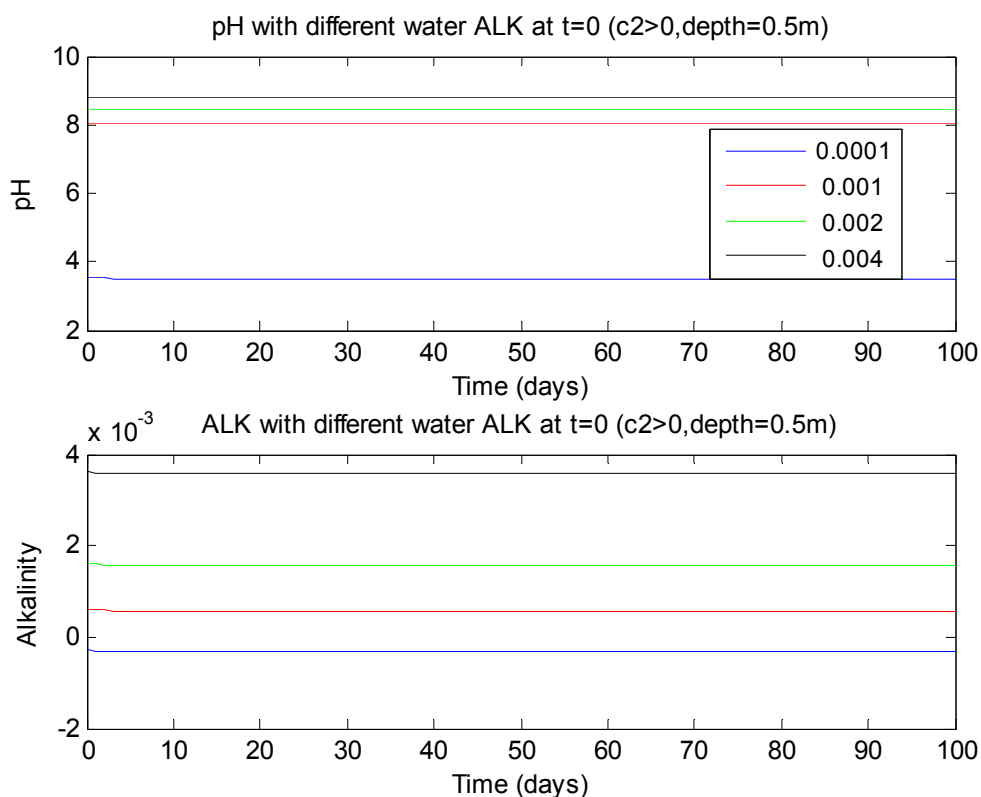


Figure 44. Modelled surface water pH and alkalinity for the Point Sturt salt water site for a 0.5m water column with different starting alkalinities (0.0001, 0.001, 0.002, and 0.004 eq L⁻¹) and c2 > 0.

3.3 Comparison to EPA Monitoring Results

Some longer term EPA monitoring results for the Boggy and Hunters Creek region of Lake Alexandrina shown in figure 45 (note log scale). An ongoing low-level presence of acidity has been observed in the water column and this appears to be lowering over time. This is generally consistent with the model predictions. There is a net alkalinity still present (figure 45, alkalinity>acidity) which is preventing water body from going acidic but the risk profile will increase under lower flow conditions (very high flows over last 18 months through Lake Alexandrina).

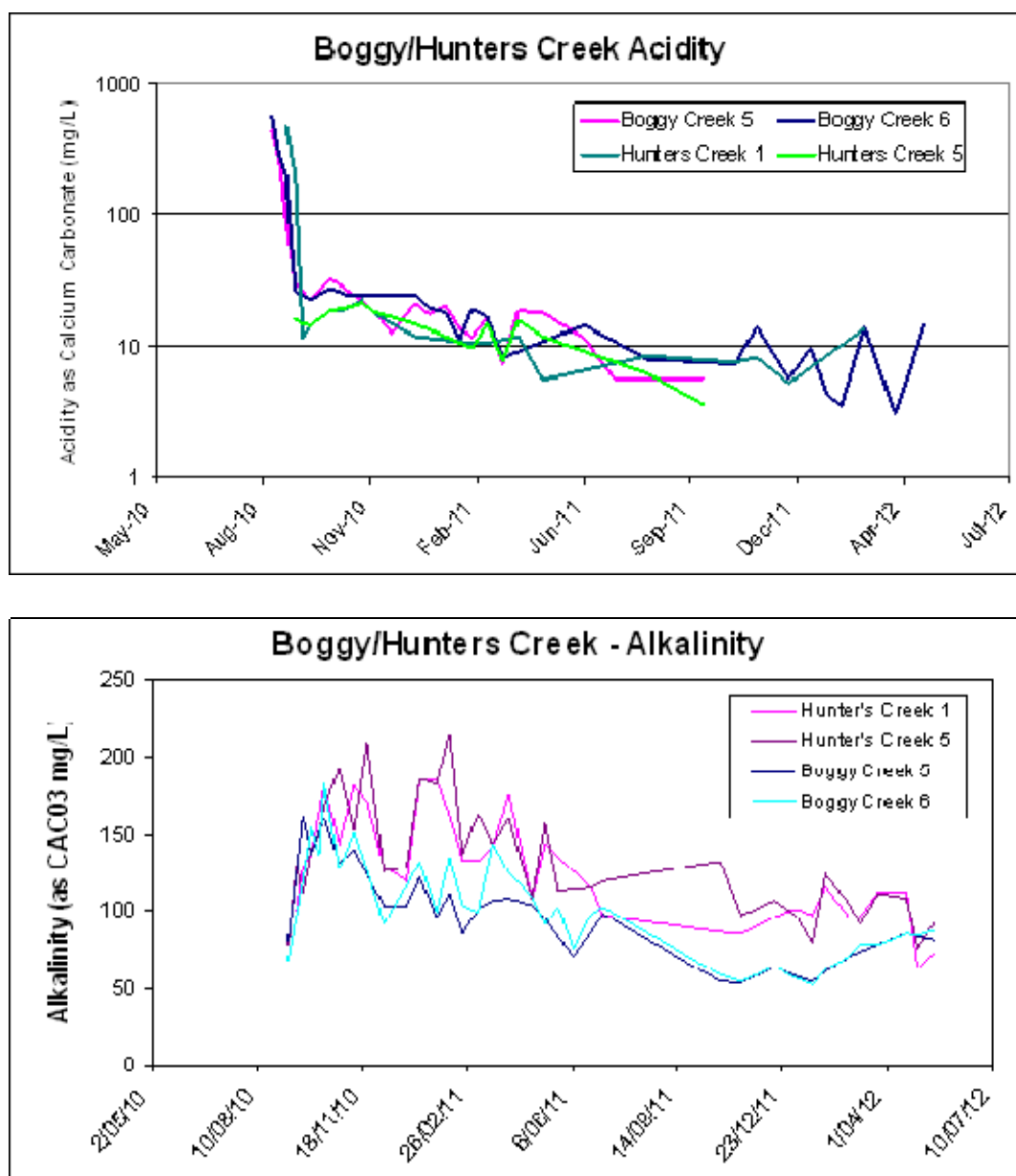


Figure 45. Measured acidity and alkalinity in the Boggy and Hunter's Creek region of Lake Alexandrina (Source: EPA).

4. DISCUSSION

The analytical solutions available and documented by van Genuchten and Alves (1982) provide a basis for exploring the fluxes of acidity from the sediments to the water column and the flux of alkalinity from the water column to the sediments. We have used these to explore the likely acidity flux from submerged sediments to the water column. The results show that if diffusion only is considered, then the flux of acidity to the water column is mainly controlled by the dispersion coefficient, the concentration of the acidity and to a lesser extent the depth of the acidic sediments. Also, with diffusion only as the mechanism for transport of acidity from the sediments

to the water column is likely that the acidity flux will continue to for a considerable time. The addition of advection with the flow into the sediments results in markedly reduced acidity flux after the initial flux of acidity, particularly in more porous sandy sediments. In this case the pore water velocity becomes one of the most important parameters determining the magnitude and time course of the flux of acidity.

When advection is out of the sediments at pore water velocities likely for seepage into the lakes the advection does not affect the acid flux greatly compared to the diffusion only transport. However, when the advection is into the sediments at the pore water velocities found by Hicks et al. (2009) the acid flux to the water column is markedly reduced. This is because the solutes get pushed down the sediment profile and the distance for diffusion to the water column becomes greater with time. In reality, in the lower lakes there are likely to be periods when the advection is into the sediments, such as when the lakes are filling and/or evaporation at the lake margin results in water transport to the sediments surrounding the lake. Cook (2011) showed that this occurred during the drying phase of the lower lakes. At other times when the surrounding soils are wet and the lake levels are low there is likely to be a seepage of water into the lakes via the sediments. Under these circumstances acidic solutes could be transported back towards the sediment surface and an increase the acidity flux to the water column may occur.

Hicks et al. (2009) measured the acidity fluxes at four specific sites using mesocosms. They used either fresh water or salt (sea) water to fill the mesocosm and monitor the chemistry of the water. We modelled these experiments using just molecular diffusion as the dispersion coefficient and were able to provide results which were generally within an order of magnitude of the measured results. The models also gave results which matched the time course of the measurements. These results suggest that the difference measured at each of the sites was mainly due to advection velocity and initial solute conditions rather than the composition of the water (fresh or sea) in the mesocosms.

Both the sensitivity analysis and the specific site modelling showed that advective flux of water into the sediments, while not changing the initial flux of acidity, could greatly reduce the acid flux with time, and hence the total amount of acidity released to the water column. This suggests that where possible a management strategy to minimise acid release to the water column should be to rewet the sediments quickly from the top so that the infiltrating water transports the acidity deeper into the sediments. This strategy would be particularly possible for small areas such as billabongs.

The coupling of the water chemistry model to the transport model indicates that if diffusion only occurred in the mesocosm experiments these would have gone acidic. The inclusion of the advective component of the transport resulted in much reduced acid fluxes and gives results more similar to those measured. The modelling of the water chemistry shows that the continued flux of acidity to water could lead to declining alkalinity in an isolated water column. The model was quite sensitive to water depth so if water levels and/or flows decline substantially acidification risks will increase in areas where the mixing of the water with the deeper lake water is restricted, such as in some shallow embayments. Results for such restricted flow areas such as Boggy Creek/Hunters Point (figure 45) suggest that continued monitoring at these sites is sensible.

A further run with the model was done to look at the long time (1000 day) estimates of the flux for the worst case scenario; diffusion-only, the highest values of the acidity and each acidity component, for the four sites from Hicks et al. (2009). These showed that especially at the Boggy Creek salt water site and the Point Sturt salt

water site considerable acidity is still being lost at 1000 days (figure 46). This is consistent with the CSIRO and EPA monitoring results showing acidity is still present in the sediment and water column of some areas of the Lower Lakes after >2 years of inundation.

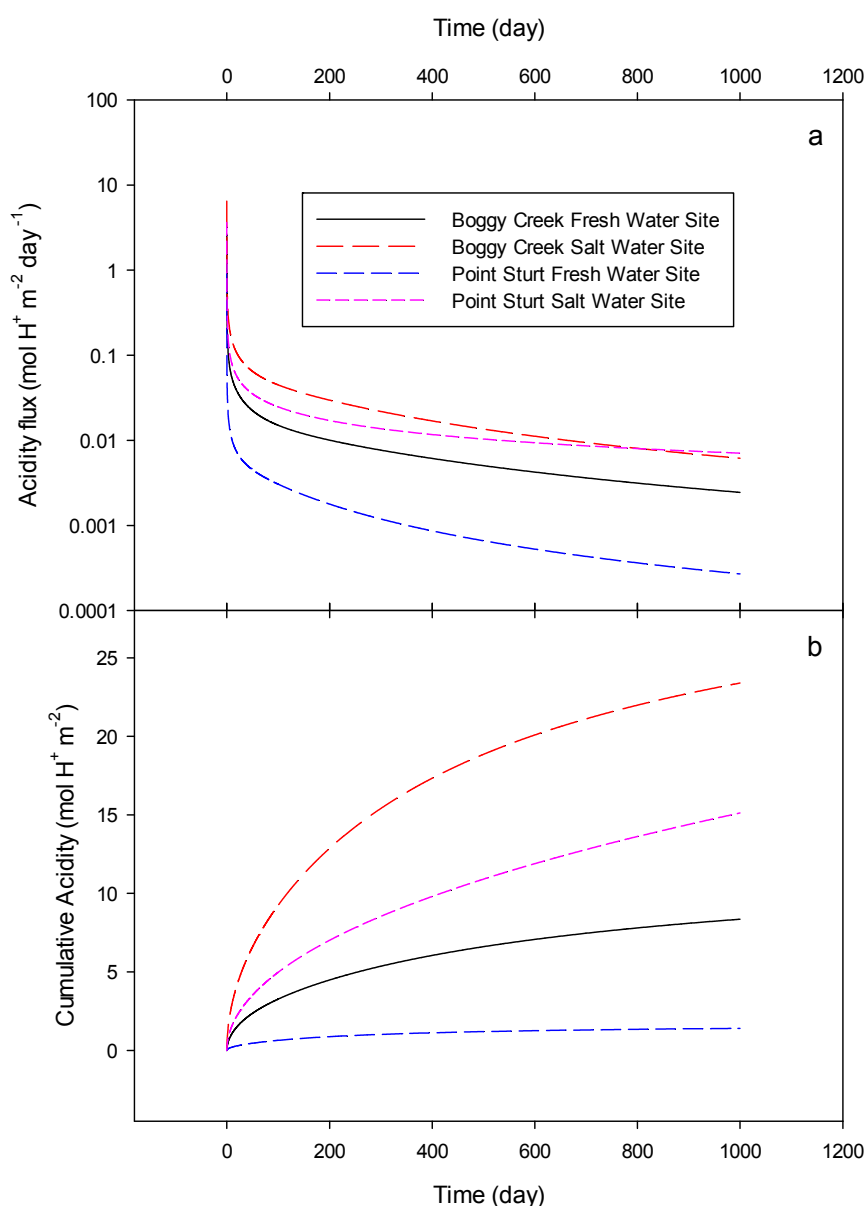


Figure 46. Long term modelling of worst case scenario at each of the four sites of Hicks et al. (2009) for a) flux of acidity and b) cumulative acidity.

The cumulative acidity at 1000 days ranges from 1.4 to 23.4 $\text{mol H}^+ \text{m}^{-2}$ for the Point Sturt fresh water site and Boggy Creek salt water site respectively. Converting these values to alkalinity would give values of 4.2, 11.7, 0.7 and 7.6 tonnes $\text{CaCO}_3 \text{ha}^{-1}$ for Boggy Creek fresh water, Boggy Creek salt water, Point Sturt fresh water and Point Sturt salt water sites respectively. The total amount of alkalinity in Lake Alexandrina was estimated to be 180,000 tonnes CaCO_3 and for Lake Albert 15,300 tonnes CaCO_3 (Cook, 2011). Since this study was completed it is likely that the total amount of total alkalinity has declined in Lake Alexandrina due to flushing post-drought but the amount for Lake Albert is likely to be similar. The rate of replenishment of alkalinity for Lake Alexandrina was estimated by Earth Systems (2008) to be 17,500

tonnes CaCO_3 per annum. For the Boggy Creek salt water site the acid flux after 1000 days is 2.4 tonnes CaCO_3 per hectare per annum. Thus an area of 7300 ha discharging acidity at the rate of the Boggy Creek salt water site would be required to use up the annual input of alkalinity. Cook (2011) estimated the exposed area of acidic sediments for Lake Alexandrina to be 3562 ha at the lowest water level reached during the recent drought (-1.19 m AHD). Thus a water level that resulted in exposure of almost twice the area exposed in the recent drought would be required before Lake Alexandrina became vulnerable to becoming acidic. This would suggest that Lake Alexandrina is not likely to go acidic in the longer term due to acid diffusion from sediments exposed from 2007-2009. This is consistent with the results of Hipsey et al. (2010) who also found that for Lake Alexandrina large-scale whole lake acidification is unlikely if water levels are maintained above -1.75 m AHD.

However, Lake Albert has much less alkalinity and the rate of replenishment of alkalinity was not estimated. However, the area of acidic sediments exposed was estimated by Cook (2011) to be approximately 1600 ha for Lake Albert at its lowest level of -1.16 m AHD. The maximum discharge in 1000 days from this area would then be 18,720 tonnes CaCO_3 , which is greater than the estimated alkalinity in Lake Albert. Despite no current evidence of acidification in EPA monitoring data, this would suggest that monitoring of the alkalinity in Lake Albert should be continued.

The present models do not include sinks and sources but it is possible to include these although the computation becomes more complicated. One reason this might be considered is that oxygen penetration into the sediments will cause the change of the Fe^{2+} to Fe^{3+} in the oxic sediments. This is likely to release H^+ ions but sulfate reduction in the anoxic sediments is likely to consume H^+ ions. The depth of the oxic/anoxic boundary is a very important property in sediments. This depth is known (DiToro, 2000) to be very dependent on the respiration rate of the sediments. Although some measurements of the sediment oxygen demand have been made (Aldridge et al. 2009) without the depth to the anoxic layer it is not possible to determine the respiration rate. Measurement of the respiration rate or sediment oxygen demand and depth to the anoxic layer would be very useful in assisting with the modelling and management of the lower lakes. The precipitation of metals near the sediment:water boundary may also have ecological implications but this is unclear at present.

5. CONCLUSIONS

The conclusions will be considered in relation to the agreed management questions in the findings of the workshop held in December 2011 (Cugley, 2011), which were:

Overarching Questions

- How long will it take for the lakes to recover and what are the indicators of recovery/problems?
- What we would do differently to manage acidification risks in the future?

Ecosystem

- What are the toxicological and synergistic effects of acidification on key aquatic organisms?
- What are the minimum water levels required to protect key species from the effects of acidification?

- What are the implications of likely functional changes to ecosystem processes?

Bioremediation

- What are the medium and longer term consequences of different bioremediation techniques/processes?

Sediment chemistry

- What are the rates of recovery of acidic sediments and what is driving recovery in different sediment types and locations?
- Are the lake sediments now more susceptible to future acidification events?

Groundwater

- How significant are surface and groundwater interactions in reducing or increasing the risk of acidification and what can we do about it?

This study has added significantly to three of these general questions:

- How long will it take for the lakes to recover and what are the indicators of recovery/problems?

Firstly the sediment transport models developed in this report have proved very useful for exploring the likely acidic fluxes from resubmerged acidic sediments. They have been shown using molecular diffusion rates for the dispersion to give realistic results compared to measured experimental values. These relatively simple models allow different scenarios for management of the lower lake sediments with some confidence. They show that in the absence of significant advection of water into the sediments that acidity in the sediments, and acid fluxes to the surface water, will remain high for some time to come. These findings are consistent with field observations of sediment and water chemistry but the ecological implications are unclear at present. Lake Alexandrina due to the large alkalinity store and continual alkalinity input is unlikely to be susceptible to whole of lake acidification. However, areas that get cut off from the main lake water body and/or have limited exchange may be susceptible to acidification. Lake Albert due to its limited alkalinity store and limited input is more susceptible to acidification. Monitoring of vulnerable areas such as, Boggy/Hunters Creek in Lake Alexandrina and Lake Albert should be continued. Continuous monitoring of sediment chemistry profiles at selected locations could assist with parameterising the models.

- What are the rates of recovery of acidic sediments and what is driving recovery in different sediment types and locations?

What these simple models indicate is that recovery will occur by the loss of acidity to the water column due to diffusion and advection and neutralization of the acidity by the alkalinity in the lake water. This recovery will be different depending on; the total acidity of the sediments, the composition of the acidity, the distribution of this acidity, the direction and velocity of the advection, and the dispersion coefficient. As noted above even the 1000 day simulations showed acidity persisting in the sediment so full recovery could take years-decades. The model findings also indicate that although the recovery of the benthic biota may result in an increase in the dispersion coefficient and hence acidity flux this increase will be relatively short lived.

- What we would do differently to manage acidification risks in the future?

The general risk of acidification can be managed in the future by preventing water levels declining to create large areas of exposed acid sulfate soils. This requires a greater amount of environmental flow to the Lower Lakes during drought. However the use of smaller-scale wetting and drying cycles as a regular management action may be beneficial to reduce the build up of pyrite in the sediments.

In this study the flux from the sediment transport model was used to drive a water chemistry model and determine the effect of these fluxes on the water alkalinity. This coupling of these two models offers the ability to explore the consequences of management options for the rewetting of acidic sediments. If flows and water levels decline again in the lower lakes the results indicate some shallow areas on the lake margins could still be susceptible to acidification. There is also a legacy of acidified sediments and indications from our modelling are that this could take many years to recover depending on the extent of advection that occurs. Our modeling suggest that ensuring as rapid a rise in the water level as possible of exposed areas could allow advection to push the acidic solutes into the sediments and reduce the rate and the amount of acidity transported to the water column.

Finally the simple models presented here do not include sources and sinks for the acidity within the sediments such as sulfate reduction (Sullivan et al. 2011) or oxic/anoxic processes. Modelling of the sensitivity of the oxic/anoxic depth was carried out and showed this was particularly sensitive to the respiration rate of the sediments. It is suggested that measurement of the respiration rate of the sediments would enhance the ability to understand the long term fate of the acidity and also regeneration of pyrites in these sediments. Modelling of the rate of sulfide production in the sediments would also seem prudent given the recent history and predicted uncertainty in the weather conditions due to climate change.

5.1 Recommendations

1. Enhance the present models with the addition of zero-order and first-order source/sink terms, including modelling the sulfide production rate of the sediments.
2. Monitor the diffusion processes and water quality in shallow embayments to determine the nature and time course of the acidity fluxes and effect on water alkalinity.
3. Ongoing monitoring of the alkalinity in the lakes, especially Lake Albert should be continued until reliable measurements of the acid fluxes are known.
4. Model the oxidation and hydrolysis of metal acidity (Mn, Al, Fe) at the redox boundary and sediment:water interface.
5. Modelling of the depth of oxygen penetration into the sediments to determine the oxic/anoxic boundary.
6. Combine acid flux measurements with benthic ecotoxicological experiments.
7. Measure the respiration rate of the sediments.

6. REFERENCES

- Aldridge KT, Deegan BM, Lamontagne S, Bissett A. and Brookes JD (2009). Spatial and temporal changes in water quality and sediment character in Lake Alexandrina and Lake Albert during a period of rapid water level drawdown. CSIRO: Water for a Healthy Country National Research Flagship, Canberra. 67pp.
- Ankley GT, Thomas AN, DiToro DM, Hansen DJ, Mahony JD, Berry WJ, Swartz RC, Hoke RA, Garrison AW, Allen HE and Zarba CS (1994). Assessing potential bioavailability of metals in sediments- A proposed approach. *Environmental Management*, **18**(3): 331-337.
- ANZECC (2000) Australian and New Zealand Guidelines for Fresh and Marine Water Quality. Australian and New Zealand Environment and Conservation Council and Agriculture and Resource Management Council of Australia and New Zealand, Canberra.
- Arnon S, Gray KA and Packman AI (2007). Biophysicochemical process coupling controls nitrate use by benthic biofilms. *Limnology and Oceanography*, **52**(4): 1665-1671.
- Braeckman U, Provoost P, Moens T, Soetaert, K, Middleburg JJ, Vincx M and Vanaverbeke J (2011). Biological vs. Physical Mixing Effects on Benthic Food Web Dynamics. *Plos One* **6**(3): 1-12.
- Baker A, Fitzpatrick RW, Simpson SL, Merry RH (2011). Temporal variations in reflooded acid sulfate soil environments around Lakes Alexandrina and Albert. South Australia. CSIRO Land and Water Science Report 4/11. Available at: <http://www.clw.csiro.au/publications/science/2011/sr04-11.pdf>
- Bourman R P and Barnett EJ (1995). Impacts of river regulation on the terminal lakes and mouth of the River Murray, South Australia. *Australian Geographical Studies* **33**, 101–115.
- Cook FJ (2011). Lake Alexandrina and Lake Albert: Analysis of groundwater measurements and estimation of acid fluxes. CSIRO: Water for a Healthy Country National Research Flagship. 62 pp.
- Cook FJ, McLachlan G, Leyden E and Mosley L (2011). Physical properties of soils/sediments of Lower Murray Lakes and modelling of acid fluxes. CSIRO: Water for a Healthy Country National Research Flagship. 60 pp. Available at: <http://www.clw.csiro.au/publications/waterforahealthycountry/2011/wfhc-LowerMurray-acid-fluxes.pdf>
- Clothier BE and Scotter DR (1985). Water and solute movement in the root zone. *New Zealand Agricultural Science*, **19**(4): 187-192.
- Cugley, J. (2011). Acid sulfate soil and ecology research workshop. John Cugley Environmental Pty Ltd, 17pp.
- Dade WB (1993). Near-bed turbulence and hydrodynamic control of diffusional mass transfer at the sea floor. *Limnology and Oceanography*, **38**(1): 52-69.
- Di Toro DM (2000). Sediment Flux Modelling. Wiley, New York, 624p.

- Duff JH and Triska FJ (2000). Nitrogen biochemistry and surface-subsurface exchange in streams, p. 197-220. *In* JB Jones and PJ Mulholland [eds.], *Streams and Groundwaters*, Academic Press.
- Earth Systems (2010). Quantification of acidity flux rates to the Lower Murray Lakes. Prepared by Earth Systems Pty Ltd. for the Department for SA Department of Environment and Natural Resources, Adelaide.
- EPA (2012 in prep.). Water quality in the lower lakes during a hydrological drought. Report by the Environment Protection Authority, South Australia.
- Fitzpatrick RW, Shand P, Marvanek S, Merry RH, Thomas M, Simpson SL, Raven MD, McClure S (2008). Acid sulfate soils in subaqueous, waterlogged and drained soil environments in Lake Albert, Lake Alexandrina and River Murray below Blanchetown (Lock 1): properties, distribution, genesis, risks and management. Prepared for Department for Environment and Heritage, SA. CSIRO Land and Water Science Report 46/08. CSIRO, Adelaide, 167. pp. Available at: <http://www.clw.csiro.au/publications/science/2008/sr46-08.pdf>
- Fitzpatrick RW, Grealish G, Shand P, Simpson SL, Merry RH, and Raven MD, (2009). Acid sulfate soil assessment in Finniss River, Currency Creek, Black Swamp and Goolwa Channel, South Australia. Prepared for the Murray Darling Basin Authority. CSIRO Land and Water Science Report 26/09. CSIRO, Adelaide, 213 pp. Available at: <http://www.clw.csiro.au/publications/science/2009/sr26-09.pdf>
- Fitzpatrick RW, Grealish G, Chappell A, Marvanek S and Shand P (2010). Spatial variability of subaqueous and terrestrial acid sulfate soils and their properties, for the lower lakes South Australia. Prepared by the Commonwealth Scientific and Industrial Research Organisation (CSIRO) Land and Water for the SA Department of Environment and Natural Resources, Adelaide. Available at: <http://www.environment.sa.gov.au/files/bea54c4b-2158-4daa-b6b0-9ebb01020c44/cllmm-gen-acidsulfatesoils-report1.pdf>
- Fitzpatrick, RW, Grealish, GJ, Shand, P. and Creeper NL. (2011). Monitoring and assessment of reflooded acid sulfate soil materials in Currency Creek and Finniss River Region, South Australia. Prepared for the South Australia Department of Environment and Natural Resources (DENR), Adelaide. Client Report R-325-8-6. CSIRO: Sustainable Agriculture Research Flagship, 101 pp. Available at: <http://www.clw.csiro.au/publications/science/2011/SAF-monitoring-ASS-Currency-Creek.pdf>
- Glud RN and Fenchel T (1999). The importance of ciliates for interstitial solute transport in benthic communities. *Marine Ecology-Progress Series* **186**: 87-93.
- Hargrave BT (1972). Aerobic decomposition of sediment and detritus as a function of particle surface-area and organic content. *Limnology and Oceanography*, **17**(4): 583-596.
- Hicks WS, Creeper N, Hutson J, Fitzpatrick RW, Grocke S and Shand P (2009). The potential for contaminant mobilisation following acid sulfate soil rewetting: field experiment. Prepared by the Commonwealth Scientific and Industrial Research Organisation (CSIRO) Land and Water for the SA Department of Environment and Natural Resources, Adelaide. Available at: <http://www.environment.sa.gov.au/files/b6b9ad2e-f460-460f-b36c-9ebb010f396f/cllmm-gen-acidsulfatesoils-report3.pdf>
- Hipsey MR, Bursch, B.D., Colleti, J. and Salmon, S.U. (2010). Lower lakes hydrogeochemical model development and assessment of acidification risks. Prepared by University of Western Australia for SA Water.
- Kirby, C. S., Cravotta, C.A., III, 2005, Net alkalinity and net acidity in mine drainage 1: Theoretical considerations, *Applied Geochemistry*, **20**: 1920–1940.

- Larned ST, Nikora VI and Biggs BJB (2004). Mass- transfer-limited nitrogen and phosphorus uptake by stream periphyton: A conceptual model and experimental evidence. *Limnology and Oceanography*, **49**: 1992-2000.
- Lichtschlag A, Felden J, Wenzhoefer F, Ertefai TF, Boetius A and deBeer D. (2010). Methane and sulfide fluxes in permanent anoxia: In situ studies at the Dvurechenskii mud volcano (Sorokin Trough, Black Sea). *Geochimica Et Cosmochimica Acta*, **74**(17): 5002-5018.
- Marion A, Bellinello M, Guymer I and Packman A (2002). Effect of bed form geometry on the penetration of nonreactive solutes into a streambed. *Water Resources Research*, **38**(10): 27-1 to 27-12.
- Marion A, Zaramella M and Packman AI (2003). Parameter estimation of the transient storage model for stream-subsurface exchange. *Journal of Environmental Engineering-ASCE*, **129**(5): 456-463.
- Meysman FJR, Galaktionov OS, Cook PLM, Janssen F, Huettel M and Middleburg JJ (2007). Quantifying biologically and physically induced flow and tracer dynamics in permeable sediments. *Biogeosciences*, **4**(4): 627-646.
- Mosley LM, Peake BM, and Hunter KA (2010). Modelling of pH and inorganic carbon speciation in estuaries using the composition of the river and seawater end members. *Environmental Modelling & Software* **25**: 1658-1663.
- Philip JR (1957). The theory of infiltration:4. Sorptivity and algebraic infiltration equations. *Soil Science*, **83**: 257-264.
- Philip, J. R. (1987). The infiltration joining problem. *Water Resources Research*, **23**(12): 2239-2245.
- Robson BJ, Hamilton DP, Webster IT and Chan T (2008). Ten steps applied to development and evaluation of process-based biogeochemical models of estuaries. *Environmental Modelling & Software*, **23**(4): 369-384.
- Stumm, W. and Morgan, J.J.(1996): Aquatic Chemistry, Chemical Equilibria and Rates in Natural Waters, 3rd ed. John Wiley & Sons, Inc., New York, 1022p.
- Sullivan LA, Bush RT, Ward NJ, Fyfe DM, Johnston M, Burton ED, Cheeseman P, Bush M, Maher C, Cheetham M, Watling KM, Wong VNL, Maher R and Weber E (2010). Lower lakes laboratory study of contaminant mobilisation under seawater and freshwater inundation. Prepared by Southern Cross GeoScience for the SA Department of Environment and Natural Resources, Adelaide. Available at: <http://www.environment.sa.gov.au/files/bc620a09-b89e-4b22-acdb-9ebb01109e53/clmm-gen-acidsulfatesoils-report5.pdf>
- Sullivan LA, Burton ED, Ward NJ, Bush RT, Coughran J, Cheetham MD, Fyfe DM, Cheeseman PJ and McIntyre T (2011). Lower lakes sulfate reduction study. Southern Cross GeoScience Technical Report No. 711. Prepared for the SA Department of Environment and Natural Resources, Adelaide.
- Van Genuchten M Th and Alves WJ (1982). Analytical solutions of the one-dimensional convective-dispersion solute transport equation. U.S. Department of Agriculture, Technical Bulletin 1661, 151p.
- van Rees KCJ, Reddy KR, and Rao PSC (1996). Influence of benthic organisms on solute transport in lake sediments. *Hydrobiologia*, **317**(1): 31-40.
- Vanýsek, P (1992). Ionic conductivity and diffusion at infinite dilution, Handbook of Chemistry and Physics, CRC Press, 1992/93 edition. Boca Raton, 1992. pp. (5-111)-(5-113).

- Vinebrooke, R.D., Schindler, D.W., Turner, M.A., Findlay, D.L., Paterson, M. and Mills, K.H. (2003). Trophic dependence of ecosystem resistance and species compensation in experimentally acidified Lake 302S (Canada). *Ecosystems* **6**: 101-113.
- Volkenborn N, Polerecky L, Welthey DS and Woodin SA (2010). Oscillatory porewater bioadvection in marine sediments induced by hydraulic activities of *Arenicola marina*. *Limnology and Oceanography*, **55**(3): 1231-1247.
- Vopel K, Gibbs M, Hickey CW and Quin J (2008). Modification of sediment-water solute exchange by sediment-capping materials: effects on O₂ and pH. *Marine and Freshwater Research*, **59**(12): 1101-1110.
- Webster DR and Weissburg MJ (2009). The Hydrodynamics of Chemical Cues Among Aquatic Organisms. *Annual Review of Fluid Mechanics*, **41**: 73-90.
- Webster IT (2003). Wave enhancement of diffusivities within surficial sediments. *Environmental Fluid Mechanics*, **3**: 269-288.

APPENDIXES

Computer programs for the modelling are listed below. These are written in MatLab.

This program is used to compute the acidity concentrations and fluxes in section 2.

```
function [ output_args ] = Sed_Acid_CC( input_args )
%Acidity output from sediment with square wave starting concentration
%profile. Surface condition concentration.

% Solute A5 of van Genuchten and Alves 1982

R = 1;
C1 = 2e-3; %Initial concentration z , z1 (kg/m3)
C2 = 0;% Initial concentration z > z1 (kg/m3)
C0 = 0; % concentration at surface (kg/m3)
v = 0; %velocity of pore water (m/day)
Ion = 1; % Specify ion species 1 = H+, 2 = Fe2+, 3 = Al3+
D = [8.06 0.61 0.47]; % Diffusion coefficient cm2/day
MW = [1 55.85 26.98]; %molecular weight g/mol, H+ 1, Fe 55.85, Al
26.98
D1 = D(Ion)/100^2;%Diffusion coefficient m2/day
z1 = 1; %depth of acidity initial pulse

filename = 'AcidCOutput21';

zrange = 3;% m

z(1:6)= [0 0.001 0.002 0.005 0.007 0.01];
E = 7;
while z(E-1) < zrange
    z(E) = (E-5)*0.01;
    E = E+1;
end

nz = size(z,2);
tmax = 100;%day
t(1:10) = [0.001 0.005 0.01 0.05 0.07 0.1 0.2 0.5 0.7 1];
i = 10
while t(i) < tmax
    t(i+1) = t(i)+1;
    i = i+1
end
tn = size(t,2);

c = zeros(tn,nz);

if v ~= 0
% full solution
    for i = 1:tn
```

```

        D2 = 2*sqrt(D1*R*t(i));
        for j = 1:nz
            Term1 = 1/2*erfc((R*(z(j)-z1)-v*t(i))/D2);
            Term2 = 1/2*exp
(v*z(j)/D1)*erfc((R*(z(j)+z1)+v*t(i))/D2);
            A = Term1 + Term2;
            Term3 = 1/2*erfc((R*z(j)-v*t(i))/D2);
            Term4 = 1/2*exp (v*z(j)/D1)*erfc((R*z(j)+v*t(i))/D2);
            B = Term3 + Term4;
            c(i,j) = C2 + (C1-C2)*A + (C0-C1)*B;
            CN(i,j) = (c(i,j)-C0)/(C1-C0);
        end
        flux(i) = D1*(c(i,1)-c(i,2))/(z(1)-z(2));
    end
else
    for i = 1:tn
        D2 = 2*sqrt(D1*R*t(i));
        for j = 1:nz
            Term1 = 1/2*erfc(R*(z(j)-z1)/D2);
            Term2 = 1/2*erfc(R*(z(j)+z1)/D2);
            A = Term1 + Term2;
            Term3 = 1/2*erfc((R*z(j))/D2);
            Term4 = 1/2*exp (v*z(j)/D1)*erfc((R*z(j))/D2);
            B = Term3 + Term4;
            c(i,j) = C2 + (C1-C2)*A + (C0-C1)*B;
            CN(i,j)= (c(i,j)-C0)/(C1-C0);
        end
        flux(i) = D1*(c(i,1)-c(i,2))/(z(1)-z(2));
    end
end
y = c(100,:);
plot(z,y)
Inames = {'R'; 'C1'; 'C2'; 'C0'; 'V'; 'D'; 'z1'};
xlswrite(filename,Inames,'Initial','A');
Initial = [R C1 C2 C0 v D1 z1];
xlswrite(filename,Initial,'Initial','B');
Heading = {'Depth (m)'; 'Time (day)'};
xlswrite(filename,Heading,'conc','A1');
xlswrite(filename,t,'conc','C1');
xlswrite(filename,z,'conc','A2');
xlswrite(filename,c,'conc','C2');
xlswrite(filename,Heading,'CN','A1');
xlswrite(filename,t,'CN','C1');
xlswrite(filename,z,'CN','A2');
xlswrite(filename,CN,'CN','C2');
dcnames = {'Time (day)'; 'flux (kg/m2/day)'; 'flux (mol_H+/m2/day)'};
xlswrite(filename,dcnames,'dcdz','A1');
xlswrite(filename,t,'dcdz','A2');
xlswrite(filename,flux,'dcdz','B2');
xlswrite(filename,flux'*Ion/MW(Ion)*1000,'dcdz','C2');

end

```

This program is used to compute the acid neutralisation in section 3.

```
%% Acid-base equilibria calculations for surface water following acid
diffusion

%% Declare global variables

global KH K1 K2 KW pCO2 ActH Alkout a b c NumIt MaxIt epsilon

sheetNames = {'Boggy Creek Fresh water', 'Boggy Creek Salt water',
'Point Sturt fresh water', 'Point Sturt salt water'};
[inputFile,txt,row] = xlsread('Acid fluxes-advection-
diffusionv3.xlsx', sheetNames{1,4});
colours = ['b', 'r', 'g', 'k', 'm', 'm', 'y'];

%% Read in initial variables

WaterDepth = 0.5; %water depth in m
WaterVolume = WaterDepth*1000; %water volume in L over 1m2 sediment
area, converted m3 unit
Acidin = inputFile(1,2)/WaterVolume; % Acid concentration following
acid addition mol/L
Alkinit = [0.0001, 0.001, 0.002, 0.004]; %initial alkalinity in the
water, mol/L
alkalinityInflow = [0.00]; % alkalinity inflow in surface water if
present
pCO2 = 0.00036; % value of the pCO2 in the water
Sal = 0.6;% Salinity of the sample (unitless approx. equivalent
to g/kg)
TempC = 25; % Temperature of water body, degrees C

%% Set iteration criteria and pH bounds for bisection method
NumIt = 0; % Initial Number of iterations
MaxIt = 1000; % Maximum number of iterations
epsilon = 10^-6; %error tolerance to consider equation solved
a = 0; % Left hand side pH guess for bisection function
b = 14; % Right hand side pH guess for bisection function

%% Convert Temperature to Kelvin

TempK = TempC + 273.15;
logTempK = log(TempK);

%% Calculate CO2 and water Thermodynamic Equilibrium Constants (KH,
K1, K2) and KW
% K1, K2, KW from Millero, Geochemica et Cosmochemica Acta
43:1651-1661, 1979,
% Millero refit data from following references to provide below
equations for K1, K2, KW
% KWrefit data of Harned and Owen, The Physical Chemistry of
% Electrolyte Solutions, 1958
% K1 from refit data from Harned and Davis,
% J American Chemical Society, 65:2030-2037, 1943.
```

```

        % K2 from refit data from Harned and Scholes,
        % J American Chemical Society, 43:1706-1709, 1941.
        % Henry's Law Constant (KH) for CO2 calculated from Weiss, R. F.,
        Marine Chemistry 2:203-215, 1974.
        % KH is also termed K0 in some texts)
        % These equations only for Sal=0 water (these are thermodynamic
        constants)
        lnKW = 148.9802 - 13847.26/TempK - 23.6521*logTempK;
        KW = exp(lnKW);
        pKW = -log10(KW);
        lnK1 = 290.9097 - 14554.21/TempK - 45.0575*logTempK;
        K1 = exp(lnK1);
        pK1 = -log10(K1);
        lnK2 = 207.6548 - 11843.79/TempK - 33.6485*logTempK;
        K2 = exp(lnK2);
        pK2 = -log10(K2);
        TempK100 = TempK/100;
        lnKH = -60.2409 + 93.4517 / TempK100 + 23.3585 * log(TempK100) +
        Sal * ...
        (0.023517 - 0.023656 * TempK100 + 0.0047036 * TempK100 ^2);
        KH = exp(lnKH); % this is in mol/kg-SW/atm (note need to check
        for NBS pH scale)
        pKH = -log10(KH);

%% Calculate activity coefficients for H+

        % First Calculate Ionic Strength from salinity
        % From the DOE CO2 system handbook, Chapter 5, p. 13/22, eq.
        7.2.4:
        % Then calculate ion activity coefficient for H+
        % Using Guntelberg approximation, Stumm and Morgan 1996, Table
        3.3 equation
        % Note, need to add equation to calculate A for various Temp
        (using
        % dielectric constant for water)

        IonicS = 19.924 * Sal / (1000 - 1.005 * Sal); % ionic
        strength correction
        logActH = -0.5 * 1^2 * ((IonicS ^0.5) / (1 + IonicS ^0.5)); %log
        activity coeff H+
        ActH = exp(logActH); %activity coeff H+

%% Calculate new alkalinity after acid addition
cResultArray = [];
C = [];
for f=1:length(Alkinit)
    AlkoutResultArray = [];
    Time = [];
    Alkout = Alkinit(1,f) - Acidin + alkalinityInflow;
    loopIt = 1;
    rawLoopIt = 2;
    while strcmp(raw(rawLoopIt,1), 'End') == 0
        Time = [Time, inputFile(loopIt,1)];
        lineAcid = inputFile(loopIt,2);
        lineAcid = lineAcid/WaterVolume;
        Alkout = Alkout - lineAcid + alkalinityInflow;
        [c, NumIt] = bisectionTEST(K1,K2,KH,KW,ActH,pCO2,Alkout, a,
        b);
        cResultArray(loopIt,1) = c;
        AlkoutResultArray(loopIt,1) = Alkout;
    end
end

```

```

        loopIt = loopIt + 1;
        rawLoopIt = rawLoopIt + 1;
    end
    C = [C cResultArray];
    subplot(2,1,1);
    plot(Time,cResultArray, colours(f));
    xlabel('Time (days)')
    ylabel('pH')
    title('pH with different water ALK at t=0
(c2>0,depth=0.5m)')
    hold on;
    subplot(2,1,2);
    plot(Time,AlkoutResultArray, colours(f));
    xlabel('Time (days)')
    ylabel('Alkalinity')
    title('ALK with different water ALK at t=0
(c2>0,depth=0.5m)')
    hold on;
end
leg = legend(cellstr(num2str(Alkinit')), 'Location',
'East');
set(leg, 'FontSize', 9);
hold off;
hold off;

```

The below function is called in the above function to solve the pH-alkalinity equation using the bisection method

```

function [c, NumIt] = bisectionTEST(K1,K2,KH,KW,ActH,pCO2,Alkout,a,b)
MaxIt = 1000;
epsilon = 10^-8;
c = (b + a)/2;
Residuala = Alkout - ((KH*pCO2)/(1/(1+K1/(10^-a)+(K1*K2)/((10^-a)^2))))*(1/(((10^-a)/K1)+1+K2/(10^-a)))+(2*((1/(((10^-a)^2)/(K1*K2))+((10^-a)/K2)+1))))-(KW/10^-a)+(10^-a/ActH);
Residualb = Alkout - ((KH*pCO2)/(1/(1+K1/(10^-b)+(K1*K2)/((10^-b)^2))))*(1/(((10^-b)/K1)+1+K2/(10^-b)))+(2*((1/(((10^-b)^2)/(K1*K2))+((10^-b)/K2)+1))))-(KW/10^-b)+(10^-b/ActH);
Residualc = Alkout - ((KH*pCO2)/(1/(1+K1/(10^-c)+(K1*K2)/((10^-c)^2))))*(1/(((10^-c)/K1)+1+K2/(10^-c)))+(2*((1/(((10^-c)^2)/(K1*K2))+((10^-c)/K2)+1))))-(KW/10^-c)+(10^-c/ActH);
NumIt = 0;
while (NumIt<=MaxIt) && (abs(Residualc)>=abs(epsilon))
    if Residuala*Residualc<=0
        b = c;
    else
        a = c;
    end
    c = (b + a)/2;
    NumIt = NumIt + 1;
    Residuala = Alkout - ((KH*pCO2)/(1/(1+K1/(10^-a)+(K1*K2)/((10^-a)^2))))*(1/(((10^-a)/K1)+1+K2/(10^-a)))+(2*((1/(((10^-a)^2)/(K1*K2))+((10^-a)/K2)+1))))-(KW/10^-a)+(10^-a/ActH);
    Residualb = Alkout - ((KH*pCO2)/(1/(1+K1/(10^-b)+(K1*K2)/((10^-b)^2))))*(1/(((10^-b)/K1)+1+K2/(10^-b)))+(2*((1/(((10^-b)^2)/(K1*K2))+((10^-b)/K2)+1))))-(KW/10^-b)+(10^-b/ActH);
    Residualc = Alkout - ((KH*pCO2)/(1/(1+K1/(10^-c)+(K1*K2)/((10^-c)^2))))*(1/(((10^-c)/K1)+1+K2/(10^-c)))+(2*((1/(((10^-c)^2)/(K1*K2))+((10^-c)/K2)+1))))-(KW/10^-c)+(10^-c/ActH);
end

```


FREEMAN COOK

ASSOCIATES /

PTY LTD

$$x = \frac{-b \pm \sqrt{b^2 - 4ac}}{2a} \quad (a+b)(a-b) = a^2 - b^2 \quad \int \frac{t^n dt}{e^t} = \frac{t^n e^t}{1} - n \int \frac{t^{n-1} e^t}{1} dt$$
$$(a-b)^2 = a^2 - 2ab + b^2 \quad \sin^2 \alpha + \cos^2 \alpha = 1 \quad (a+b)(a-b) = a^2 - b^2 \quad ax^2 + bx + c = 0 \quad (a+b)(a-b) = a^2 - b^2 \quad \sin^2 \alpha + \cos^2 \alpha = 1$$

Ph: 0409 613 932
Email: freeman.j.cook@gmail.com
PO Box 97 Glasshouse Mountains Q 4518 Australia